Isotopic ages of post-Paleocene igneous rocks within and bordering the Clifton 1°×2° quadrangle, Arizona–New Mexico

by R. F. Marvin, C. W. Naeser, M. Bikerman,
H. H. Mehnert, and J. C. Ratté

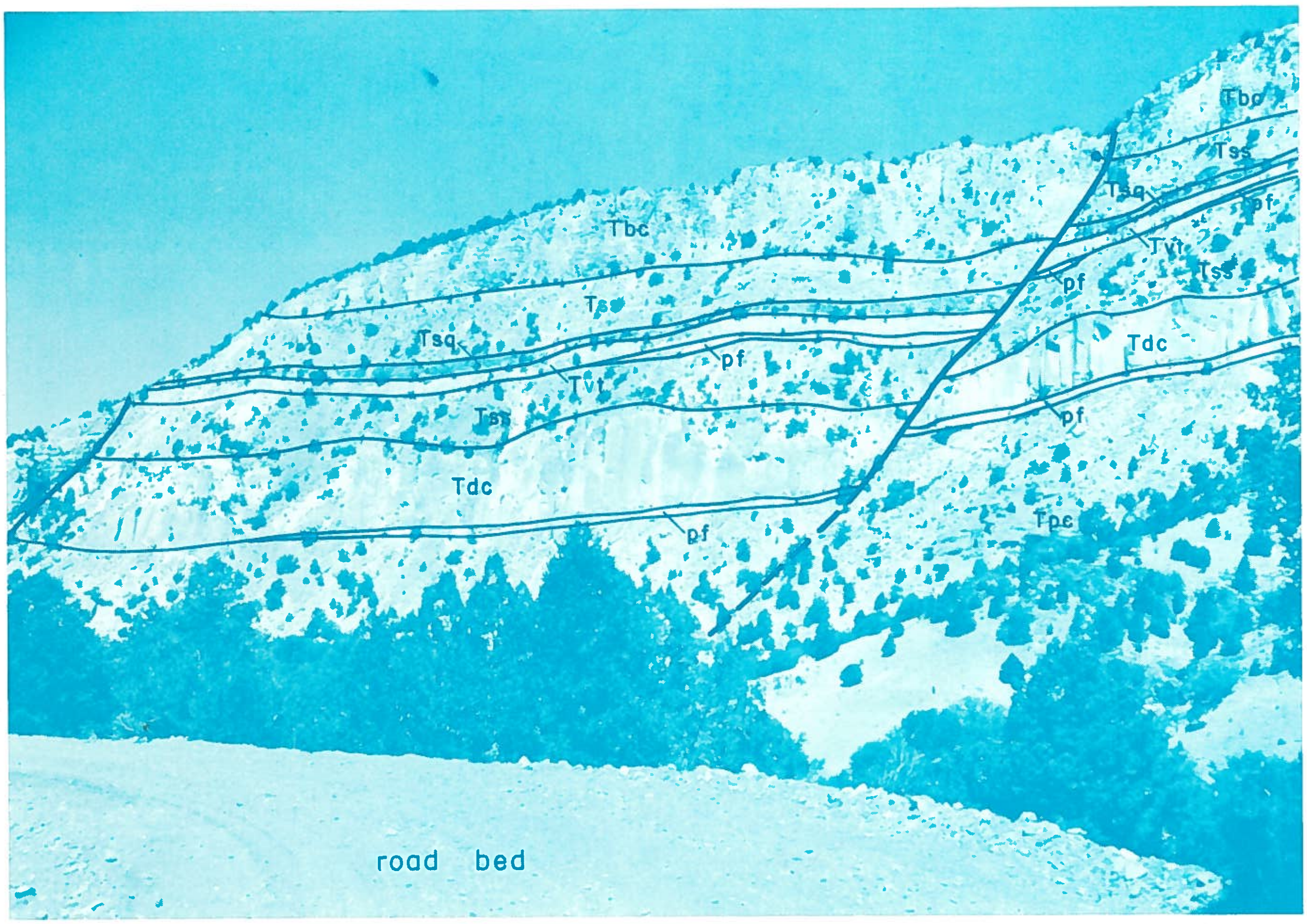

BULLETIN 118 New Mexico Bureau of Mines & Mineral Resources 1987

A DIVISION OF

NEW MEXICO INSTITUTE OF MINING & TECHNOLOGY

Bulletin 118

New Mexico Bureau of Mines & Mineral Resources

A DIVISION OF
NEW MEXICO INSTITUTE OF MINING & TECHNOLOGY

Isotopic ages of post-Paleocene igneous rocks within and bordering the Clifton 1° x 2° quadrangle, Arizona—New Mexico

by R. F. Marvin[1], C. W. Naeser[1], M. Bikerman[2], H. H. Mehnert[1], and J. C. Ratté[1]

[1]U.S. Geological Survey, Denver, Colorado 80225;
[2]Department of Geology and Planetary Science, University of Pittsburgh, Pittsburgh, Pennsylvania 15260

SOCORRO 1987

Original Printing 1987

Published by Authority of State of New Mexico, NMSA 1953 Sec. 63-1-4
Printed by University of New Mexico Printing Plant, December 1987

Available from New Mexico Bureau of Mines & Mineral Resources, Socorro, NM 87801

Contents

Tables

Figures

Plate

Abstract

This report is a compilation of isotopic ages and analytical data from more than 200 samples of volcanic and subvolcanic igneous rocks of the western and central parts of the Mogollon—Datil volcanic field of middle to late Cenozoic age. More than one-half of the tabulated ages have never been published. In addition to the compilation of ages, the report includes brief discussions of some of the problems involved in conventional K—Ar and fission-track dating of rapidly erupted volcanic sequences in a large, complex volcanic field and includes some of the specific volcano-stratigraphic problems in the central and western parts of the Mogollon—Datil field.

Introduction

In recent years, numerous K—Ar and fission-track ages have been determined for volcanic rocks of the Mogollon—Datil volcanic field. Most of these dated rocks were collected within or peripheral to the Clifton 1° x 2° quadrangle of Arizona and New Mexico. However, the Clifton quadrangle encompasses only part of the Mogollon—Datil volcanic field.

This compilation of isotopic ages lists more than 200 samples of post-Paleocene igneous rocks. Slightly more than one-half of the tabulated ages have never been published. Also included in this compilation are unpublished analytical data pertaining to tabulated ages that have already appeared in print.

The purposes of this compilation are:

1) to present the currently available age data that are pertinent to establishment of viable volcanic stratigraphic sequences in the western and central parts of the Mogollon—Datil volcanic field.
2) to describe some of the problems associated with dating the rocks of a complex volcanic field and the efficacy of different radiometric dating methods.
3) to discuss the application of the ages in the compilation to certain specific geologic problems in the western and central parts of the Mogollon—Datil field.

Present study

Approximately 70% of the ages and analytical data in the compilation are the work of Marvin, Naeser, and Mehnert in the U.S. Geological Survey laboratories in Denver, Colorado, since about 1972, and about 12% are the work of Bikerman at the University of Pittsburgh, over roughly the same period. Some of the U.S. Geological Survey samples were collected by T. L. Finnell, D. C. Hedlund, W. E. Brooks, and B. B. Houser, but most were collected by Ratté. Biker-man, Marvin, and Mehnert are responsible for the conventional K—Ar age determinations and interpretation of the analytical data; Naeser is responsible for the fission-track ages and analyses; Ratté is largely responsible for the geologic interpretations and stratigraphic correlations. The geologic interpretations are based mainly upon published and unpublished mapping by T. L. Finnell, D. L. Gaskill, D. C. Hedlund, E. R. Landis, W. E. Brooks, B. B. Houser, D. H. Richter, V. A. Lawrence, and Ratté, all of the U.S. Geological Survey. Marvin and Ratté are principally responsible for preparation of the manuscript.

Acknowledgments

Ages and analytical data previously published by workers other than the authors comprise nearly 20% of the compilation. P. E. Damon, M. Shafiqullah, and D. York are the major contributors of published ages and analytical data for rocks collected by R. C. Rhodes, E. I. Smith, R. V. Fodor, T. J. Bornhorst, W. E. Elston, and others. V. A. Lawrence, M. R. Oakman, W. E. Brooks, and E. Rivera assisted in various aspects of field and laboratory work and manuscript preparation.

M. Bikerman acknowledges support from the New Mexico Bureau of Mines and Mineral Resources for field work in western New Mexico. This is publication no. 665 of the Department of Geology and Planetary Science, University of Pittsburgh, Pittsburgh, Pennsylvania.

We have profited from the informal cooperation of the New Mexico Bureau of Mines and Mineral Resources, particularly through numerous field excursions with C. E. Chapin, G. R. Osburn, W. C. McIntosh, and S. M. Cather. Paleomagnetic studies and precision $^{40}Ar/^{39}Ar$ dating, presently in progress by W. C. McIntosh, have been shared freely with us and promise to provide important new dimensions toward establishing a volcanic stratigraphic framework for the Mogollon—Datil volcanic field. The manuscript was greatly improved by the very thorough editing of Jane Calvert Love, Associate Editor, New Mexico Bureau of Mines and Mineral Resources.

Organization of compilation

The compilation consists basically of separate entries of descriptive and analytical data for more than 200 rock samples. From this body of data, two master lists were made, Tables 1 and 8; both lists give the same information: entry number, name or correlation, age(s), and quadrangle location. In Table 1, the samples are listed in numerical sequence by entry number, according to their location in 7$^1/2$- and 15-min quadrangles, whereas in Table 8 (pp. 24-29) they are rearranged in approximate order of increasing age, as interpreted from geologic relationships, as well as from isotopic ages. The sample localities are designated by entry number on a map showing the 7$^1/2$-and 15-min quadrangles in which they occur (Pl. 1, in back pocket). Some of the samples are from localities outside the Clifton 1° x 2° quadrangle (Fig. 1), and they were included because their ages are relevant to the volcanic stratigraphy in the Clifton quadrangle.

In the main body of the compilation, the source of the age is indicated, and an accurate sample location is given. The entry number is followed by the author and date of publication, if the age has been published previously. If the age is new, the entry number is followed by a field number, which is preceded by USGS(D) if the sample was collected and analyzed by the authors or others with the U.S. Geological Survey in Denver. For a few samples, the published age was not accompanied by a sample number; for those few samples, the sample number is shown with a USGS(D) prefix. The entry line is followed by the rock name or stratigraphic unit; the correlations are generally those of the authors unless a reference is given. Where the correlation differs from that of other workers, an explanation commonly follows in the *Comment.* Samples are located according to latitude and longitude, section and township and range, name of $7^1/2$- or 15-min topographic quadrangle (Pl. 1, in back pocket; Fig. 1), county, state, and additional descriptive location if available and useful. Section and township and range locations usually refer to published U.S. Geological Survey topographic quadrangles but in some cases refer to U.S. Forest Service maps because the land net on some of the U.S. Geological Survey quadrangles is incomplete. In cases where latitude and longitude of previously published sample localities are inconsistent with respect to accompanying section and township and range, we commonly report revised locations. Two or more samples may be grouped

(text continued on page 13)

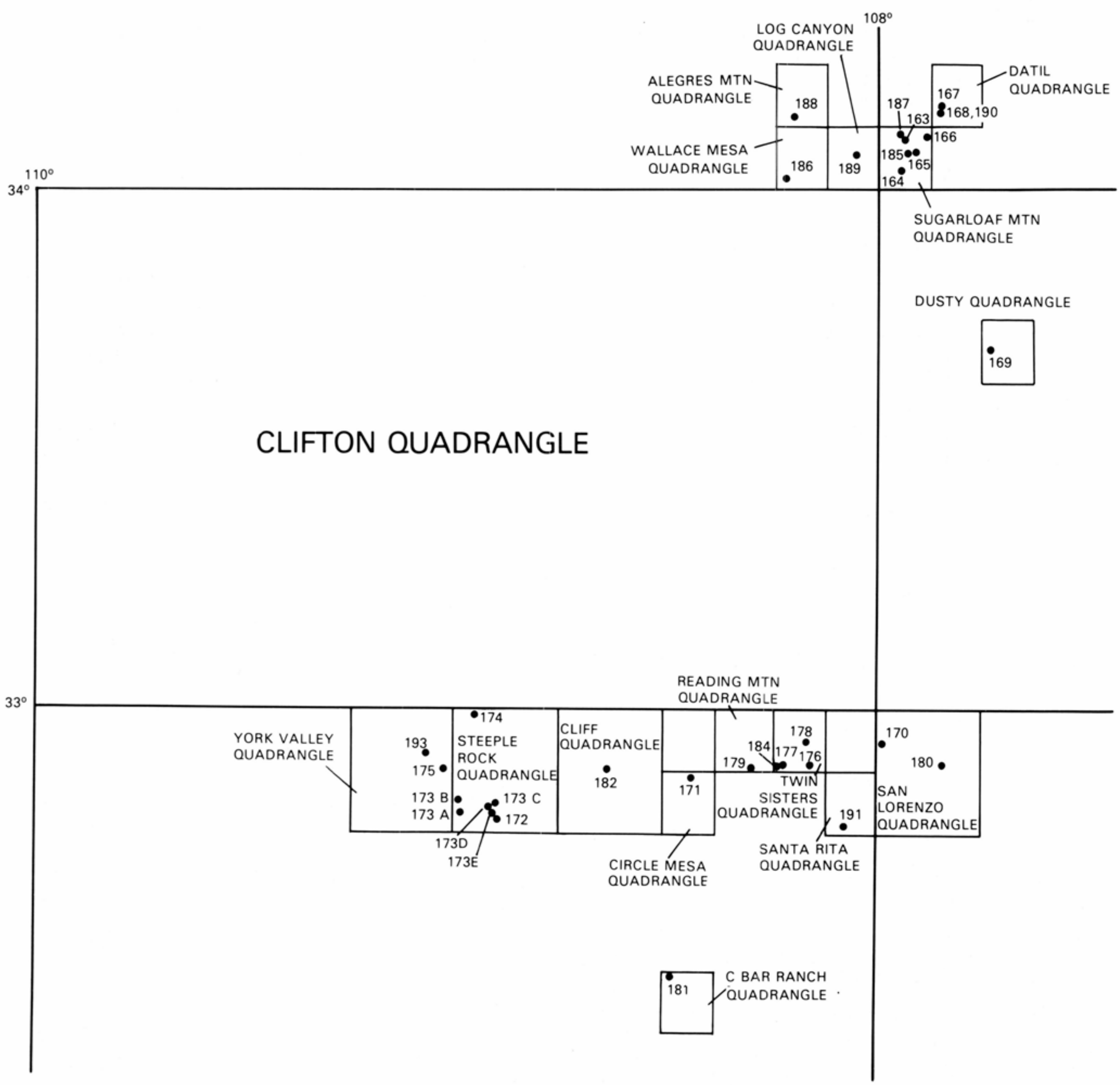

FIGURE 1—Location of dated samples bordering the Clifton 1° × 2° quadrangle.

TABLE 1—Numerical list of dated mid-Tertiary volcanic rocks in the Clifton 1° × 2° quadrangle, Arizona–New Mexico, and peripheral areas. Letter(s) indicates mineral or material dated: S, sanidine; B, biotite; P, plagioclase; H, hornblende; F, K-feldspar; Al, alunite; W, whole-rock; G, glass—obsidian; Z, zircon; Sp, sphene; A, apatite; Ad, adularia. Letter not repeated for replicate analyses of same sample. Entry no. with * means that rubidium and strontium isotopic data are listed with the analytical data under this entry number. Quadrangle name followed by [1] indicates that sample was collected outside of Clifton 1° × 2° quadrangle; see Fig. 1. Use of "at" as in basalt at Apache Creek implies more restricted distribution than use of "of" as in rhyolite of Hells Hole.

Entry no.	Correlation	Mineral dated and calculated age (m.y.)		Quadrangle (see Pl. 1)
1	Quartz latite at Baldy Peak	F	8.8 ± 0.4	Mount Ord
2	Basalt NE of Mt. Baldy	W	9.1 ± 0.9	Mount Ord
3	Basaltic-andesite flow in Barlow Pass area	W	28.7 ± 0.5	Point of Pines West
4	Basalt beneath pyroclastic rocks, Barlow Pass area	W	26.1 ± 0.9 28.3 ± 1.3	Point of Pines West
5	Rhyolite ash-flow tuff at Nantac Rim	B B B S S	24.6 ± 0.9 24.9 ± 0.9 33.7 ± 1.3 22.0 ± 0.9 22.9 ± 0.8	Point of Pines East
6	Porphyritic andesite east of Barlow Pass	P	21.3 ± 0.7 29.1 ± 1.5	Point of Pines East
7	Andesites at Bryce Mountain	W	13 ages ranging from 27–35	Bryce Mountain
8	Bloodgood Canyon Tuff	S	25.5 ± 0.7	Blue
9*	Bloodgood Canyon Tuff	B S	28.3 ± 1.0 28.3 ± 1.0 28.6 ± 1.0	Blue
10	Bloodgood Canyon Tuff	B S	30.6 ± 1.0 27.3 ± 1.3	Blue
11	Shelley Peak Tuff	B	30.1 ± 1.0	Blue
12	Older andesite in Blue Range	H	38.3 ± 3.9	Rose Peak
13	Older andesite in Blue Range	H	36.1 ± 2.7	Rose Peak
14	Quartz-latite domes of Blue Range	B	23.9 ± 0.7	Dutch Blue Creek
15	Andesite at Rose Peak, Blue Range	W	23.9 ± 0.7	Rose Peak
16	Rhyolite intrusive along lower San Francisco River	Z	33.0 ± 4.8	Big Lue Mountains
17	Amygdaloidal andesite	W	27.9 ± 1.0	Big Lue Mountains
18	Rhyolite of Hells Hole	P	28.4 ± 1.0	Big Lue Mountains
19	Rhyolite of Hells Hole	B P	27.1 ± 1.0 32.9 ± 1.2	Big Lue Mountains
20	Rhyolite of Hells Hole	Z	28.7 ± 3.7	Big Lue Mountains
21	Rhyolite dike at Chalk Peak	B Z	28.6 ± 1.0 25.5 ± 2.6	Big Lue Mountains
22	Porphyritic rhyolite dike in Soapbox Canyon	B Z A	28.4 ± 1.0 26.1 ± 3.2 20.7 ± 6.0	Big Lue Mountains
23	Rhyolite at Rattlesnake Gap	W	27.5 ± 1.0	Big Lue Mountains
24	Porphyritic rhyolite, north of Sawmill Creek	Z	27.6 ± 5.5	Big Lue Mountains
25	Tuff interlayered with mafic lava flows	Z	28.6 ± 3.7	Big Lue Mountains
26	Rhyodacite at Pat Creek	P	27.8 ± 1.6	Big Lue Mountains
27	Rhyodacite at Pat Creek	B P	30.4 ± 1.1 25.7 ± 1.6	Big Lue Mountains
28	Tuff interlayered with flows at Bird Canyon	B	28.0 ± 1.0	Big Lue Mountains
29	Pumice—rhyolite of Mule Creek	Z	26.5 ± 3.4	Big Lue Mountains
30	Porphyritic andesite in Rustlers Canyon	P P	29.5 ± 1.1 28.7 ± 1.1	Big Lue Mountains
31	Porphyritic andesite near Hamilton Spring	P	25.0 ± 0.9	Big Lue Mountains
32	Porphyritic andesite dike near Cold Spring Mountain	P	26.2 ± 1.0	Big Lue Mountains
33	Dacite of Tennessee Creek	H	21.8 ± 1.4	Big Lue Mountains
34	Rhyolite of Mule Creek	G	19.0 ± 0.9	Big Lue Mountains
35	Rhyolite of Mule Creek	G	18.3 ± 0.7	Big Lue Mountains

(*continued on page 8*)

TABLE 1 continued

Entry no.	Correlation	Mineral dated and calculated age (m.y.)		Quadrangle (see Pl. 1)
36	Rhyolite of Mule Creek	G	17.7 ± 0.6	Big Lue Mountains
37	Rhyolite at Coal Creek	W	19.0 ± 0.7	Big Lue Mountains
38	Basalt feeder dike for flow (Entry 39)	W	19.0 ± 1.2	Big Lue Mountains
39	Basalt overlying rhyolite of Mule Creek	W	19.1 ± 1.1	Big Lue Mountains
40	Rhyolite of Hells Hole	Z	26.7 ± 3.5	Mule Creek
41	Rhyodacite dome of Sawmill Creek	B Z	25.4 ± 0.9 19.0 ± 5.0	Mule Creek
42	Rhyolite dike	B Z	25.3 ± 0.9 24.3 ± 3.5	Mule Creek
43	Intrusive andesite at Tillie Hall Canyon	P A	24.5 ± 0.8 16.9 ± 4.3	Mule Creek
44	Rhyolite of Mule Creek	Z	17.7 ± 1.9	Mule Creek
45	Dacite of Mineral Spring Canyon	B Z	26.1 ± 0.9 26.1 ± 3.3	Wilson Mountain
46	Dacite of Mineral Spring Canyon	Z	25.0 ± 2.3	Wilson Mountain
47	Andesite at Wilson Mountain	W	24.7 ± 0.8	Wilson Mountain
48	Rhyolite at The Box	B P Z	19.3 ± 0.7 18.7 ± 0.9 18.9 ± 2.1	Wilson Mountain
49	Rhyolite of Potholes Country	B Z	21.1 ± 0.7 18.9 ± 1.4	Wilson Mountain
50	Rhyolite of Potholes Country	Z	18.4 ± 2.1	Wilson Mountain
51	Basalt beneath rhyolite of Mule Creek	W	18.3 ± 0.7	Wilson Mountain
52	Porphyritic andesite in Burnt Stump Canyon	P	25.6 ± 1.3	Moon Ranch
53	Altered and mineralized rhyolite	Al W	33.8 ± 1.2 32.0 ± 1.7	Holt Mountain
54	Porphyritic dacite flow in Bursum caldera wall	B Z	29.9 ± 1.1 28.5 ± 3.5	Holt Mountain
55	Cooney(?) Tuff or Shelley Peak(?) Tuff	B Z	28.5 ± 1.0 26.7 ± 4.0	Holt Mountain
56	Nabours Mountain Quartz Latite	Sp	28.3 ± 3.9	Holt Mountain
57	Nabours Mountain Quartz Latite	S	28.4 ± 0.8	Holt Mountain
58	Cooney Canyon Member of Cooney Tuff	B	33.1 ± 1.5	Holt Mountain
59	Dacite of Goat Basin volcano	P H Z	28.6 ± 2.0 26.4 ± 1.6 26.5 ± 3.4	Glenwood
60	Rhyolite dike in Goat Basin	P	28.5 ± 1.0	Glenwood
61	Andesite at "Glenwood" Brushy Mountain	W	25.9 ± 0.5	Glenwood
62	Rhyolite dome at "Glenwood" Brushy Mountain	W	23.3 ± 0.8	Glenwood
63	Basalt at Harve Gulch	W	5.6 ± 0.3	Glenwood
64	Whitewater Creek Member of Cooney Tuff	Z	31.8 ± 2.8	Mogollon
65	Cooney Tuff	B	24.3 ± 0.8	Mogollon
66	Cooney Tuff	B	33.7 ± 1.0	Clifton
67	Cooney Tuff	Z	33.1 ± 2.8	Clifton
68	Fall Canyon Tuff	Z	29.4 ± 3.1	Mogollon
69	Shelley Peak Tuff	Z	28.4 ± 2.4	Mogollon
70	Shelley Peak Tuff	B Z	24.4 ± 0.8 23.4 ± 0.8 27.3 ± 2.6	Mogollon
71	Andesite intrusive on upper Devils Creek	H	30.4 ± 1.9	Mogollon
72	Fanney Rhyolite	S	26.9 ± 1.0	Mogollon
73	Mineral Creek Andesite	W	25.7 ± 0.5	Mogollon
74	Lower part of Last Chance Andesite	W	25.0 ± 0.8	Mogollon
75	Upper part of Last Chance Andesite	W	23.2 ± 0.8	Mogollon

TABLE 1 continued

Entry no.	Correlation	Mineral dated and calculated age (m.y.)		Quadrangle (see Pl. 1)
76	Last Chance(?) Andesite	W	17.7 ± 0.3	Mogollon
			17.6 ± 0.3	
77	Intrusive andesite at Silver Creek	B	27.1 ± 0.9	Mogollon
		Z	23.5 ± 2.8	
		A	14.7 ± 2.7	
78	Vein—Last Chance mine	Ad	17.5 ± 0.6	Mogollon
		W	18.5 ± 0.7	
			16.5 ± 0.6	
79	Basalt at Cooney Peak	W	15.2 ± 0.4	Bearwallow Mountain
80	Bearwallow Mountain Andesite	W	23.1 ± 0.8	Bearwallow Mountain
81	Andesite at Negrito Mountain	W	25.6 ± 0.9	Negrito Mountain
82	Rhyolite at Ewe Canyon	G	27.6 ± 1.8	Negrito Mountain
83	Dacite in the porphyritic latite of Willow Creek	B	27.5 ± 0.5	Negrito Mountain
			27.9 ± 0.5	
84	Apache Spring Tuff	B	27.9 ± 0.8	Grouse Mountain
85	Apache Spring Tuff	B	28.1 ± 1.0	Grouse Mountain
		Z	29.3 ± 3.6	
86	Apache Spring Tuff	Sp	29.9 ± 4.6	Grouse Mountain
		Sp	28.5 ± 5.6	
		Sp	30.0 ± 4.8	
		Sp	30.2 ± 4.8	Bearwallow Mountain
87	Quartz-porphyry dike of Fanney Rhyolite age	Sp	26.6 ± 3.7	Rice Ranch
88	Cooney Tuff	P	34 ± 2	Rice Ranch
89	Quartz-porphyry dike, rhyolite of the Diablo Range	B	28.2 ± 1.0	Shelley Peak
		Sp	27.8 ± 2.7	
		S	26.8 ± 0.9	
90	Volcanic complex of Brock Canyon	B	31.7 ± 0.8	Canteen Canyon
91	Volcanic complex of Brock Canyon	B	33.5 ± 0.8	Canteen Canyon
92	Volcanic complex of Brock Canyon	Z	31.0 ± 6.4	Canteen Canyon
93	Volcanic complex of Brock Canyon	Z	31.2 ± 5.5	Canteen Canyon
		Z	27.8 ± 5.3	
94	Dacite intrusive at Holt Gulch	Z	22.7 ± 2.3	Holt Mountain
95	Fall Canyon Tuff	S	15.8 ± 1.0	Canyon Hill
96	Bloodgood Canyon Tuff	Sp	24.9 ± 5.6	Granny Mountain
97	Bloodgood Canyon Tuff	Sp	29.4 ± 4.0	Little Turkey Park
98	Lava flows of Gila Flat	B	30.3 ± 0.7	Copperas Peak
		S	30.0 ± 0.7	
99	Granite dike—volcanic complex of Alum Mountain	F	30.4 ± 0.7	Copperas Peak
100	Basalt at Roberts Lake Dam	W	21.1 ± 0.5	Copperas Peak
101	Granite of North Star Mesa	Z	42.6 ± 5.2	North Star Mesa
		A	42.7 ± 5.3	
102	Bloodgood Canyon Tuff	S	26.0 ± 1.5	Gila Hot Springs
		B	26.9 ± 1.5	
103	Bloodgood Canyon Tuff	S	28.0 ± 1.0	Wall Lake
104	Taylor Creek Rhyolite	S	27.7 ± 0.9	Wall Lake
105	Taylor Creek Rhyolite	S	24.6 ± 0.5	Spring Canyon
106	Tuff of Slash Ranch	S	22.2 ± 0.7	Black Mountain
107	Rhyolite at Canyon Creek	B	27.7 ± 2.0	Loco Mountain
		W	24.8 ± 2.0	
108	Bloodgood Canyon Tuff	S	27.7 ± 0.9	Indian Peaks West
		Z	26.0 ± 2.7	
109	Bloodgood Canyon Tuff	S	23.4 ± 0.7	Indian Peaks West
110	Andesite at Pelona Mountain	W	26.6 ± 1.0	Pelona Mountain
111	Andesite at O Bar O Mountain	W	25.7 ± 0.9	O Bar O Canyon West
112*	Rhyolite of Shaw Canyon	S	28.7 ± 1.5	Shaw Mountain
			28.3 ± 1.5	
		S	29.7 ± 1.5	

(*continued on page 10*)

TABLE 1 continued

Entry no.	Correlation	Mineral dated and calculated age (m.y.)		Quadrangle (see Pl. 1)
113	Davis Canyon(?) Tuff	S Z	29.2 ± 1.0 27.3 ± 3.1	Shaw Mountain
114	Rhyolite at Horse Mountain	P Z H	12.0 ± 3.0 10.4 ± 1.3 35.3 ± 6.1	Horse Mountain East
115	Blue Canyon Tuff	S S	33.3 ± 1.0 32.7 ± 4.6	Horse Mountain West
116	Datil Well Tuff	S	36.7 ± 1.3	Horse Mountain West
117	Datil Well(?) Tuff	B	35.4 ± 2.0	Horse Mountain West
118	Tuff breccia of Horse Springs Canyon(?)	B P	35.5 ± 2.2 33.9 ± 1.2	Bell Peak
119	Clast in tuff breccia of Horse Springs Canyon	Z	32.4 ± 3.4	Bell Peak
120	Rhyolite of Wye Hill	Z	30.3 ± 6.1	Bell Peak
121	Rhyolite of Wye Hill	S	27.3 ± 0.6	Bell Peak
122	Rhyolite of Wye Hill	S	32.2 ± 2.0	Bell Peak
123*	Tuff breccia of Horse Springs Canyon(?)	B B	36.2 ± 2.0 32.2 ± 1.0 31.2 ± 1.0	Bell Peak
124	Shelley Peak Tuff	F B	31.7 ± 1.5 27.4 ± 1.3	Bell Peak
125	Bloodgood Canyon Tuff	B S	28.8 ± 1.0 28.2 ± 1.0	Tularosa Canyon
126	John Kerr Peak Quartz Latite	Sp Sp A Z Z	22.7 ± 4.8 20.6 ± 4.8 22.7 ± 5.2 21.4 ± 2.2 19.9 ± 2.2	John Kerr Peak
127	John Kerr Peak Quartz Latite	B Z	13.6 ± 0.5 12.0 ± 1.6	John Kerr Peak
128*	Andesite along Cox Canyon Road	W	20.4 ± 1.5	Collins Park
129*	Rhyolite in Y Canyon	S	26.2 ± 1.2	Collins Park
130*	Bloodgood Canyon Tuff	S B	26.4 ± 1.5 27.3 ± 1.5	Salvation Peak
131	Shelley Peak Tuff	B	28.7 ± 1.0 25.7 ± 1.7	Squirrel Springs Canyon
132*	Basalt at Apache Creek	W	0.9 ± 0.2	Squirrel Springs Canyon
133	Basalt at Apache Creek	W	1.0 ± 0.1	Squirrel Springs Canyon
134	Older basalt at Apache Creek	P	13.7 ± 1.4	Squirrel Springs Canyon
135	Tuff of Luna	S B Z	31.9 ± 0.7 36.5 ± 1.3 32.5 ± 3.4	Luna
136	Tuff of Luna	S B Z	31.8 ± 0.7 35.3 ± 1.3 39.5 ± 4.0	Centerfire Bog
137	Basalt at Luna	W	2.65 ± 0.10	Luna
138	Tuff of Bishop Peak	B S	37.1 ± 1.3 34.3 ± 1.2	Underwood Lake
139	Tuff lens in early andesite sequence	S Z	34.0 ± 1.2 32.8 ± 3.5	Bull Basin
140	Quartz-diorite intrusive at Wet Leggett Spring	B H Z	17.7 ± 0.6 13.9 ± 0.7 11.9 ± 1.4	Bull Basin
141	Rhyolite east of Maverick Peak	S	14.0 ± 0.5	Bull Basin
142	Tuff lens in early andesite sequence	S B Z	32.4 ± 1.1 29.7 ± 1.0 28.2 ± 1.0 32.3 ± 2.4	Saliz Pass
143	Tuff lens in early andesite sequence	S B	30.2 ± 2.0 31.8 ± 2.0 26.7 ± 2.0 24.4 ± 2.0	Saliz Pass

TABLE 1 continued

Entry no.	Correlation	Mineral dated and calculated age (m.y.)		Quadrangle (see Pl. 1)
144	Davis Canyon Tuff	B	30.7 ± 1.0	Saliz Pass
		S	28.9 ± 1.0	
145	Shelley Peak Tuff	B	30.5 ± 1.5	Saliz Pass
146	Shelley Peak Tuff	B	29.1 ± 1.0	Saliz Pass
		S	28.1 ± 1.0	
		Z	28.5 ± 2.4	
147	Bloodgood Canyon Tuff	S	28.2 ± 1.0	Saliz Pass
			28.0 ± 1.0	
			25.9 ± 0.9	
		S	27.6 ± 0.9	
		Z	27.4 ± 3.4	
148	Vitrophyre from early andesite complex	B	33.6 ± 1.1	Saliz Pass
149	Basalt of Saliz Hill	W	12.2 ± 0.5	Saliz Pass
150	Basalt of Pueblo Park	P	19.2 ± 2.7	Saliz Pass
151	Rhyolite at Frying Pan Creek	Z	26.6 ± 4.2	O Block Canyon
		W	30.5 ± 1.0	
152	Tuff lens in andesite sequence near Devils Park	Z	26.2 ± 2.4	O Block Canyon
		S	67.0 ± 2.3	
153	Bloodgood Canyon Tuff	S	24.3 ± 1.5	Reserve
			27.3 ± 0.9	
154	Shelley Peak Tuff	G	28.9 ± 1.8	Reserve
155	Bloodgood Canyon Tuff	S	23.7 ± 0.7	Milligan Mountain
156	Bloodgood Canyon Tuff	B	28.0 ± 1.0	Milligan Mountain
		S	27.1 ± 0.9	
		Z	28.9 ± 3.0	
157	Bloodgood Canyon Tuff	S	26.6 ± 0.9	Milligan Mountain
			26.9 ± 0.9	
		S	27.8 ± 0.9	
		Sp	27.9 ± 4.0	
		S	27.4 ± 0.9	
			28.0 ± 1.0	
		Z	27.3 ± 2.8	
		Sp	30.4 ± 5.0	
158	Davis Canyon(?) Tuff	B	29.7 ± 1.5	Milligan Mountain
		F	27.1 ± 2.0	
159	Davis Canyon(?) Tuff	Sp	31.6 ± 2.0	Eagle Peak
160	Squirrel Springs Canyon Andesite	P	24.3 ± 1.5	Eagle Peak
161	Bloodgood Canyon Tuff	S	26.1 ± 0.9	Eagle Peak
			27.3 ± 1.5	
162	Deadwood Gulch Member, Fanney Rhyolite	S	24.4 ± 1.5	Grouse Mountain
163	Vicks Peak(?) Tuff	S	27.2 ± 0.9	Sugarloaf Mountain[1]
		Z	22.9 ± 2.1	
164	Porphyritic intrusive at Cerrito Viejo	Z	21.4 ± 2.3	Sugarloaf Mountain[1]
		B	30.2 ± 1.1	
165	Hells Mesa Tuff	B	$^{40}Ar/^{39}Ar$ 32.11 ± 0.19	Sugarloaf Mountain[1]
			33.2 ± 1.1	
			33.0 ± 1.1	
		S	30.9 ± 1.1	
		Z	31.4 ± 2.6	
166	Hells Mesa Tuff	B	$^{40}Ar/^{39}Ar$ 32.09 ± 0.10	Sugarloaf Mountain[1]
			32.3 ± 1.5	
		S	$^{40}Ar/^{39}Ar$ 31.87 ± 0.07	
			28.6 ± 1.0	
		P	31.1 ± 1.9	
		Z	29.3 ± 3.0	
167	Rock House Canyon Tuff	Z	28.3 ± 3.3	Datil[1]
168	Datil Well Tuff	S	35.6 ± 1.3	Datil[1]
169	La Jencia(?) Tuff	S	27.0 ± 1.0	Dusty[1]
		Z	16.8 ± 3.2	
170	Basalt at Mimbres Valley	W	6.47 ± 0.41	San Lorenzo[1]
171	Fall Canyon(?) Tuff	B	34.7 ± 1.2	Circle Mesa[1]
		Z	30.8 ± 3.4	

(*continued on page 12*)

TABLE 1 continued

Entry no.	Correlation		Mineral dated and calculated age (m.y.)	Quadrangle (see Pl. 1)
172	Fall Canyon(?) Tuff	B	$^{40}Ar/^{39}Ar$ 32.42 ± 0.14	Steeple Rock[1]
			32.5 ± 1.2	
		S	29.2 ± 1.1	
173	Bloodgood Canyon Tuff	Z	30.0 ± 1.7 (average of 15 ages)	Steeple Rock[1]
174	Andesite at "Radar" Brushy Mountain	W	23.7 ± 0.5	Steeple Rock[1]
		W	25.6 ± 0.5	
175	Alunitic rhyolite	Al	31.3 ± 1.1	York Valley[1]
176	Bloodgood Canyon Tuff	B	30.0 ± 1.0	Twin Sisters[1]
			30.5 ± 1.0	
		S	26.4 ± 0.9	
177	Tadpole Ridge Quartz Latite	B	31.9 ± 1.0	Twin Sisters[1]
178	Tadpole Ridge Quartz Latite	B	31.7 ± 1.0	Twin Sisters[1]
179	Kneeling Nun(?) Tuff	B	$^{40}Ar/^{39}Ar$ 35.88 ± 0.11	Reading Mountain[1]
			35.1 ± 0.8	
		S	32.7 ± 0.8	
		Z	34.6 ± 4.0	
180	Porphyritic rhyolite intrusive at Dry Gallinas Campground	B	35.7 ± 1.2	San Lorenzo[1]
		S	33.3 ± 1.2	
			34.7 ± 1.2	
181	Kneeling Nun(?) Tuff	B	$^{40}Ar/^{39}Ar$ 34.13 ± 0.11	C Bar Ranch[1]
			34.6 ± 0.8	
182	Bloodgood Canyon Tuff	S	27.1 ± 1.2	Cliff[1]
			27.0 ± 0.8	
183	Andesite of Dry Leggett Canyon(?)	W	29.6 ± 1.4	Queens Head
184	Tadpole Ridge Quartz Latite	B	31.9 ± 1.0	Twin Sisters[1]
185	Hells Mesa Tuff	S	32.1 ± 0.7	Sugarloaf Mountain[1]
186	Tuff breccia of Horse Springs Canyon	Z	32.7 ± 3.8	Wallace Mesa[1]
187	Vicks Peak(?) Tuff	Z	31.3 ± 5.0	Sugarloaf Mountain[1]
188	Tularosa Canyon(?) Rhyolite Tuff	Z	30.5 ± 3.8	Alegres Mountain[1]
189	Blue Canyon Tuff	Z	33.2 ± 3.2	Log Canyon[1]
190	Datil Well Tuff	S	35.6 ± 0.7	Datil[1]
		Z	37.7 ± 3.8	
191	Kneeling Nun Tuff	B	34.2 ± 1.0	Santa Rita[1]
192	Andesite at Black Mountain	W?	23.9	Black Mountain
193	Bloodgood Canyon Tuff	Z	25.7 ± 2.1	York Valley[1]
194	Bloodgood Canyon Tuff	Z	24.0 ± 2.3	Big Lue Mountains
195	Dacite of Tennessee Creek	P	21.3 ± 1.8	Big Lue Mountains
196	Dacite in Seep Spring Canyon	W	24.2 ± 0.9	Big Lue Mountains
197	Dacite in Limestone Gulch	H	27.2 ± 1.0	Big Lue Mountains
		P	20.1 ± 1.1	
198	Basalt in Dix Creek	W	17.7 ± 0.6	Big Lue Mountains
199	Amygdaloidal andesite in Buzzard Roost Canyon	W	27.5 ± 1.0	Big Lue Mountains
200	Basalt in Saliz Canyon	W	15.4 ± 0.6	Bull Basin
201	Rhyolite of Hells Hole(?)	H	29.5 ± 0.9	Big Lue Mountains
202	Andesite in Keller Canyon	W	25.2 ± 0.9	Alma Mesa
203	Rhyolite of Enebro Mountain	W	20.9 ± 0.8	Clifton
			20.6 ± 0.7	
204	Dacite at Eagle Peak	W	8.6 ± 0.3	Eagle Peak
			9.9 ± 0.4	
			10.0 ± 0.4	
205	Rhyolite dike near Haystack Mountain	F	23.1 ± 1.0	Rice Ranch
206	Vitric ash in Gila Conglomerate	Z	2.01 ± 0.97	Canteen Canyon
207	Andesite at Saddle Mountain	P	33.3 ± 1.2	Blue
208	Rhyolite at Sheridan Mountain	P	25.9 ± 0.9	Moon Ranch
209	Rhyolite of the Mogollon Mountains	S	28.2 ± 1.0	Shelley Peak
210	Rhyolite of the Diablo Range	S	27.7 ± 1.5	Diablo Range
211	Rhyodacite of the Big Lue Mountains	B	28.1 ± 1.0	Big Lue Mountains
		P	24.1 ± 1.3	
212	Rhyolite of Bat Cave Wells	F	27.4 ± 1.0	Fullerton

under the same entry number if the samples are from essentially the same outcrop or represent a vertical sequence of the same stratigraphic unit.

Analytical data are presented for all except a very few samples, for which such data were not available. If potassium content was represented by percent K in previously published sources, we have made the conversion to percent K_20, and likewise with other parameters where necessary to make the presentation of analytical data as consistent as possible. All K-Ar ages have been recalculated using the decay constants and isotopic abundances of Steiger and Jager (1977). The quoted analytical uncertainty for all new ages for U.S. Geological Survey samples and for Bikerman's samples (University of Pittsburgh) is 2 standard deviations (± 2 sigma). The level of uncertainty for other ages may be determined from the cited reference, as, for instance, Bornhorst et al. (1982), where the level of uncertainty is given as one standard deviation (1 sigma). For some ages, such as those from Strangway et al. (1976), the level of uncertainty is not known. Most fission-track ages have been recalculated using presently accepted constants, and analytical uncertainty is listed as ± 2 sigma.

Rubidium-strontium data for these volcanic rocks are quite sparse. At present, analytical data are reported for seven samples.

Under the subheading *Comment,* we mainly explain analytical problems that may affect the interpretation of the ages and differences in stratigraphic correlation between different workers. Some of the previously published ages will not agree exactly with the ages for the same samples cited in this compilation because we have attempted to update revised or incorrect data. Some ages previously reported as recalculated ages in Ratté et al. (1984, tables 3 and 6) inadvertently were not recalculated as stated, but they have been recalculated for this compilation, as in Entries 176, 177, 181, and 182.

Most of the dated samples in the compilation are from rocks in the eastern two-thirds of the Clifton 1° x 2° quadrangle. They represent volcanic activity that preceded, accompanied, and followed the development of a major Oligocene caldera complex in the Mogollon Mountains volcanic source region (Ratté et al., 1984; Elston and Northrop, 1976; Chapin and Elston, 1978). The western one-third of the Clifton 1° x 2° quadrangle consists largely of lands that are part of the Fort Apache and San Carlos Indian Reservations, for which detailed geologic studies are largely unavailable. However, a few ages for rocks in the Baldy Peak area—White Mountains volcanic center—in the northwestern part of the Clifton quadrangle (Merrill, 1974; Finnell et al., 1967) and for rocks in the Point of Pines and Bryce Mountain areas in the southwestern part of the quadrangle (Bromfield et al., 1972; Strangway et al., 1976) have been included in the compilation for completeness.

Discussion

Conventional K-Ar and fission-track dating of suitable minerals has been generally useful in fitting the volcanic sequences in the western and central parts of the Mogollon-Datil volcanic field into an absolute time frame. However, these dating methods are of more limited use in establishing the sequence of closely spaced eruptive events in late Oligocene and early Miocene time when most of the volcanic activity occurred. Undue reliance on isotopic dating, particularly on single-mineral ages, in establishing volcanic sequences during past reconnaissance studies has caused considerable confusion in the correlation of volcanic units and timing of eruptive events upon which structural and petrogenetic interpretations must be based.

In this section of the report, we will consider some of the analytical problems in dating the eruptive history of a complex volcanic pile where closely spaced eruptions and intrusions commonly proceeded concurrently at different eruptive centers. In the absence of suitable regional volcanic stratigraphic marker units or the intertonguing of flows and pyroclastics from adjacent volcanic centers, isotopic dating may become critical, and the method with the greatest resolution for the time span involved must be applied. Where Oligocene and early Miocene events are separated by 1-2 m. y. or less, conventional K-Ar and fission-track ages are generally ineffective, but the $^{40}Ar/^{39}Ar$ method holds great promise for providing the necessary resolution.

A few $^{40}Ar/^{39}Ar$ ages for samples previously dated by conventional K-Ar and fission-track methods have been made available by John F. Sutter (USGS, Reston, Va.), Entries 172, 179, and 181, and Laura L. Kedzie, Entries 165 and 166 (Kedzie, 1984). In addition, Table 2 presents the results of preliminary $^{40}Ar/^{39}Ar$ dating of several major ash-flow tuffs of the Mogollon-Datil volcanic field (McIntosh et al., 1986, table 1) for comparison with the conventional K-Ar and fission-track ages compiled here.

Fission-track ages have the additional capability of providing information on the cooling history of a rock through low-temperature annealing of fission tracks

TABLE 2—$^{40}Ar/^{39}Ar$ ages of some major ash-flow tuffs of the Mogollon–Datil volcanic field (McIntosh et al., 1986)

Name of tuff	$^{40}Ar/^{39}Ar$ age (m.y.)
Bloodgood Canyon Tuff	28.36
Shelley Peak Tuff	28.52
Vicks Peak Tuff	28.46
La Jencia Tuff	28.78
Davis Canyon Tuff	29.03
Hells Mesa Tuff	32.04
Blue Canyon Tuff	33.93
Tadpole Ridge Quartz Latite	35.14*
Kneeling Nun Tuff	35.28
Datil Well Tuff	35.51

*New correlations of tuffs mapped in the North Star Mesa quadrangle (Aldrich, 1976) show that Tadpole Ridge Quartz Latite is younger than 31.9-m.y. Caballo Blanco Tuff (McIntosh, pers. comm. 1987), and therefore the conventional biotite K-Ar ages in Entries 177 and 178 are more accurate than the $^{40}Ar/^{39}Ar$ age reported in this table.

and recognition of post-emplacement thermal events (Naeser, 1976; 1979). Thus, discordant K—Ar and fission-track ages may not only be clues to post-depositional thermal events, such as an intrusive episode, but, in a mining district, may allow mapping of thermal anomalies related to blind intrusives that could be important in mineral exploration (Naeser et al., 1980). As a possible case in point, in the Mogollon mining district, intrusive andesite (Entry 77) east of the mineralized Queen fault has a biotite K—Ar age of 27.1 m.y.; thus, it appears to be related to the Bearwallow Mountain Andesite. However, fission-track ages (zircon = 23.5 m.y. and apatite = 14.7 m.y.) suggest a partial annealing of fission tracks in the zircon and probably complete annealing of apatite at a later time, possibly coincident with the mineralization in the Mogollon district, presently indicated as about 17 m.y. ago from K—Ar dating of vein adularia (Entry 78). Additional fission-track dating might define a thermal anomaly that would be useful in further mineral exploration in the district.

Comparative age data for Bloodgood Canyon and Apache Spring Tuffs

The Bloodgood Canyon and Apache Spring Tuffs are major caldera-forming ash-flow tuffs whose volumes each exceed 1,000 km^3. They are virtually indistinguishable in age by standard isotopic methods (Table 3), but geologic relationships show that the Bloodgood Canyon Tuff is older than the Apache Spring Tuff. Both tuffs are believed to represent a compositionally zoned sequence that was erupted from a high-level magma chamber beneath the Bursum caldera (Ratté et al., 1984).

Fifty-eight separate K—Ar and fission-track age determinations on biotite, sanidine, zircon, and sphene from Bloodgood Canyon Tuff (51 ages) and Apache Spring Tuff (seven ages) are listed in Table 3. The large number of Bloodgood Canyon Tuff ages was generated by correlation problems resulting from the nearly 10 m.y. spread in ages (Fig. 2) obtained from widespread outcrops of the outflow sheet of the tuff (Ratté et al., 1984). The ages obtained by different techniques or on different minerals range beyond stated analytical uncertainty. The differences in the K—Ar ages can be examined either as (1) the discordancy of ages between coexisting biotite and sanidine or (2) the discordancy of ages amongst all biotites, all sanidines, all whole-rocks, etc., from different outcrops of the same volcanic formation. In the first case, the discordancy is now considered to be mainly an analytical one, probably related to the incomplete extraction of argon from alkali feldspars (McDowell, 1983). Of seven Bloodgood Canyon Tuff samples for which biotitesanidine pairs were dated, six of the biotite ages are older than the corresponding sanidine ages by amounts ranging from 0.6 to 3.3 m.y. (2-12%); in the remaining sample, the biotite—sanidine ages were the same. Similarly, within this entire compilation of isotopic ages in the Clifton 1° x 2° quadrangle and vicinity, biotite ages are older for 15 out of 19 biotite—feldspar pairs; for one sample, the biotite age is older than the cor-

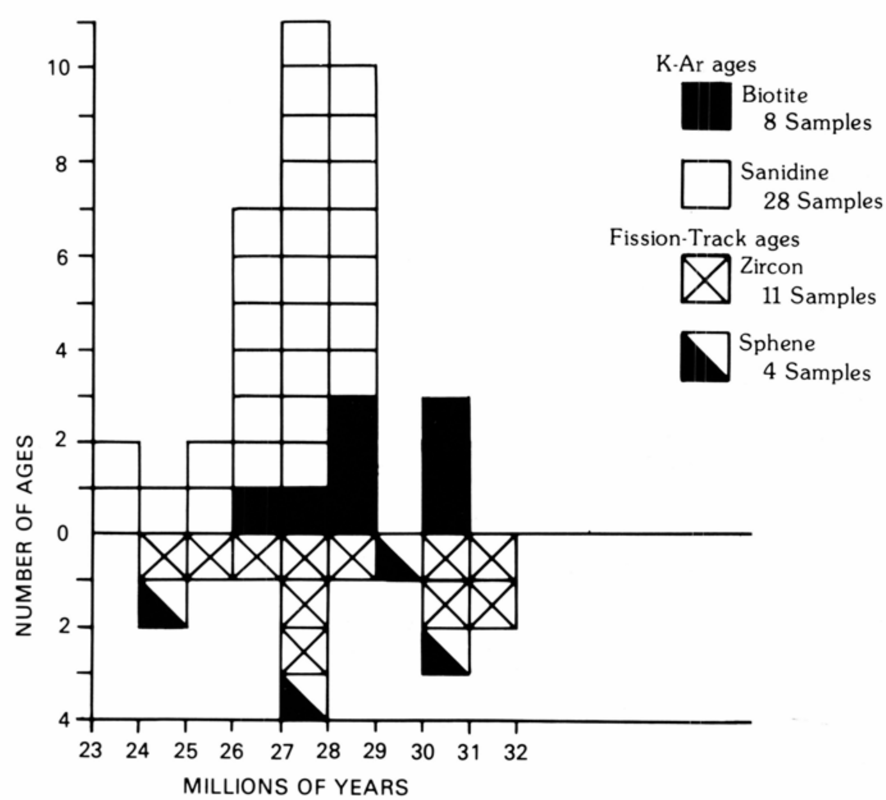

FIGURE 2—Histogram of Bloodgood Canyon Tuff ages.

TABLE 3—Ages of Bloodgood Canyon and Apache Spring Tuffs. Quadrangle name followed by [1] indicates that sample was collected outside of Clifton 1° × 2° quadrangle; see Fig. 1. [2] Eliminating sanidine ages younger than 25 m.y. results in an average of 27.2 ± 0.8 m.y.

Entry no.	K–Ar ages (m.y.) Biotite	Sanidine	Fission-track ages (m.y.) Zircon	Sphene	Quadrangle (see Pl. 1)
		Bloodgood Canyon Tuff			
147a		28.2 ± 1.0 28.0 ± 1.0 25.9 ± 0.9			Saliz Pass
147b			27.4 ± 3.4		Saliz Pass
147c		27.6 ± 0.9			Saliz Pass
9	28.3 ± 1.0	28.3 ± 1.0 28.6 ± 1.0			Blue
8		25.5 ± 0.7			Blue
153		24.3 ± 1.5 27.3 ± 0.9			Reserve
155		23.7 ± 0.7			Milligan Mountain
156	28.0 ± 1.0	27.1 ± 0.9	28.9 ± 3.0		Milligan Mountain
157a		26.6 ± 0.9 26.9 ± 0.9			Milligan Mountain
157b		27.8 ± 0.9		27.9 ± 4.0	Milligan Mountain
157c		27.4 ± 0.9 28.0 ± 1.0	27.3 ± 2.8	30.4 ± 5.0	Milligan Mountain
161		27.3 ± 1.5 26.1 ± 0.9			Eagle Peak
130	27.3 ± 1.5	26.4 ± 1.5			Salvation Peak
125	28.8 ± 1.0	28.2 ± 1.0			Tularosa Canyon
108		27.7 ± 0.9	26.0 ± 2.7		Indian Peaks West
109		23.4 ± 0.7			Indian Peaks West
102	26.9 ± 1.5	26.0 ± 1.5			Gila Hot Springs
97				29.4 ± 4.0	Little Turkey Park
96				24.9 ± 5.6	Granny Mountain
10	30.6 ± 1.0	27.3 ± 1.3			Blue
173			30.3 ± 1.9 31.0 ± 2.1 27.4 ± 1.2 30.0 ± 1.4 31.0 ± 1.5		Steeple Rock[1]
176	30.0 ± 1.0 30.5 ± 1.0	26.4 ± 0.9			Twin Sisters[1]
193			25.7 ± 2.1		York Valley[1]
194			24.0 ± 2.3		Big Lue Mountains
182		27.1 ± 1.2 27.0 ± 0.8			Cliff[1]
103		28.0 ± 1.0			Wall Lake
Averages	28.8 ± 1.3 (s.d.)	26.9 ± 1.3 (s.d.)[2]	28.1 ± 2.2 (s.d.)	28.2 ± 2.1 (s.d.)	
		Apache Spring Tuff			
84	27.9 ± 0.8				Grouse Mountain
85	28.1 ± 1.0		29.3 ± 3.6		Grouse Mountain
86a				29.9 ± 4.6	Grouse Mountain
86b				28.5 ± 5.6	Grouse Mountain
86c				30.0 ± 4.8	Grouse Mountain
86d				30.2 ± 4.8	Bearwallow Mountain
Averages	28.0 ± 0.1 (s.d.)		29.3	29.6 ± 0.7 (s.d.)	

responding whole-rock age by 5% . Since the general recognition of this problem in the late 1970's, argon extraction from the sanidines in Bloodgood Canyon Tuff has generally improved, and the later sanidine K-Ar ages are in better agreement with the biotite KAr ages. The three sanidines that gave ages less than 24.5 m.y. (Entries 109, 153, and 155) have been re-dated using the same sample (Entry 153) or different samples from the same outcrops (Entries 108 and 156); the second ages are all between 27.3 and 28.0 m.y.

Zircon and sphene fission-track ages for Bloodgood Canyon and Apache Spring Tuffs (Fig. 2) show a spread (24.0-31.0 m.y.) comparable to the K-Ar ages (23.430.5 m.y.). Although sphene ages have a relatively large analytical uncertainty because of the very low uranium content of the sphene, five of eight sphene samples give ages ranging between 29.4 and 30.4 m.y. for both tuffs.

From the data in Table 3, it seems reasonable to conclude that the age of the Bloodgood Canyon and Apache Spring Tuffs is about 28-29 m.y. It also seems clear that single-mineral ages on Bloodgood Canyon Tuff, which is the most widespread volcanic stratigraphic marker in the western Mogollon-Datil volcanic field, have been quite misleading. Thus, rocks that previously have been described as Railroad Canyon Tuff (Elston and Damon, 1970; Elston et al., 1973) and thought to be about 23 m.y. old, actually are Bloodgood Canyon Tuff (Ratté et al., 1984). This assignment removes the need for a separate Railroad Canyon source such as the Corduroy Canyon depression of Elston (1984, table 1, no. 27). The name Railroad Canyon was abandoned by Lawrence and Richter (1986) in favor of Bloodgood Canyon.

Volcano-stratigraphic correlations

Despite some fairly concentrated efforts in geologic mapping in the Mogollon-Datil volcanic field during the past 20 yrs by several groups, mainly from the University of New Mexico, New Mexico Institute of Mining and Technology, and the U.S. Geological Survey, an integrated volcanic stratigraphy for the major parts of the field only now is beginning to take form. A large step in this direction is the publication of Stratigraphic Chart 1 by the New Mexico Bureau of Mines and Mineral Resources (Osburn and Chapin, 1983) and the initial results of combined paleomagnetic studies and $^{40}Ar/^{39}Ar$ dating (McIntosh et al., 1986).

The distribution and correlation of some of the major ash-flow sheets in the Mogollon-Datil volcanic field are shown in Fig. 3. The principal eruptive centers represented by the tuffs shown in Fig. 3 are:

1) Socorro-Magdalena-San Mateo Mountains caldera cluster in the northeastern part of the Mogollon-Datil volcanic field, outside of the Clifton 1° x 2° quadrangle. Some of the associated tuffs include Tuff of Turkey Springs, South Canyon Tuff, Lemitar Tuff, Vicks Peak Tuff, La Jencia Tuff, and Hells Mesa Tuff and correlatives—Fall Canyon Tuff (in part?) and tuff of Luna.

2) Mogollon Mountains caldera cluster in the central and western parts of the MogollonDatil volcanic field. The associated tuffs include Bloodgood Canyon Tuff, Apache Spring Tuff (not shown in Fig. 3 because it occurs only

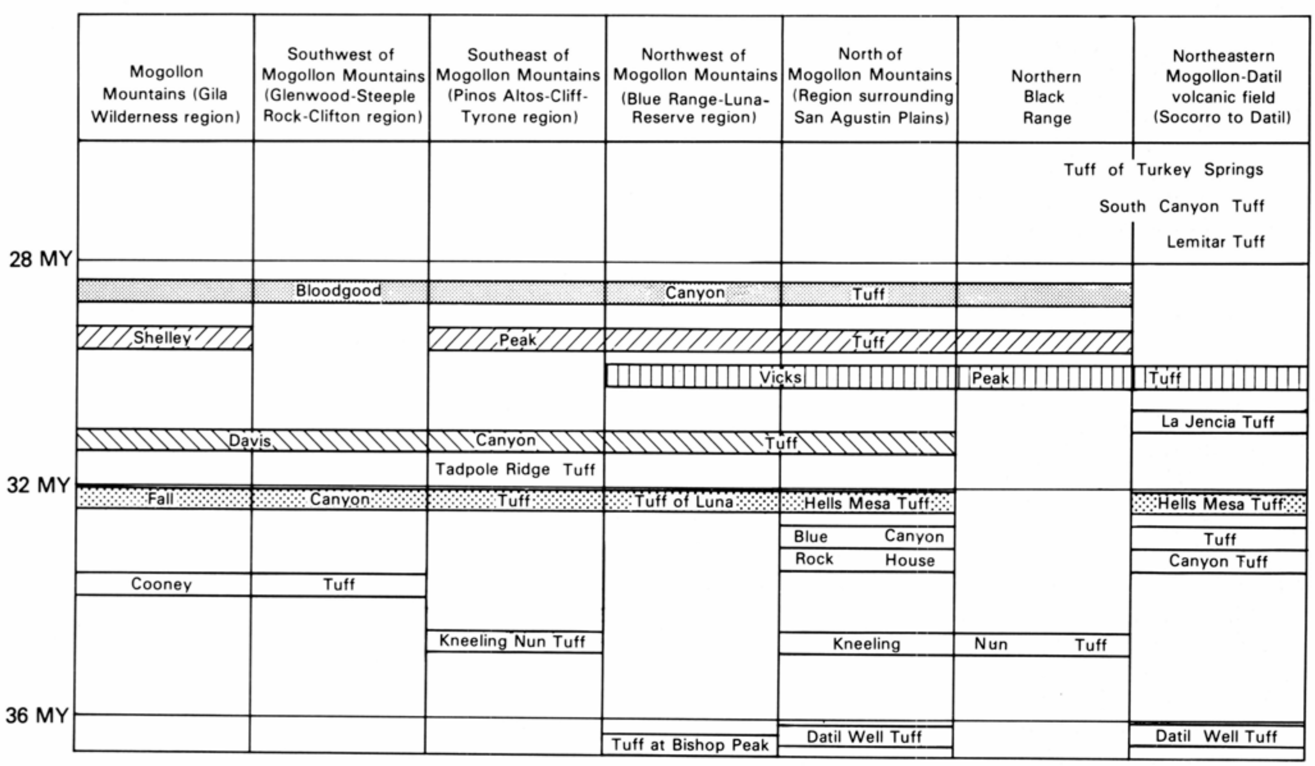

FIGURE 3—Distribution and correlation of some major ash-flow tuffs of the Mogollon Mountains and the northeastern part of the Mogollon–Datil volcanic field. Some of the correlations are based on the $^{40}Ar/^{39}Ar$ ages and paleomagnetic data of McIntosh et al. (1986).

within the Bursum caldera), Shelley Peak Tuff, Davis Canyon Tuff, and Cooney Tuff.

3) Emory cauldron center in the southern Black Range, east of the Clifton 1° x 2° quadrangle. Two of the associated tuffs are Kneeling Nun Tuff and Fall Canyon Tuff (in part?).

4) Pinos Altos—Cliff—Tyrone region mainly in the northeastern part of the Silver City 1° x 2° quadrangle (Drewes et al., 1985), south of the Clifton 1° x 2° quadrangle (Fig. 1). The Tadpole Ridge Quartz Latite Tuff (Fig. 3) is only one of several tuffs in a major eruptive sequence that represents a caldera cluster in this region (Wahl, 1980; Ratté, unpubl. reconnaissance 1985-1986).

The 28-29 m.y. old Bloodgood Canyon Tuff, which is distributed over an area of approximately 15,000 km^2 (Ratté et al., 1984, fig. 6), is the most widespread volcano-stratigraphic marker presently known in this field. Throughout much of its outcrop area, Bloodgood Canyon Tuff occurs with the underlying Shelley Peak and Davis Canyon Tuffs. Where the phenocryst-rich, brick-red Shelley Peak Tuff is sandwiched between white to gray Bloodgood Canyon and Davis Canyon Tuffs, they make a distinctive stratigraphic triplet, which provides even more convincing volcano-stratigraphic control than Bloodgood Canyon Tuff alone. However, in the critical areas where tuffs from different centers in the Mogollon, Black Range, and Socorro source areas interfinger, look-alike tuffs of very similar age, petrographic character, and stratigraphic position can be only tentatively distinguished at this time. In the northeastern part of the Clifton quadrangle, all possible criteria must be utilized to separate 28-29 m.y. old, crystal-poor tuffs, such as Davis Canyon, Vicks Peak, and La Jencia Tuffs.

Similarly, several phenocryst-rich tuffs have proven to be very difficult or impossible to distinguish by field criteria alone. The Kneeling Nun and Hells Mesa Tuffs are 3-4 m.y. different in age (Table 2) but are so similar petrographically that where stratigraphic control is inadequate and precise dating and paleomagnetic data are lacking, they have often been miscorrelated or given local names where correlation is uncertain. Fall Canyon Tuff and tuff of Luna could be correlated by lithology with either Kneeling Nun or Hells Mesa Tuffs. However, preliminary paleomagnetic analysis of the tuff of Luna suggests that it correlates with Hells Mesa Tuff (McIntosh, pers. comm. 1986), which is compatible with conventional K—Ar sanidine ages reported here for tuff of Luna (Entries 135 and 136) but incompatible with K—Ar biotite ages for the same samples.

Correlation of Fall Canyon Tuff with either Kneeling Nun or Hells Mesa Tuffs from present data is more complicated. It may be that in some places Fall Canyon Tuff is Kneeling Nun, and in other places it is Hells Mesa. When Ratté et al. (1984) suggested that Fall Canyon Tuff in the Mogollon Mountains might correlate with Kneeling Nun Tuff, the accepted age of Kneeling Nun Tuff was about 34 m.y. (Entry 191). Since then, new $^{40}Ar/^{39}Ar$ ages indicate that its age is greater than 35 m.y. (Entries 179, 180, and 181). Also, new ages of about 32 m.y. for Fall Canyon Tuff (Entry 172) suggest a correlation of Fall Canyon Tuff in the Steeple Rock quadrangle (Fig. 1) with the Hells Mesa Tuff. However, correlation of Fall Canyon Tuff with Hells Mesa Tuff throughout the Mogollon—Datil volcanic field creates a source problem. If Hells Mesa Tuff originated in the Socorro caldera, as is generally accepted (Osburn and Chapin, 1983), correlation with Fall Canyon Tuff in the Mogollon Mountains and Steeple Rock regions would require a highly asymmetric distribution of Hells Mesa Tuff, with a lobe extending 200 km or more southwestward from the assumed source cauldron at Socorro. Correlation of the tuff of Luna and Hells Mesa Tuff is seemingly less problematic, but correlation of all three tuffs would require the source to be close to the geographic center of distribution.

Other lithologically similar phenocryst-rich tuffs that commonly are difficult to distinguish in the field are Bloodgood Canyon and South Canyon Tuffs and the tuff of Turkey Springs. Precision $^{40}Ar/^{39}Ar$ dating and paleomagnetic analysis have been critical in separating these units in the northern Black Range, east of the northeastern part of the Clifton 1° x 2° quadrangle, where tuffs from the various eruptive source areas do not conform to the familiar stratigraphic context found in the source areas (McIntosh et al., 1986).

It is probably most difficult to identify the very thin to discontinuous distal edges of ash-flow tuff outflow sheets, where the tuffs are least likely to be in a recognizable stratigraphic context. A number of such thin, discontinuous tuffs (including Entries 139, 142, and 143) are interlayered with the andesitic lava flows, mudflow breccias, and volcaniclastic sedimentary rocks that unconformably underlie Davis Canyon Tuff in the Saliz Pass, Reserve, and Bull Basin quadrangles (Pl. 1). These andesitic rocks of the Pueblo Creek Formation (Ratté, 1986) and interlayered tuffs are largely correlative with the Spears Formation and Datil Group of Osburn and Chapin (1983). Thus some of the thin interlayered tuffs may correlate with the tuffs of the Datil Group, which include the Blue Canyon, Rock House Canyon, and Datil Well Tuffs.

Flow-banded rhyolites of the central and western parts of the Mogollon—Datil volcanic field

The so-called flow-banded rhyolites are designated thus to distinguish extensive tracts of intrusive—extrusive rhyolite flows, domes, and subvolcanic intrusives from the rhyolite ash-flow tuff sheets of similar age and composition, which blanket much of the region. From the Black Range to the Mogollon Mountains and south toward Steeple Rock and the Big Lue Mountains, the flow-banded rhyolites cover on the order of 1,000 km', i.e. about 10% of the approximately 10,000 km^2 in the central and western parts of the Mogollon—Datil volcanic field. From surface exposures they appear to have a volume of at least 300 km^3 and perhaps much more. The rhyolites range in composition from rhyodacite to high-silica rhyolite and have been mapped and described under many

TABLE 4—Ages of flow-banded rhyolites in the western and central Mogollon–Datil volcanic field. Letter(s) indicates mineral or material dated: B, biotite; H, hornblende; P, plagioclase; S, sanidine; W, whole-rock; G, whole-rock glass; Z, zircon; Sp, sphene. [1] Rhyolite dike in Goat Basin included with rhyolite of Hells Hole, dikes (dH) in Fig. 4A.

Entry no.	Correlation	Mineral dated and calculated age (m.y.)		Quadrangle (see Pl. 1)
18	Rhyolite of Hells Hole	P	28.4 ± 1.0	Big Lue Mountains
19	Rhyolite of Hells Hole	B P	27.1 ± 1.0 32.9 ± 1.2	Big Lue Mountains
20	Rhyolite of Hells Hole	Z	28.7 ± 3.7	Big Lue Mountains
21	Rhyolite of Hells Hole; dike at Chalk Peak	B Z	28.6 ± 1.0 25.5 ± 2.6	Big Lue Mountains
22	Rhyolite of Hells Hole; porphyritic dike in Soapbox Canyon	B Z	28.4 ± 1.0 26.1 ± 3.2	Big Lue Mountains
23	Rhyolite of Hells Hole; rhyolite at Rattlesnake Gap	W	27.5 ± 1.0	Big Lue Mountains
40	Rhyolite of Hells Hole	Z	26.7 ± 3.5	Mule Creek
56	Nabours Mountain Quartz Latite	Sp	28.3 ± 3.9	Holt Mountain
57	Nabours Mountain Quartz Latite, rhyolite	S	28.4 ± 0.8	Holt Mountain
60	Rhyolite dike in Goat Basin[1]	P	28.5 ± 1.0	Glenwood
62	Rhyolite dome at "Glenwood" Brushy Mountain	W	23.3 ± 0.8	Glenwood
72	Fanney Rhyolite	S	26.9 ± 1.0	Mogollon
82	Jerky Mountains Rhyolite; (rhyolite at Ewe Canyon)	G	27.6 ± 1.8	Negrito Mountain
83	Dacite in the porphyritic latite of Willow Creek	B	27.5 ± 0.5 27.9 ± 0.5	Negrito Mountain
87	Quartz-porphyry dike of Fanney Rhyolite age	Sp	26.6 ± 3.7	Rice Ranch
89	Rhyolite of Diablo Range, quartz-porphyry dike	B Sp S	28.2 ± 1.0 27.8 ± 2.7 26.8 ± 0.9	Shelley Peak
104	Taylor Creek Rhyolite	S	27.7 ± 0.9	Wall Lake
105	Taylor Creek Rhyolite	S	24.6 ± 0.5	Spring Canyon
107	Jerky Mountains Rhyolite; (rhyolite at Canyon Creek)	B W	27.7 ± 2.0 24.8 ± 2.0	Loco Mountain
112	Rhyolite at Shaw Canyon	S S	28.7 ± 1.5 28.3 ± 1.5 29.7 ± 1.5	Shaw Mountain
129	Jerky Mountains Rhyolite; (rhyolite in Y Canyon)	S	26.2 ± 1.2	Collins Park
151	Rhyolite at Frying Pan Creek	Z W	26.6 ± 4.2 30.5 ± 1.0	O Block Canyon
201	Rhyolite of Hells Hole(?)	H	29.5 ± 0.9	Big Lue Mountains
208	Rhyolite at Sheridan Mountain (Fanney Rhyolite)	P	25.9 ± 0.9	Moon Ranch
209	Rhyolite of the Mogollon Mountains	S	28.2 ± 1.0	Shelley Peak
210	Rhyolite of the Diablo Range	S	27.7 ± 1.5	Diablo Range

local names, such as Fanney Rhyolite (Ferguson, 1927), Jerky Mountains Rhyolite (Elston, 1968, p. 237; 1976), rhyolite of the Diablo Range (Ratté and Gaskill, 1975), rhyolite of Hells Hole (Ratté and Hedlund, 1981), Taylor Creek Rhyolite (Elston, 1968, p. 238; Lawrence, 1986; Duffield, 1986), and rhyolite-flow map units (Tdf, Tdr) of Willard and Stearns (1971). The flow-banded rhyolites have long presented stratigraphic and structural problems because of petrographic similarities, their complex field relationships, and their many separate eruptive centers.

Some of the rhyolite bodies are localized along caldera ring-fracture zones, such as those around the Bursum caldera (Ratté and Gaskill, 1975), but large masses elsewhere have no known relationship to caldera structures. Rather they seem to represent a general rise of rhyolitic magma to subvolcanic levels, from where large volumes were erupted onto the surface toward the end of the caldera cycle of activity in the volcanic field. Because the flow-banded rhyolites apparently are the final manifestation of silicic volcanic activity before the onset of voluminous andesitic volcanism, they would seem to record temporal and compositional variations at different locations in the upper part of the batholith-size magma chamber immediately prior to its consolidation.

Accurate dating is a prerequisite for the study of the late caldera-cycle sequence of rhyolitic eruptive

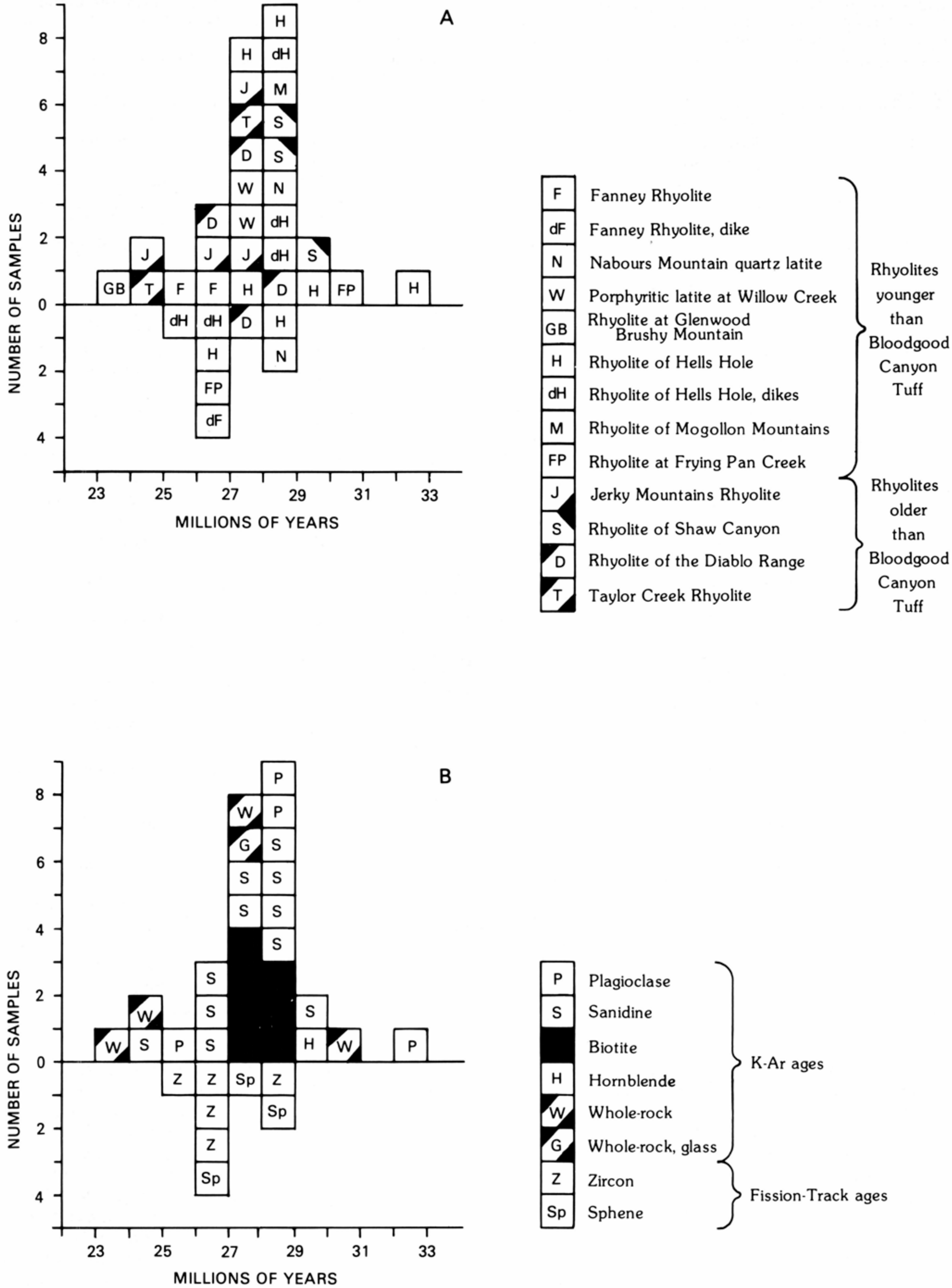

FIGURE 4—Histograms of flow-banded rhyolite ages. A, Ages as identified by map unit. B, Ages identified by mineral dated; samples correspond directly to samples in same position in Fig. 4A.

events. A list of ages of flow-banded or flow—dome rhyolites is compiled separately in Table 4, and the ages are summarized in histograms according to the minerals dated and the correlation of units in Fig. 4A, B. Seventy-five percent of the rhyolite ages cluster between 26 and 29 m.y., and more than half of all the ages, and all seven biotite ages, are between 27 and 29 m.y. However, field relationships indicate that the rhyolites were not erupted all at the same time.

Two age groups of flow-banded rhyolite are known, based on their stratigraphic position relative to the Bloodgood Canyon Tuff. Flow—dome rhyolites younger than Bloodgood Canyon Tuff include the Jerky Mountains Rhyolite of Elston (1968) where it is present within the Bursum caldera, Fanney Rhyolite, rhyolite of Nabours Mountain, other rhyolites along the western ring-fracture zone of the Bursum caldera, and rhyolite of Hells Hole. The rhyolite of Rocky Canyon in the North Star Mesa quadrangle (Ratté and Gaskill, 1975) has not been dated, but it also overlies Bloodgood Canyon Tuff.

Flow-banded rhyolites older than Bloodgood Canyon Tuff include Taylor Creek Rhyolite and its correlatives in the northeastern part of the Clifton 1° x 2° quadrangle and probably most or all of the Jerky Mountains Rhyolite previously mapped in reconnaissance (Rhodes and Smith, 1976; Elston, Rhodes et al., 1976; Coney, 1976) outside of the Bursum caldera.

Another rhyolite flow—dome complex that is older than Bloodgood Canyon Tuff is the rhyolite of the Diablo Range, which covers more than 200 km^2 in the southern walls of both the Gila Cliff Dwellings and Bursum calderas (Ratté and Gaskill, 1975). However, the rhyolite of the Diablo Range (Entry 210) and the petrographically similar Jerky Mountains Rhyolite in the Mogollon Mountains within the Bursum caldera (Entry 209) are indistinguishable in age according to conventional K—Ar dating of sanidines. Further complicating the relationship between these two seemingly identical rhyolites, which are in contact across the Bursum caldera wall, is the association of agglutinates and/or ash-flow tuffs interlayered in the rhyolite of the Diablo Range. Although the thick (0-150 m), welded, near-source pyroclastic rocks closely resemble Bloodgood Canyon Tuff and led Ratté to speculate that the rhyolite of the Diablo Range might be intrusive and thus younger than Bloodgood Canyon (Ratté et al., 1984, p. 8720), reexamination in the field (1987) and additional petrographic and chemical data (Seamans and Elston, 1987) clearly show that the rhyolite of the Diablo Range is older than Bloodgood Canyon Tuff as originally mapped by Ratté and Gas-kill (1975).

If the rhyolite of the Diablo Range and the intracaldera Jerky Mountains Rhyolite of Elston (1968) are separated in time by the Bloodgood Canyon Tuff, as interpreted here, then their ages would probably bracket the major events in the development of the Bursum caldera. These ages may be resolved by future $^{40}Ar/^{39}Ar$ dating.

Taylor Creek Rhyolite was proposed by Rhodes (1976b) as a cauldron rhyolite of the Gila Cliff Dwellings caldera (Elston, 1984), and he believed it marked the ring-fracture zone of that caldera. However, recent geologic mapping of the Wall Lake, Indian Peaks West, and Indian Peaks East quadrangles (Pl. 1, Fig. 1; Richter, 1986; Richter and Lawrence, 1986; Lawrence and Richter, 1986) shows the Taylor Creek Rhyolite

TABLE 5—Ages of rocks included in or correlated (Last Chance Andesite, Mineral Creek Andesite) with Bearwallow Mountain Andesite. All ages are whole-rock K–Ar ages unless indicated otherwise; P indicates a plagioclase K–Ar age.

Entry no.	Correlation	Mineral dated and calculated age (m.y.)		Quadrangle (see Pl. 1)
80	Bearwallow Mountain Andesite		23.1 ± 0.8	Bearwallow Mountain
81	Andesite at Negrito Mountain		25.6 ± 0.9	Negrito Mountain
111	Andesite at O Bar O Mountain		25.7 ± 0.9	O Bar O Canyon West
110	Andesite at Pelona Mountain		26.6 ± 1.0	Pelona Mountain
192	Andesite at Black Mountain		23.9	Black Mountain
73	Mineral Creek Andesite		25.7 ± 0.5	Mogollon
74	Lower part of Last Chance Andesite		25.0 ± 0.8	Mogollon
75	Upper part of Last Chance Andesite		23.2 ± 0.8	Mogollon
61	Andesite at "Glenwood" Brushy Mountain		25.9 ± 0.5	Glenwood
174	Andesite at "Radar" Brushy Mountain		23.7 ± 0.5 25.6 ± 0.5	Steeple Rock (see Fig. 1)
43	Intrusive andesite at Tillie Hall Canyon	P	24.5 ± 0.8	Mule Creek
47	Andesite at Wilson Mountain		24.7 ± 0.8	Wilson Mountain
202	Andesite in Keller Canyon		25.2 ± 0.9	Alma Mesa
52	Porphyritic andesite in Burnt Stump Canyon	P	25.6 ± 1.3	Moon Ranch
31	Porphyritic andesite near Hamilton Spring	P	25.0 ± 0.9	Big Lue Mountains
32	Porphyritic andesite dike near Cold Spring Mountain	P	26.2 ± 1.0	Big Lue Mountains
15	Andesite at Rose Peak, Blue Range		23.9 ± 0.7	Rose Peak

TABLE 6—Ages of basaltic lava flows and more silicic volcanic rocks that previously were included in the Bearwallow Mountain Formation. Letter indicates mineral or material dated: W, whole-rock; P, plagioclase; Z, zircon; H, hornblende; S, sanidine.

Entry no.	Correlation	Mineral dated and calculated age (m.y.)		Quadrangle (see Pl. 1)
100	Basalt at Roberts Lake Dam	W	21.1 ± 0.5	Copperas Peak
150	Basalt of Pueblo Park	P	19.2 ± 2.7	Saliz Pass
39	Basalt overlying rhyolite of Mule Creek	W	19.1 ± 1.1	Big Lue Mountains
38	Basalt feeder dike for flow (Entry 39)	W	19.0 ± 1.2	Big Lue Mountains
51	Basalt beneath rhyolite of Mule Creek	W	18.3 ± 0.7	Wilson Mountain
79	Basalt at Cooney Peak	W	15.2 ± 0.4	Bearwallow Mountain
134	Older basalt at Apache Creek	P	13.7 ± 1.4	Squirrel Springs Canyon
149	Basalt of Saliz Hill	W	12.2 ± 0.5	Saliz Pass
106	Tuff of Slash Ranch (Jordan Canyon Rhyolite)	S	22.2 ± 0.7	Black Mountain
114	Rhyolite at Horse Mountain	P	12.0 ± 3.0	Horse Mountain East
		H	35.3 ± 6.1	
		Z	10.4 ± 1.3	
204	Dacite at Eagle Peak	W	8.6 ± 0.3	Eagle Peak
			9.9 ± 0.4	
			10.0 ± 0.4	

beneath and older than Bloodgood Canyon Tuff, making it very difficult for the rhyolite to be the defluidized residue of Bloodgood Canyon Tuff as proposed by Rhodes. New ages for Taylor Creek Rhyolite (Entry 104) and unpublished ages (Maxwell and Marvin, pers. comm. 1985) range from 26 to 28 m.y., significantly older than the 24.5 m.y. age for Taylor Creek Rhyolite (Entry 105) reported by Elston and Damon (1970).

Again it is worth emphasizing that fission-track and conventional K—Ar dating are inadequate for resolving time relationships amongst closely spaced events of caldera ring-fracture volcanism in the Oligocene to early Miocene age range.

Bearwallow Mountain Formation redefined and revised

The Bearwallow Mountain Formation is here redefined as Bearwallow Mountain Andesite to clarify its age and the volcanic units that are included in it (Table 5). As formally defined (Elston, 1976, pp. 132-133), the Bearwallow Mountain Formation is about 21 m.y. old; its lower part is intertongued with John Kerr Peak Quartz Latite (21.4 ± 1.1 m.y.; Entry 126) and Jordan Canyon Rhyolite (21.7 ± 0.7 m.y.; Entry 106), and the upper part (21.1 ± 0.5 m.y.; Entry 100) intertongues with Gila Conglomerate at Roberts Lake Dam. The formation was expanded by Rhodes (1976a, p. 47) to include all post-Deadwood Gulch Rhyolite (24.4 ± 1.5 m.y.; Entry 162) mafic and intermediate rocks. However, recent K—Ar dating of andesite at Bearwallow Mountain, the type locality, and elsewhere shows that the ages of the most voluminous members of the Bearwallow Mountain, such as the shield-type volcanoes at Bearwallow Mountain, Negrito Mountain, Pelona Mountain, 0 Bar 0 Mountain, and Black Mountain (Entries 80, 81, 110, 111, and 192) are between 23 and 27 m.y. Compositionally, these rocks range from dacite to basaltic andesite but are dominantly andesitic rather than basaltic (Stinnett, 1980; USGS, unpubl. data 1986), whereas less voluminous mafic lavas less than about 21 m.y. old, including those used originally to define the age of the Bearwallow Mountain Formation, are basaltic and range from basaltic andesite to alkali basalt. Limited isotopic data (Stinnett, 1980; USGS, unpubl. data 1986) also indicate that the younger, more basaltic lavas, less than about 21 m.y. old (Table 6), are chemically distinct from the 23-27 m.y. old andesitic lavas of the Bearwallow Mountain Andesite, as redefined here. More silicic volcanoes that previously were included in the Bearwallow Mountain (Table 6), such as Eagle Peak (Elston, 1976, p. 132) and Horse Mountain (Bornhorst, 1980, p. 1011), are in a group of middle to late Miocene intermediate to silicic volcanic centers (Table 7) that lie along the Morenci—Reserve fault zone (Ratté, 1986).

To more accurately reflect the age and composition of the rock at the type locality at Bearwallow Mountain (Elston, 1976, pp. 132-133), we are changing the Bearwallow Mountain Formation to Bearwallow Mountain Andesite, and we are limiting the unit to include those predominantly calc-alkalic andesites and basaltic-andesite eruptives and intrusives of a series of low-profile cones or small shield volcanoes that range in age from 23 to 27 m.y. Most of the rocks originally included in the Bearwallow Mountain Formation of Elston (1976, pp. 132-133) fit these criteria. Dated units that we include in the Bearwallow Mountain Andesite are listed in Table 5.

Excluded from our usage of Bearwallow Mountain Andesite (Table 6) are younger intermediate to silicic rocks, such as the dacitic volcano at Eagle Peak (Entry 204) and the rhyolitic volcano at Horse Mountain (Entry 114), that were formerly included in the Bearwallow Mountain Formation of Elston (1976) but are not related to the Bearwallow Mountain Andesite. Also excluded are the more basaltic lavas (mainly alkalic and tholeiitic) that are younger than 21-22 m.y. These basaltic lava flows, which are notably thinner

TABLE 7—Ages of post-Bearwallow Mountain Andesite volcanic rocks along the Morenci–Reserve fault zone in the western Mogollon–Datil volcanic field. Letter(s) indicates mineral or material dated: W, whole-rock; P, plagioclase; B, biotite; S, sanidine; G, whole-rock glass; H, hornblende; Ad, adularia; Z, zircon; A, apatite; Sp, sphene.

Entry no.	Correlation	Mineral dated and calculated age (m.y.)		Quadrangle (see Pl. 1)
132	Basalt at Apache Creek	W	0.9 ± 0.2	Squirrel Springs Canyon
133	Basalt at Apache Creek	W	1.0 ± 0.1	Squirrel Springs Canyon
137	Basalt at Luna	W	2.65 ± 0.10	Luna
63	Basalt at Harve Gulch	W	5.6 ± 0.3	Glenwood
203	Rhyolite of Enebro Mountain	W	20.9 ± 0.8	Clifton
			20.6 ± 0.7	
204	Dacite at Eagle Peak	W	8.6 ± 0.3	Eagle Peak
			9.9 ± 0.4	
			10.0 ± 0.4	
114	Rhyolite at Horse Mountain	P	12.0 ± 3.0	Horse Mountain East
		Z	10.4 ± 1.3	
		H	35.3 ± 6.1	
127	John Kerr Peak Quartz Latite	B	13.6 ± 0.5	John Kerr Peak
		Z	12.0 ± 1.6	
126	John Kerr Peak Quartz Latite	Sp	22.7 ± 4.8	John Kerr Peak
		Sp	20.6 ± 4.8	
		A	22.7 ± 5.2	
		Z	21.4 ± 2.2	
		Z	19.9 ± 2.2	
149	Basalt of Saliz Hill	W	12.2 ± 0.5	Saliz Pass
134	Older basalt at Apache Creek	P	13.7 ± 1.4	Squirrel Springs Canyon
140	Quartz-diorite intrusive at Wet Leggett Spring	B	17.7 ± 0.6	Bull Basin
		H	13.9 ± 0.7	
		Z	11.9 ± 1.4	
198	Basalt at Dix Creek	W	17.7 ± 0.6	Big Lue Mountains
141	Rhyolite of Maverick Peak	S	14.0 ± 0.5	Bull Basin
79	Basalt at Cooney Peak	W	15.2 ± 0.4	Bearwallow Mountain
200	Basalt in Saliz Canyon	W	15.4 ± 0.6	Bull Basin
78	Vein gangue at Last Chance mine	Ad	17.5 ± 0.6	Mogollon
		W	18.5 ± 0.7	
			16.5 ± 0.6	
39	Basalt overlying rhyolite of Mule Creek	W	19.1 ± 1.1	Big Lue Mountains
38	Basalt feeder dike for flow (Entry 39)	W	19.0 ± 1.2	Big Lue Mountains
36	Rhyolite of Mule Creek	G	17.7 ± 0.6	Big Lue Mountains
44	Rhyolite of Mule Creek	Z	17.7 ± 1.9	Mule Creek
35	Rhyolite of Mule Creek	G	18.3 ± 0.7	Big Lue Mountains
34	Rhyolite of Mule Creek	G	19.0 ± 0.9	Big Lue Mountains
37	Rhyolite at Coal Creek	W	19.0 ± 0.7	Big Lue Mountains
48	Rhyolite at The Box	B	19.3 ± 0.7	Wilson Mountain
		P	18.7 ± 0.9	
		Z	18.9 ± 2.1	
51	Basalt beneath rhyolite of Mule Creek	W	18.3 ± 0.7	Wilson Mountain
150	Basalt of Pueblo Park	P	19.2 ± 2.7	Saliz Pass
49	Rhyolite of Potholes Country	B	21.1 ± 0.7	Wilson Mountain
		Z	18.9 ± 1.4	
50	Rhyolite of Potholes Country	Z	18.4 ± 2.1	Wilson Mountain
33	Dacite of Tennessee Creek	H	21.8 ± 1.4	Big Lue Mountains
195	Dacite of Tennessee Creek	P	21.3 ± 1.8	Big Lue Mountains
164	Porphyritic intrusive at Cerrito Viejo	Z	21.4 ± 2.3	Sugarloaf Mountain (see Fig. 1)
		B	30.2 ± 1.1	

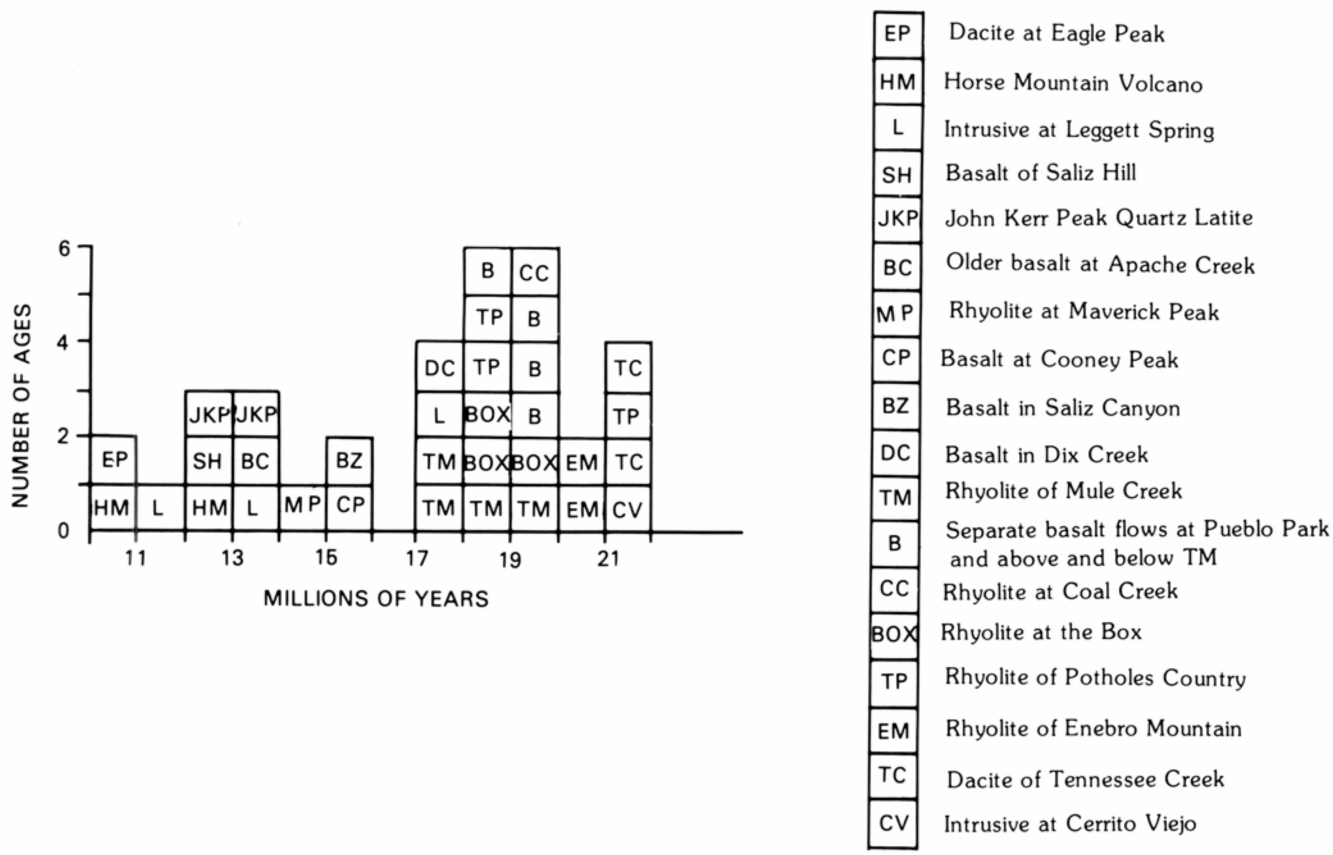

FIGURE 5—Histogram of ages of volcanic rocks between 10 and 21 m.y. in the Morenci–Reserve fault zone.

than most accumulations of Bearwallow Mountain Andesite, generally occur at the base of or interlayered with Gila Conglomerate.

Basalts about 12-22 m.y. old, here excluded from the Bearwallow Mountain Andesite (Table 5), may b€ more closely akin to the 1-6 m.y. old alkali basalts (Entries 63, 170, 132, 133, and 137), for which initial ^{87}Sr/^{86}Sr ratios of 0.703-0.704 have been reported (Bikerman, 1976; Stinnett, 1980, 1976; Elston, Rhodes, and Erb, 1976, p. 127), than to the Bearwallow Mountain andesites, which have initial 'Sr/'Sr ratios between 0.7078 and 0.7083 for 11 of 12 samples (Stinnett, 1980, p. 81).

Miocene volcanism along the Morenci-Reserve fault zone

New ages for volcanic rocks along the north-north-east-trending Morenci-Reserve fault zone tend to partially fill in that part of the age spectrum of volcanic rocks commonly referred to as the mid-Miocene lull, about 20-14 m.y. ago (Fig. 5; Chapin and Seager, 1975). Ages for rocks along this zone have been compiled separately in Table 7. They include a bimodal suite of rhyolites and basalts in the southwestern part of the Morenci-Reserve zone, as follows: the rhyolites of Potholes Country (Entries 49 and 50) and Mule Creek (Entries 34, 35, 36, and 44), the rhyolites of Coal Creek and The Box (Entries 37 and 48), and basalt flows interlayered in Gila Conglomerate (Entries 38, 39, 51, 79, 198, and 200); ages of these rhyolites and basalts range between 15 and 21 m.y.

In the northern part of the fault zone, from the vicinity of Reserve to Horse Mountain, volcanic rocks of basaltic to rhyolitic composition (including intermediate rock compositions) range between 8 and 19 m.y. in age. Included are calc-alkaline medium- to high-K rhyolites of the Horse Mountain composite volcano (Entry 114; Bornhorst, 1980, chemical analyses 580-584); domes of high-K rhyolite in the John Kerr Peak dome complex (Entry 126, Smith, 1976; Entry 127), high-K dacite in the intrusive at Wet Leggett Spring (Entry 140; Ratté and Grotbo, 1979, chemical analysis 78; Bornhorst, 1980, chemical analyses 565, 1016-1019), dacite at Eagle Peak (Entry 204; Ratté and Grotbo, 1979, chemical analysis 72), and high-silica rhyolite of Maverick Peak (Entry 141). Also, along this zone and adjacent to it, are Pliocene and Quaternary basalt flows (Entries 63, 132, 133, and 137) and andesitic volcanic centers of Bearwallow Mountain Andesite age-23-27 m.y. Thus, the MorenciReserve fault zone has long localized leakage of magma along the western margin of the Mogollon-Datil volcanic field; the fault zone probably provided access to the surface during and following crystallization of the batholith underlying this volcanic field.

At present, the limited strontium isotopic data suggests that the younger mafic volcanics (Pliocene and younger) have initial ^{87}Sr/^{86}Sr ratios of 0.703-0.704. The older mafic volcanics, such as the Bearwallow Mountain Andesite (23-27 m.y.), have initial ^{87}Sr/^{86}Sr ratios around 0.708. The decreasing initial strontium ratios with decreasing age may indicate faster magma ascent and less crustal contamination for the younger volcanics and/or differences in source region.

TABLE 8—List of dated mid-Tertiary volcanic rocks in the Clifton 1° × 2° quadrangle, Arizona–New Mexico, and peripheral areas. Dated samples are listed in approximate order of increasing age. If discordant ages were obtained from different samples of the same stratigraphic unit or from different minerals from the same sample and if the field relationships of the unit are uncertain, the sample is listed according to our assessment of the most reliable age obtained. Letter(s) indicates mineral or material dated: S, sanidine; B, biotite; P, plagioclase; H, hornblende; F, K-feldspar; Al, alunite; W, whole-rock; G, glass—obsidian; Z, zircon; Sp, sphene; A, apatite; Ad, adularia. Letter not repeated for replicate analyses of same sample. Quadrangle name followed by [1] indicates that sample was collected outside of Clifton 1° × 2° quadrangle; see Fig. 1.

Entry no.	Correlation	Mineral dated and calculated age (m.y.)		Quadrangle (see Pl. 1)
132	Basalt at Apache Creek	W	0.9 ± 0.2	Squirrel Springs Canyon
133	Basalt at Apache Creek	W	1.0 ± 0.1	Squirrel Springs Canyon
206	Vitric ash in Gila Conglomerate	Z	2.01 ± 0.97	Canteen Canyon
137	Basalt at Luna	W	2.65 ± 0.10	Luna
63	Basalt at Harve Gulch	W	5.6 ± 0.3	Glenwood
170	Basalt at Mimbres Valley	W	6.47 ± 0.41	San Lorenzo[1]
204	Dacite at Eagle Peak	W	8.6 ± 0.3	Eagle Peak
			9.9 ± 0.4	
			10.0 ± 0.4	
1	Quartz latite at Baldy Peak	F	8.8 ± 0.4	Mount Ord
2	Basalt NE of Mt. Baldy	W	9.1 ± 0.9	Mount Ord
114	Rhyolite at Horse Mountain	P	12.0 ± 3.0	Horse Mountain East
		Z	10.4 ± 1.3	
		H	35.3 ± 6.1	
127	John Kerr Peak Quartz Latite	B	13.6 ± 0.5	John Kerr Peak
		Z	12.0 ± 1.6	
126	John Kerr Peak Quartz Latite	Sp	22.7 ± 4.8	John Kerr Peak
		Sp	20.6 ± 4.8	
		A	22.7 ± 5.2	
		Z	21.4 ± 2.2	
		Z	19.9 ± 2.2	
149	Basalt of Saliz Hill	W	12.2 ± 0.5	Saliz Pass
134	Older basalt at Apache Creek	P	13.7 ± 1.4	Squirrel Springs Canyon
140	Quartz-diorite intrusive at Wet Leggett Spring	B	17.7 ± 0.6	Bull Basin
		H	13.9 ± 0.7	
		Z	11.9 ± 1.4	
141	Rhyolite east of Maverick Peak	S	14.0 ± 0.5	Bull Basin
79	Basalt at Cooney Peak	W	15.2 ± 0.4	Bearwallow Mountain
200	Basalt in Saliz Canyon	W	15.4 ± 0.6	Bull Basin
78	Vein—Last Chance mine	Ad	17.5 ± 0.6	Mogollon
		W	18.5 ± 0.7	
			16.5 ± 0.6	
198	Basalt in Dix Creek	W	17.7 ± 0.6	Big Lue Mountains
39	Basalt overlying rhyolite of Mule Creek	W	19.1 ± 1.1	Big Lue Mountains
38	Basalt feeder dike for flow (Entry 39)	W	19.0 ± 1.2	Big Lue Mountains
36	Rhyolite of Mule Creek	G	17.7 ± 0.6	Big Lue Mountains
44	Rhyolite of Mule Creek	Z	17.7 ± 1.9	Mule Creek
35	Rhyolite of Mule Creek	G	18.3 ± 0.7	Big Lue Mountains
34	Rhyolite of Mule Creek	G	19.0 ± 0.9	Big Lue Mountains
29	Pumice—rhyolite of Mule Creek	Z	26.5 ± 3.4	Big Lue Mountains
37	Rhyolite at Coal Creek	W	19.0 ± 0.7	Big Lue Mountains
48	Rhyolite at The Box	B	19.3 ± 0.7	Wilson Mountain
		P	18.7 ± 0.9	
		Z	18.9 ± 2.1	
51	Basalt beneath rhyolite of Mule Creek	W	18.3 ± 0.7	Wilson Mountain
203	Rhyolite at Enebro Mountain	W	20.9 ± 0.8	Clifton
			20.6 ± 0.7	
150	Basalt of Pueblo Park	P	19.2 ± 2.7	Saliz Pass
49	Rhyolite of Potholes Country	B	21.1 ± 0.7	Wilson Mountain
		Z	18.9 ± 1.4	
50	Rhyolite of Potholes Country	Z	18.4 ± 2.1	Wilson Mountain
33	Dacite of Tennessee Creek	H	21.8 ± 1.4	Big Lue Mountains
195	Dacite of Tennessee Creek	P	21.3 ± 1.8	Big Lue Mountains

TABLE 8 continued

Entry no.	Correlation	Mineral dated and calculated age (m.y.)		Quadrangle (see Pl. 1)
164	Porphyritic intrusive at Cerrito Viejo	Z B	21.4 ± 2.3 30.2 ± 1.1	Sugarloaf Mountain[1]
100	Basalt at Roberts Lake Dam	W	21.1 ± 0.5	Copperas Peak
6	Porphyritic andesite east of Barlow Pass	P	21.3 ± 0.7 29.1 ± 1.5	Point of Pines East
106	Tuff of Slash Ranch	S	22.2 ± 0.7	Black Mountain
94	Dacite intrusive at Holt Gulch	Z	22.7 ± 2.3	Holt Mountain
205	Rhyolite dike near Haystack Mountain	F	23.1 ± 1.0	Rice Ranch
62	Rhyolite dome at "Glenwood" Brushy Mountain	W	23.3 ± 0.8	Glenwood
14	Quartz-latite domes of Blue Range	B	23.9 ± 0.7	Dutch Blue Creek
25	Tuff interlayered with mafic lava flows	Z	28.6 ± 3.7	Big Lue Mountains
162	Deadwood Gulch Member, Fanney Rhyolite	S	24.4 ± 1.5	Grouse Mountain
196	Dacite in Seep Spring Canyon	W	24.2 ± 0.9	Big Lue Mountains
	Bearwallow Mountain Andesite (23–27 m.y.) and correlatives			
80	Bearwallow Mountain Andesite	W	23.1 ± 0.8	Bearwallow Mountain
192	Andesite at Black Mountain	W?	23.9	Black Mountain
174	Andesite at "Radar" Brushy Mountain	W W	23.7 ± 0.5 25.6 ± 0.5	Steeple Rock[1]
75	Upper part of Last Chance Andesite	W	23.2 ± 0.8	Mogollon
74	Lower part of Last Chance Andesite	W	25.0 ± 0.8	Mogollon
15	Andesite at Rose Peak, Blue Range	W	23.9 ± 0.7	Rose Peak
76	Last Chance(?) Andesite	W	17.7 ± 0.3 17.6 ± 0.3	Mogollon
81	Andesite at Negrito Mountain	W	25.6 ± 0.9	Negrito Mountain
111	Andesite at O Bar O Mountain	W	25.7 ± 0.9	O Bar O Canyon West
110	Andesite at Pelona Mountain	W	26.6 ± 1.0	Pelona Mountain
43	Intrusive andesite at Tillie Hall Canyon	P A	24.5 ± 0.8 16.9 ± 4.3	Mule Creek
47	Andesite at Wilson Mountain	W	24.7 ± 0.8	Wilson Mountain
202	Andesite in Keller Canyon	W	25.2 ± 0.9	Alma Mesa
52	Porphyritic andesite in Burnt Stump Canyon	P	25.6 ± 1.3	Moon Ranch
61	Andesite at "Glenwood" Brushy Mountain	W	25.9 ± 0.5	Glenwood
73	Mineral Creek Andesite	W	25.7 ± 0.5	Mogollon
31	Porphyritic andesite near Hamilton Spring	P	25.0 ± 0.9	Big Lue Mountains
32	Porphyritic andesite dike near Cold Spring Mountain	P	26.2 ± 1.0	Big Lue Mountains
128	Andesite along Cox Canyon Road	W	20.4 ± 1.5	Collins Park
	Pre-Bearwallow Mountain Andesite			
45	Dacite of Mineral Spring Canyon	B Z	26.1 ± 0.9 26.1 ± 3.3	Wilson Mountain
46	Dacite of Mineral Spring Canyon	Z	25.0 ± 2.3	Wilson Mountain
41	Rhyodacite dome of Sawmill Creek	B Z	25.4 ± 0.9 19.0 ± 5.0	Mule Creek
42	Rhyolite dike	B Z	25.3 ± 0.9 24.3 ± 3.5	Mule Creek
5	Rhyolite ash-flow tuff at Nantac Rim	B B B S S	24.6 ± 0.9 24.9 ± 0.9 33.7 ± 1.3 22.0 ± 0.9 22.9 ± 0.8	Point of Pines East
7	Andesites at Bryce Mountain	W	13 ages ranging from 27–35	Bryce Mountain
4	Basalt beneath pyroclastic rocks, Barlow Pass area	W	26.1 ± 0.9 28.3 ± 1.3	Point of Pines West
3	Basaltic-andesite flow in Barlow Pass area	W	28.7 ± 0.5	Point of Pines West

(*continued on page 26*)

TABLE 8 continued

Entry no.	Correlation	Mineral dated and calculated age (m.y.)		Quadrangle (see Pl. 1)
197	Dacite of Limestone Gulch	H	27.2 ± 1.0	Big Lue Mountains
		P	20.1 ± 1.1	
199	Amygdaloidal andesite in Buzzard Roost Canyon	W	27.5 ± 1.0	Big Lue Mountains
17	Amygdaloidal andesite	W	27.9 ± 1.0	Big Lue Mountains
26	Rhyodacite at Pat Creek	P	27.8 ± 1.6	Big Lue Mountains
27	Rhyodacite at Pat Creek	B	30.4 ± 1.1	Big Lue Mountains
		P	25.7 ± 1.6	
28	Tuff interlayered with flows at Bird Canyon	B	28.0 ± 1.0	Big Lue Mountains
152	Tuff lens in andesite sequence near Devils Park	Z	26.2 ± 2.4	O Block Canyon
		S	67.0 ± 2.3	
77	Intrusive andesite at Silver Creek	B	27.1 ± 0.9	Mogollon
		Z	23.5 ± 2.8	
		A	14.7 ± 2.7	
87	Quartz-porphyry dike of Fanney Rhyolite age	Sp	26.6 ± 3.7	Rice Ranch
208	Rhyolite at Sheridan Mountain	P	25.9 ± 0.9	Moon Ranch
72	Fanney Rhyolite	S	26.9 ± 1.0	Mogollon
151	Rhyolite at Frying Pan Creek	Z	26.6 ± 4.2	O Block Canyon
		W	30.5 ± 1.0	
82	Rhyolite at Ewe Canyon	G	27.6 ± 1.8	Negrito Mountain
107	Rhyolite at Canyon Creek	B	27.7 ± 2.0	Loco Mountain
		W	24.8 ± 2.0	
129	Rhyolite in Y Canyon	S	26.2 ± 1.2	Collins Park
89	Quartz-porphyry dike, rhyolite of the Diablo Range	B	28.2 ± 1.0	Shelley Peak
		Sp	27.8 ± 2.7	
		S	26.8 ± 0.9	
209	Rhyolite of the Mogollon Mountains	S	28.2 ± 1.0	Shelley Peak
210	Rhyolite of the Diablo Range	S	27.7 ± 1.5	Diablo Range
212	Rhyolite of Bat Cave Wells	F	27.4 ± 1.0	Fullerton
112	Rhyolite of Shaw Canyon	S	28.7 ± 1.5	Shaw Mountain
			28.3 ± 1.5	
		S	29.7 ± 1.5	
104	Taylor Creek Rhyolite	S	27.7 ± 0.9	Wall Lake
105	Taylor Creek Rhyolite	S	24.6 ± 0.5	Spring Canyon
56	Nabours Mountain Quartz Latite	Sp	28.3 ± 3.9	Holt Mountain
57	Nabours Mountain Quartz Latite, rhyolite	S	28.4 ± 0.8	Holt Mountain
83	Dacite in the porphyritic latite of Willow Creek	B	27.5 ± 0.5	Negrito Mountain
			27.9 ± 0.5	
24	Porphyritic rhyolite, north of Sawmill Creek	Z	27.6 ± 5.5	Big Lue Mountains
211	Rhyodacite of the Big Lue Mountains	B	28.1 ± 1.0	Big Lue Mountains
		P	24.1 ± 1.3	
30	Porphyritic andesite in Rustlers Canyon	P	29.5 ± 1.1	Big Lue Mountains
			28.7 ± 1.1	
18	Rhyolite of Hells Hole	P	28.4 ± 1.0	Big Lue Mountains
19	Rhyolite of Hells Hole	B	27.1 ± 1.0	Big Lue Mountains
		P	32.9 ± 1.2	
20	Rhyolite of Hells Hole	Z	28.7 ± 3.7	Big Lue Mountains
40	Rhyolite of Hells Hole	Z	26.7 ± 3.5	Mule Creek
201	Rhyolite of Hells Hole(?)	H	29.5 ± 0.9	Big Lue Mountains
21	Rhyolite dike at Chalk Peak	B	28.6 ± 1.0	Big Lue Mountains
		Z	25.5 ± 2.6	
22	Porphyritic rhyolite dike in Soapbox Canyon	B	28.4 ± 1.0	Big Lue Mountains
		Z	26.1 ± 3.2	
		A	20.7 ± 6.0	
23	Rhyolite at Rattlesnake Gap	W	27.5 ± 1.0	Big Lue Mountains
59	Dacite of Goat Basin volcano	P	28.6 ± 2.0	Glenwood
		H	26.4 ± 1.6	
		Z	26.5 ± 3.4	
60	Rhyolite dike in Goat Basin	P	28.5 ± 1.0	Glenwood

TABLE 8 continued

Entry no.	Correlation	Mineral dated and calculated age (m.y.)		Quadrangle (see Pl. 1)
183	Andesite of Dry Leggett Canyon(?)	W	29.6 ± 1.4	Queens Head
54	Porphyritic dacite flow in Bursum caldera wall	B	29.9 ± 1.1	Holt Mountain
		Z	28.5 ± 3.5	
	Major caldera-forming ash-flow tuffs and associated rocks			
84	Apache Spring Tuff	B	27.9 ± 0.8	Grouse Mountain
85	Apache Spring Tuff	B	28.1 ± 1.0	Grouse Mountain
		Z	29.3 ± 3.6	
86	Apache Spring Tuff	Sp	29.9 ± 4.6	Grouse Mountain
		Sp	28.5 ± 5.6	
		Sp	30.0 ± 4.8	
		Sp	30.2 ± 4.8	Bearwallow Mountain
109	Bloodgood Canyon Tuff	S	23.4 ± 0.7	Indian Peaks West
155	Bloodgood Canyon Tuff	S	23.7 ± 0.7	Milligan Mountain
153	Bloodgood Canyon Tuff	S	24.3 ± 1.5	Reserve
			27.3 ± 0.9	
96	Bloodgood Canyon Tuff	Sp	24.9 ± 5.6	Granny Mountain
8	Bloodgood Canyon Tuff	S	25.5 ± 0.7	Blue
102	Bloodgood Canyon Tuff	S	26.0 ± 1.5	Gila Hot Springs
		B	26.9 ± 1.5	
182	Bloodgood Canyon Tuff	S	27.1 ± 1.2	Cliff[1]
			27.0 ± 0.8	
130	Bloodgood Canyon Tuff	S	26.4 ± 1.5	Salvation Peak
		B	27.3 ± 1.5	
161	Bloodgood Canyon Tuff	S	26.1 ± 0.9	Eagle Peak
			27.3 ± 1.5	
108	Bloodgood Canyon Tuff	S	27.7 ± 0.9	Indian Peaks West
		Z	26.0 ± 2.7	
156	Bloodgood Canyon Tuff	B	28.0 ± 1.0	Milligan Mountain
		S	27.1 ± 0.9	
		Z	28.9 ± 3.0	
157	Bloodgood Canyon Tuff	S	26.6 ± 0.9	Milligan Mountain
			26.9 ± 0.9	
		S	27.8 ± 0.9	
		Sp	27.9 ± 4.0	
		S	27.4 ± 0.9	
			28.0 ± 1.0	
		Z	27.3 ± 2.8	
		Sp	30.4 ± 5.0	
147	Bloodgood Canyon Tuff	S	28.2 ± 1.0	Saliz Pass
			28.0 ± 1.0	
			25.9 ± 0.9	
		S	27.6 ± 0.9	
		Z	27.4 ± 3.4	
103	Bloodgood Canyon Tuff	S	28.0 ± 1.0	Wall Lake
9	Bloodgood Canyon Tuff	B	28.3 ± 1.0	Blue
		S	28.3 ± 1.0	
			28.6 ± 1.0	
10	Bloodgood Canyon Tuff	B	30.6 ± 1.0	Blue
		S	27.3 ± 1.3	
176	Bloodgood Canyon Tuff	B	30.0 ± 1.0	Twin Sisters[1]
			30.5 ± 1.0	
		S	26.4 ± 0.9	
125	Bloodgood Canyon Tuff	B	28.8 ± 1.0	Tularosa Canyon
		S	28.2 ± 1.0	
97	Bloodgood Canyon Tuff	Sp	29.4 ± 4.0	Little Turkey Park
173	Bloodgood Canyon Tuff	Z	30.0 ± 1.7 (average of 15 ages)	Steeple Rock[1]
193	Bloodgood Canyon Tuff	Z	25.7 ± 2.1	York Valley[1]
194	Bloodgood Canyon Tuff	Z	24.0 ± 2.3	Big Lue Mountains
69	Shelley Peak Tuff	Z	28.4 ± 2.4	Mogollon
70	Shelley Peak Tuff	B	24.4 ± 0.8	Mogollon
			23.4 ± 0.8	
		Z	27.3 ± 2.6	
55	Cooney(?) Tuff or Shelley Peak(?) Tuff	B	28.5 ± 1.0	Holt Mountain
		Z	26.7 ± 4.0	

(continued on page 28)

TABLE 8 continued

Entry no.	Correlation	Mineral dated and calculated age (m.y.)		Quadrangle (see Pl. 1)
11	Shelley Peak Tuff	B	30.1 ± 1.0	Blue
145	Shelley Peak Tuff	B	30.5 ± 1.5	Saliz Pass
146	Shelley Peak Tuff	B	29.1 ± 1.0	Saliz Pass
		S	28.1 ± 1.0	
		Z	28.5 ± 2.4	
154	Shelley Peak Tuff	G	28.9 ± 1.8	Reserve
131	Shelley Peak Tuff	B	28.7 ± 1.0	Squirrel Springs Canyon
			25.7 ± 1.7	
124	Shelley Peak Tuff	F	31.7 ± 1.5	Bell Peak
		B	27.4 ± 1.3	
160	Squirrel Springs Canyon Andesite	P	24.3 ± 1.5	Eagle Peak
144	Davis Canyon Tuff	B	30.7 ± 1.0	Saliz Pass
		S	28.9 ± 1.0	
158	Davis Canyon(?) Tuff	B	29.7 ± 1.5	Milligan Mountain
		F	27.1 ± 2.0	
159	Davis Canyon(?) Tuff	Sp	31.6 ± 2.0	Eagle Peak
188	Tularosa Canyon(?) Rhyolite Tuff	Z	30.5 ± 3.8	Alegres Mountain[1]
113	Davis Canyon(?) Tuff	S	29.2 ± 1.0	Shaw Mountain
		Z	27.3 ± 3.1	
187	Vicks Peak(?) Tuff	Z	31.3 ± 5.0	Sugarloaf Mountain[1]
163	Vicks Peak(?) Tuff	S	27.2 ± 0.9	Sugarloaf Mountain[1]
		Z	22.9 ± 2.1	
169	La Jencia(?) Tuff	S	27.0 ± 1.0	Dusty[1]
		Z	16.8 ± 3.2	
120	Rhyolite of Wye Hill	Z	30.3 ± 6.1	Bell Peak
121	Rhyolite of Wye Hill	S	27.3 ± 0.6	Bell Peak
122	Rhyolite of Wye Hill	S	32.2 ± 2.0	Bell Peak
71	Andesite intrusive on upper Devils Creek	H	30.4 ± 1.9	Mogollon
98	Lava flows of Gila Flat	B	30.3 ± 0.7	Copperas Peak
		S	30.0 ± 0.7	
99	Granite dike—volcanic complex of Alum Mountain	F	30.4 ± 0.7	Copperas Peak
177	Tadpole Ridge Quartz Latite	B	31.9 ± 1.0	Twin Sisters[1]
178	Tadpole Ridge Quartz Latite	B	31.7 ± 1.0	Twin Sisters[1]
184	Tadpole Ridge Quartz Latite	B	31.9 ± 1.0	Twin Sisters[1]
175	Alunitic rhyolite	Al	31.3 ± 1.1	York Valley[1]
135	Tuff of Luna	S	31.9 ± 0.7	Luna
		B	36.5 ± 1.3	
		Z	32.5 ± 3.4	
136	Tuff of Luna	S	31.8 ± 0.7	Centerfire Bog
		B	35.3 ± 1.3	
		Z	39.5 ± 4.0	
172	Fall Canyon(?) Tuff	B	$^{40}Ar/^{39}Ar$ 32.42 ± 0.14	Steeple Rock[1]
		B	32.5 ± 1.2	
		S	29.2 ± 1.1	
171	Fall Canyon(?) Tuff	B	34.7 ± 1.2	Circle Mesa[1]
		Z	30.8 ± 3.4	
68	Fall Canyon Tuff	Z	29.4 ± 3.1	Mogollon
95	Fall Canyon Tuff	S	15.8 ± 1.0	Canyon Hill
165	Hells Mesa Tuff	B	$^{40}Ar/^{39}Ar$ 32.11 ± 0.19	Sugarloaf Mountain[1]
			33.2 ± 1.1	
			33.0 ± 1.1	
		S	30.9 ± 1.1	
		Z	31.4 ± 2.6	
166	Hells Mesa Tuff	B	$^{40}Ar/^{39}Ar$ 32.09 ± 0.10	Sugarloaf Mountain[1]
			32.3 ± 1.5	
		S	$^{40}Ar/^{39}Ar$ 31.87 ± 0.07	
			28.6 ± 1.0	
		P	31.1 ± 1.9	
		Z	29.3 ± 3.0	
185	Hells Mesa Tuff	S	32.1 ± 0.7	Sugarloaf Mountain[1]
91	Volcanic complex of Brock Canyon	B	33.5 ± 0.8	Canteen Canyon

TABLE 8 continued

Entry no.	Correlation	Mineral dated and calculated age (m.y.)		Quadrangle (see Pl. 1)
90	Volcanic complex of Brock Canyon	B	31.7 ± 0.8	Canteen Canyon
92	Volcanic complex of Brock Canyon	Z	31.0 ± 6.4	Canteen Canyon
93	Volcanic complex of Brock Canyon	Z	31.2 ± 5.5	Canteen Canyon
		Z	27.8 ± 5.3	
142	Tuff lens in early andesite sequence	S	32.4 ± 1.1	Saliz Pass
		B	29.7 ± 1.0	
			28.2 ± 1.0	
		Z	32.3 ± 2.4	
207	Andesite at Saddle Mountain	P	33.3 ± 1.2	Blue
143	Tuff lens in early andesite sequence	S	30.2 ± 2.0	Saliz Pass
			31.8 ± 2.0	
		B	26.7 ± 2.0	
			24.4 ± 2.0	
139	Tuff lens in early andesite sequence	S	34.0 ± 1.2	Bull Basin
		Z	32.8 ± 3.5	
148	Vitrophyre from early andesite complex	B	33.6 ± 1.1	Saliz Pass
53	Altered and mineralized rhyolite	Al	33.8 ± 1.2	Holt Mountain
		W	32.0 ± 1.7	
58	Cooney Canyon Member of Cooney Tuff	B	33.1 ± 1.5	Holt Mountain
64	Whitewater Creek Member of Cooney Tuff	Z	31.8 ± 2.8	Mogollon
88	Cooney Tuff	P	34 ± 2	Rice Ranch
65	Cooney Tuff	B	24.3 ± 0.8	Holt Mountain
66	Cooney Tuff	B	33.7 ± 1.0	Clifton
67	Cooney Tuff	Z	33.1 ± 2.8	Clifton
16	Rhyolite intrusive along lower San Francisco River	Z	33.0 ± 4.8	Big Lue Mountains
118	Tuff breccia of Horse Springs Canyon(?)	B	35.5 ± 2.2	Bell Peak
		P	33.9 ± 1.2	
119	Clast in tuff breccia of Horse Springs Canyon	Z	32.4 ± 3.4	Bell Peak
123	Tuff breccia of Horse Springs Canyon(?)	B	36.2 ± 2.0	Bell Peak
		B	32.2 ± 1.0	
			31.2 ± 1.0	
186	Tuff breccia of Horse Springs Canyon	Z	32.7 ± 3.8	Wallace Mesa[1]
115	Blue Canyon Tuff	S	33.3 ± 1.0	Horse Mountain West
		S	32.7 ± 4.6	
189	Blue Canyon Tuff	Z	33.2 ± 3.2	Log Canyon[1]
167	Rock House Canyon Tuff	Z	28.3 ± 3.3	Datil[1]
191	Kneeling Nun Tuff	B	34.2 ± 1.0	Santa Rita[1]
179	Kneeling Nun(?) Tuff	B	^{40}Ar/^{39}Ar 35.88 ± 0.11	Reading Mountain[1]
			35.1 ± 0.8	
		S	32.7 ± 0.8	
		Z	34.6 ± 4.0	
181	Kneeling Nun(?) Tuff	B	^{40}Ar/^{39}Ar 34.13 ± 0.11	C Bar Ranch[1]
			34.6 ± 0.8	
180	Porphyritic rhyolite intrusive at Dry Gallinas Campground	B	35.7 ± 1.2	San Lorenzo[1]
		S	33.3 ± 1.2	
			34.7 ± 1.2	
190	Datil Well Tuff	S	35.6 ± 0.7	Datil[1]
		Z	37.7 ± 3.8	
168	Datil Well Tuff	S	35.6 ± 1.3	Datil[1]
116	Datil Well Tuff	S	36.7 ± 1.3	Horse Mountain West
117	Datil Well(?) Tuff	B	35.4 ± 2.0	Horse Mountain West
138	Tuff of Bishop Peak	B	37.1 ± 1.3	Underwood Lake
		S	34.3 ± 1.2	
12	Older andesite in Blue Range	H	38.3 ± 3.9	Rose Peak
13	Older andesite in Blue Range	H	36.1 ± 2.7	Rose Peak
101	Granite of North Star Mesa	Z	42.6 ± 5.2	North Star Mesa
		A	42.7 ± 5.3	

Isotopic-age compilation

1. *Merrill, 1974, no. F–1966* K–Ar
Rhyolite flow (near 33°54′25″N, 109°33′43″W; top of Mount Baldy (or Baldy Peak), Mount Ord quad., White Mountains, Apache Co., AZ). *Analyzed by*: Geochron Laboratories, Inc.
(K-feldspar) 8.8 ± 0.4 m.y.

2. *Merrill, 1974; Merrill and Péwé, 1971, no. R–1162* K–Ar
Basalt (NW1/4 SE1/4 NW1/4 sec. 33, T7N, R27E, near 33°57′40″N, 109°30′10″W; Sheep Crossing on northeast flank of Mount Baldy, Mount Ord quad., White Mountains, Apache Co., AZ). *Analyzed by*: Geochron Laboratories, Inc. *Comment*: Basalt flow lies unconformably above the Sheep Crossing Formation of Merrill and Péwé (1971).
(whole-rock) 9.1 ± 0.9 m.y.

3. *Strangway et al., 1976, table 1, no. NP1A* K–Ar
Basaltic andesite (approx. 33°17′30″N, 109°50′W; roadcut on Natanes Plateau, Point of Pines West quad., Graham Co., AZ). *Comment*: The collection site of this sample is uncertain, but its apparent position at the north edge of Ash Flat (Strangway et al., 1976, fig. 1) suggests that this andesite and the andesite of Entry 4 (this paper) are from the same unit.
(whole-rock) 28.7 ± 0.5 m.y.

4. *Bromfield et al., 1972, no. AMZ–287* K–Ar
Basalt (33°17′58″N, 109°46′36″W; roadcut on west side of Barlow Pass, Point of Pines West quad., Graham Co., AZ). *Analytical data*: (Geochron Laboratories, Inc.) K_2O = 2.049, 2.066%; $^{40}Ar^*$ = 0.8507, 0.8407 × 10^{-10} mol/gm; $^{40}Ar^*/\Sigma^{40}Ar$ = 12, 15%; (USGS in 1978) K_2O = 1.94, 1.96%; $^{40}Ar^*$ = 0.7362 × 10^{-10} mol/gm; $^{40}Ar^*/\Sigma^{40}Ar$ = 73%. *Comment*: Basalt or basaltic andesite underlies a pyroclastic sequence in the Barlow Pass area.
Geochron **(whole-rock) 28.3 ± 1.3 m.y.**
USGS **(whole-rock) 26.1 ± 0.9 m.y.**

5. *Bromfield et al., 1972, no. AMZ–283* K–Ar
Rhyolite ash-flow tuff (33°18′24″N, 109°42′48″W; along Black River Road, east of Barlow Pass, Point of Pines East quad., Graham Co., AZ). *Analytical data*: (Geochron Laboratories, Inc.) (biotite) K_2O = 8.336, 8.348%; $^{40}Ar^*$ = 4.178, 4.003 × 10^{-10} mol/gm; $^{40}Ar^*/\Sigma^{40}Ar$ = 20, 22%; (sanidine) K_2O = 5.058, 5.234, 5.060%; $^{40}Ar^*$ = 1.624, 1.641 × 10^{-10} mol/gm; $^{40}Ar^*/\Sigma^{40}Ar$ = 22, 27%; (USGS) (biotite) K_2O = 8.28, 8.24%; $^{40}Ar^*$ = 2.941 × 10^{-10} mol/gm; $^{40}Ar^*/\Sigma^{40}Ar$ = 67%; (biotite–1) K_2O = 8.38, 8.32%; $^{40}Ar^*$ = 3.019 × 10^{-10} mol/gm; $^{40}Ar^*/\Sigma^{40}Ar$ = 70%; (sanidine–1) K_2O = 8.10, 8.11%; $^{40}Ar^*$ = 2.684 × 10^{-10} mol/gm; $^{40}Ar^*/\Sigma^{40}Ar$ = 94%. *Comment*: USGS laboratories dated the same biotite separate prepared by Geochron Laboratories, Inc. In addition, samples biotite–1 and sanidine–1 were prepared by the USGS from a portion of sample AMZ–283 that was held in reserve. Geochron's 33.7 m.y. biotite age appears spurious.
This sample is from the upper ash-flow tuff unit of the pyroclastic sequence in the Barlow Pass area.
Geochron **(biotite) 33.7 ± 1.3 m.y.**
(sanidine) 22.0 ± 0.9 m.y.
USGS **(biotite) 24.6 ± 0.9 m.y.**
(biotite–1) 24.9 ± 0.9 m.y.
(sanidine–1) 22.9 ± 0.8 m.y.

6. *Bromfield et al., 1972, no. AMZ–284* K–Ar
Andesite (33°18′14″N, 109°41′30″W; east of Barlow Pass and Black River Road, Point of Pines East quad., Graham Co., AZ). *Analytical data*: (Geochron Laboratories, Inc.) K_2O = 1.240, 1.238%; $^{40}Ar^*$ = 0.5054, 0.5404 × 10^{-10} mol/gm; $^{40}Ar^*/\Sigma^{40}Ar$ = 19, 23%; (USGS) K_2O = 1.18, 1.18%; $^{40}Ar^*$ = 0.3632 × 10^{-10} mol/gm; $^{40}Ar^*/\Sigma^{40}Ar$ = 55%. *Comment*: Coarsely porphyritic andesite flow (turkey-track type) overlies pyroclastic sequence of Barlow Pass area. Geochron's age is apparently spurious; USGS age is compatible with the stratigraphic position of the andesite in the volcanic sequence.
Geochron **(plagioclase) 29.1 ± 1.5 m.y.**
USGS **(plagioclase) 21.3 ± 0.7 m.y.**

7. *Strangway et al., 1976, table 1* K–Ar
Basaltic andesite (approx. 33°00′25″N, 109°41′10″W; SW1/4 sec. 9, T5S, R26E; Bryce Mountain in the Gila Mountains, Bryce Mountain quad., Graham Co., AZ). *Comment*: Nine samples from a sequence of 29 andesite lava flows were dated as part of a magnetic stratigraphy study. Flows were numbered from no. 1 at the top to no. 20 at the bottom of the sequence. The listed ages were determined at the University of Toronto, Canada, with additional ages—indicated by asterisks—supplied by Geochron Laboratories, Inc. The anomalously old ages given by sample AV15B are probably caused by the presence of xenoliths, according to Strangway et al. (1976, p. 119).

Field no.	Whole-rock age (m.y.)	Flow no.
AV2A	27.6 ± 1.4	2
AV4B	28.9 ± 0.9	4
AV8A	29.6 ± 0.5	8
AV11A	27.7 ± 0.5	11

AV11B	*28.9 ± 1.0	11
AV14B	*27.4 ± 0.9	14
AV15B	34.8 ± 0.6	15
	34.6 ± 0.8	15
	34.6 ± 0.4	15
	32.9 ± 0.7	15
AV17B	*29.6 ± 0.9	17
AV18B	29.8 ± 0.5	18
	31.1 ± 0.5	18

8. *Ratté et al., 1969, no. BR–85* K–Ar
Bloodgood Canyon Tuff (33°35′45″N, 109°07′38″W; NW1/4 sec. 22, T3N, R31E; low cliffs on east side of Blue River, Blue quad., Greenlee Co., AZ). *Analytical data*: K_2O = 6.86%; $^{40}Ar^*$ = 2.54 × 10^{-10} mol/gm; $^{40}Ar^*/\Sigma^{40}Ar$ = 99%. *Collected by*: J. C. Ratté. *Dated by*: P. E. Damon, Univ. of Arizona (Damon and Assoc., 1968, p. 44, sample PED–31–67).
(sanidine) 25.5 ± 0.7 m.y.

9. *UP–G23* K–Ar
Bloodgood Canyon Tuff (33°36′45″N, 109°05′28″W; SW1/4 sec. 12, T3N, R31E; near Blue Post Office, Blue quad., Greenlee Co., AZ). *Analytical data*: (biotite) K_2O = 7.40%; $^{40}Ar^*$ = 3.036 × 10^{-10} mol/gm; $^{40}Ar^*/\Sigma^{40}Ar$ = 76%; (sanidine–1) K_2O = 5.38%; $^{40}Ar^*$ = 2.211 × 10^{-10} mol/gm; $^{40}Ar^*/\Sigma^{40}Ar$ = 93%; (sanidine–2) K_2O = 4.65%; $^{40}Ar^*$ = 1.930 × 10^{-10} mol/gm; $^{40}Ar^*/\Sigma^{40}Ar$ = 78%. Rb–Sr analytical data for whole-rock material: Rb = 266 ppm, Sr = 20.0 ppm, $^{87}Rb/^{86}Sr$ = 38.48, $^{87}Sr/^{86}Sr$ = 0.7248, calculated initial $^{87}Sr/^{86}Sr$ = 0.7093 ± 0.0005. *Collected and dated by*: M. Bikerman, Univ. of Pittsburgh. *Comment*: Sample is from one of the westernmost outcrops of outflow Bloodgood Canyon Tuff.
(biotite) 28.3 ± 1.0 m.y.
(sanidine–1) 28.3 ± 1.0 m.y.
(sanidine–2) 28.6 ± 1.0 m.y.

10. *UP–G51* K–Ar
Bloodgood Canyon Tuff (33°38′38″N, 109°01′09″W; along Forest Service Road 209, 0.8 km north of turnoff to Saddle Mountain Lookout at Hinkle Park, Blue quad., Catron Co., NM). *Analytical data*: (biotite) K_2O = 7.17%; $^{40}Ar^*$ = 3.185 × 10^{-10} mol/gm; $^{40}Ar^*/\Sigma^{40}Ar$ = 87.5%; (sanidine) K_2O = 5.90%; $^{40}Ar^*$ = 2.337 × 10^{-10} mol/gm; $^{40}Ar^*/\Sigma^{40}Ar$ = 64.3%. *Collected and dated by*: M. Bikerman, Univ. of Pittsburgh. *Comment*: Tuff is correlated with the Bloodgood Canyon Tuff on the basis of stratigraphic position, petrography, and radiometric age (Ratté, unpubl. mapping 1976).
(biotite) 30.6 ± 1.0 m.y.
(sanidine) 27.3 ± 1.3 m.y.

11. *UP–G58* K–Ar
Shelley Peak Tuff (33°38′31.2″N, 109°01′07″W; sec 4, T8S, R21W; below Forest Service Road 209 in Hinkle Park, Blue quad., Catron Co., NM). *Analytical data*: K_2O = 7.79%; $^{40}Ar^*$ = 3.403 × 10^{-10} mol/gm; $^{40}Ar^*/\Sigma^{40}Ar$ = 68%. *Collected and dated by*: M. Bikerman, Univ. of Pittsburgh. *Comment*: At this locality, Shelley Peak Tuff underlies the Bloodgood Canyon Tuff of Entry 10.
(biotite) 30.1 ± 1.0 m.y.

12. *Ratté et al., 1969, no. BR–89R* K–Ar
Andesite (33°23′43″N, 109°19′55″W; outcrop along US–666, Blue Range, Rose Peak quad., Greenlee Co., AZ). *Analytical data*: K_2O = 0.619%; $^{40}Ar^*$ = 0.345 × 10^{-10} mol/gm; $^{40}Ar^*/\Sigma^{40}Ar$ = 18%. *Collected by*: J. C. Ratté. *Dated by*: P. E. Damon, Univ. of Arizona (Damon and Assoc., 1969, p. 49, sample PED–33–67). *Comment*: Pyroxene–hornblende andesite is the basal unit of the volcanic sequence exposed in this area.
(hornblende) 38.3 ± 3.9 m.y.

13. *Damon and Assoc., 1970, no. BR–120B* K–Ar
Andesite (33°25′06″N, 109°17′07″W; along Rousensock Creek, Blue Range, Rose Peak quad., Greenlee Co., AZ). *Analytical data*: K_2O = 0.587%; $^{40}Ar^*$ = 0.308 × 10^{-10} mol/gm; $^{40}Ar^*/\Sigma^{40}Ar$ = 24%. *Collected by*: J. C. Ratté. *Dated by*: P. E. Damon, Univ. of Arizona (Damon and Assoc., 1970, p. 40, sample PED–9–69). *Comment*: Pyroxene–hornblende andesite flow or sill is part of an andesite volcano centered near Brigham Peak; it correlates with the andesite of Entry 12.
(hornblende) 36.1 ± 2.7 m.y.

14. *Ratté et al., 1969, no. BR–109A* K–Ar
Vitrophyre (33°23′39″N, 109°12′58″W; along Rousensock Creek, below junction with Thomas Creek, Blue Range, Dutch Blue Creek quad., Greenlee Co., AZ). *Analytical data*: K_2O = 7.71%; $^{40}Ar^*$ = 2.67 × 10^{-10} mol/gm; $^{40}Ar^*/\Sigma^{40}Ar$ = 50%. *Collected by*: J. C. Ratté. *Dated by*: P. E. Damon, Univ. of Arizona (Damon and Assoc., 1968, p. 44, sample PED–36–67). *Comment*: Perlitic vitrophyre is part of a quartz-latite–rhyolite dome complex that is younger than the andesite unit of Entries 12 and 13.
(biotite) 23.9 ± 0.7 m.y.

15. *Ratté et al., 1969, no. BR–89A* K–Ar
Basaltic andesite (33°26′40″N, 109°22′10″W; roadcut at junction of road to Rose Peak Lookout Tower and US–666, Blue Range, Rose Peak quad., Greenlee Co., AZ). *Analytical data*: K_2O = 2.43%; $^{40}Ar^*$ = 0.841 × 10^{-10} mol/gm; $^{40}Ar^*/\Sigma^{40}Ar$ = 64%. *Collected by*: J. C. Ratté. *Dated by*:

P. E. Damon, Univ. of Arizona (Damon and Assoc., 1968, p. 44, sample PED–32–67). *Comment*: This is a minimum age for the youngest major andesite flow unit in this area.

(whole-rock) 23.9 ± 0.7 m.y.

16. *Ratté, 1982, table 2, no. VI (no. BL–55–80)* Fission-track
Rhyolite intrusion(?) (33°12′13″N, 109°08′09″W; NE¼ sec. 3, T3S, R32E; west side of San Francisco River opposite mouth of Harden Cienega, Big Lue Mountains quad., Greenlee Co., AZ). *Analytical data*: (6 zircons) P_s = 2.29 × 10^6 tracks/cm^2 (393); P_i = 4.40 × 10^6 tracks/cm^2 (377); ϕ = 1.06 × 10^{15} n/cm^2; U = 130 ppm. *Comment*: Gray porphyritic rock contains about 5% phenocrysts, mainly 1–3 mm pink alkali feldspar and 1–2 mm brown biotite, both too altered for K–Ar age analysis. Rhyolite is mapped as part of the volcanic rocks of Indian Creek (Ratté, 1982), which apparently are the oldest volcanic rocks exposed along the San Francisco River between Glenwood, NM, and the Blue River.

(zircon) 33.0 ± 4.8 m.y.

17. *USGS(D)–BL–64–82* K–Ar
Andesite (33°01′18″N, 109°07′08″W; sec. 2, T5S, R31E; northwest flank of hill 5413, north of Lop Ear Creek, Big Lue Mountains quad., Greenlee Co., AZ). *Analytical data*: K_2O = 2.72, 2.70%; $^{40}Ar^*$ = 1.097 × 10^{-10} mol/gm; $^{40}Ar^*/\Sigma^{40}Ar$ = 91%. *Comment*: Massive, fine-grained andesite forms a small dome that may mark a local eruptive center of the amygdaloidal andesite sequence that overlies Bloodgood Canyon Tuff in the Big Lue Mountains quad.

(whole-rock) 27.9 ± 1.0 m.y.

18. *USGS(D)–BL–85–79* K–Ar
Rhyolite of Hells Hole (Ratté and Hedlund, 1981) (33°02′10″N, 109°06′46″W; sec. 36, T4S, R31W; at 5,131-ft elevation on ridge south of Black Jack Spring, Big Lue Mountains quad., Greenlee Co., AZ). *Analytical data*: K_2O = 1.12, 1.17, 1.22, 1.22%; $^{40}Ar^*$ = 0.4869 × 10^{-10} mol/gm; $^{40}Ar^*/\Sigma^{40}Ar$ = 78%. *Comment*: Fine-grained intrusive–extrusive domal rhyolite contains sparse sodic-plagioclase and rare biotite phenocrysts.

(plagioclase) 28.4 ± 1.0 m.y.

19. *USGS(D)–BL–48–82* K–Ar
Rhyolite of Hells Hole (Ratté and Hedlund, 1981) (33°01′00″N, 109°08′17″W; NE¼ sec. 10, T5S, R31E; east of AZ–78, south of Black Jack Canyon, Big Lue Mountains quad., Greenlee Co., AZ). *Analytical data*: (biotite) K_2O = 8.22, 8.20, 8.03, 8.08%; $^{40}Ar^*$ = 3.151 and 3.242 × 10^{-10} mol/gm; $^{40}Ar^*/\Sigma^{40}Ar$ = 29, 81%; (plagioclase) K_2O = 1.00, 0.97, 1.05, 0.98%; $^{40}Ar^*$ = 0.4812 and 0.4761 × 10^{-10} mol/gm; $^{40}Ar^*/\Sigma^{40}Ar$ = 81, 50%. *Comment*: Dated sample is a rhyolite vitrophyre from an intrusive(?) contact. The plagioclase age is apparently too old when compared to other ages obtained from presumed correlatives of this rhyolite.

(biotite) 27.1 ± 1.0 m.y.
(plagioclase) 32.9 ± 1.2 m.y.

20. *USGS(D)–BL–117–81* Fission-track
Rhyolite of Hells Hole (Ratté and Hedlund, 1981) (33°03′36″N, 109°04′22″W; east of AZ–78 and in west bank of White Mule Creek, Big Lue Mountains quad., Greenlee Co., AZ). *Analytical data*: (6 zircons) P_s = 2.68 × 10^6 tracks/cm^2 (484); P_i = 5.45 × 10^6 tracks/cm^2 (492); ϕ = 0.976 × 10^{15} n/cm^2; U = 180 ppm. *Comment*: Fine-grained lithophysal rhyolite with minor plagioclase phenocrysts.

(zircon) 28.7 ± 3.7 m.y.

21. *USGS(D)–BL–11–81* K–Ar, Fission-track
Rhyolite dike (33°04′15″N, 109°12′07″W; SW¼ sec. 19, T3S, R31E; lower end of talus slope on east flank of Chalk Peak, Big Lue Mountains quad., Greenlee Co., AZ). *Analytical data*: (biotite) K_2O = 5.93, 5.96%; $^{40}Ar^*$ = 2.466 × 10^{-10} mol/gm; $^{40}Ar^*/\Sigma^{40}Ar$ = 66%; (6 zircons) P_s = 5.31 × 10^6 tracks/cm^2 (787); P_i = 10.27 × 10^6 tracks/cm^2 (762); ϕ = 0.828 × 10^{15} n/cm^2; U = 390 ppm. *Comment*: Porphyritic rhyolite dike is petrographically similar to and probably correlates with conspicuous rhyolite plugs that constitute the White Peaks in this area. Age appears to be the same as the rhyolite of Hells Hole.

K–Ar (biotite) 28.6 ± 1.0 m.y.
Fission-track (zircon) 25.5 ± 2.6 m.y.

22. *USGS(D)–BL–47–81* K–Ar, Fission-track
Rhyolite dike (33°03′13″N, 109°13′45″W; near center of sec. 26, T4S, R30E; east side of Soapbox Canyon, Big Lue Mountains quad., Greenlee Co., AZ). *Analytical data*: (biotite) K_2O = 8.90, 8.86%; $^{40}Ar^*$ = 3.653 × 10^{-10} mol/gm; $^{40}Ar^*/\Sigma^{40}Ar$ = 82%; (6 zircons) P_s = 2.27 × 10^6 tracks/cm^2 (484); P_i = 5.13 × 10^6 tracks/cm^2 (546); ϕ = 0.988 × 10^{15} n/cm^2; U = 160 ppm; (50 apatites) P_s = 0.054 × 10^6 tracks/cm^2 (113); P_i = 0.138 × 10^6 tracks/cm^2 (288); ϕ = 0.883 × 10^{15} n/cm^2; U = 5.0 ppm. *Comment*: The porphyritic rhyolite dike with biotite and plagioclase phenocrysts cuts the Cooney Tuff (~33 m.y.). The biotite and zircon ages indicate that the dike is close in age to the rhyolite of Hells Hole; the apatite age suggests a later thermal event.

K–Ar (biotite) 28.4 ± 1.0 m.y.
Fission-track (zircon) 26.1 ± 3.2 m.y.
Fission-track (apatite) 20.7 ± 6.0 m.y.

23. *USGS(D)–BL–392–81* K–Ar
Rhyolite (33°06′17″N, 109°10′09″W; sec. 8, T4S, R31E; ~1 km northwest of Rattlesnake Gap, Big Lue Mountains quad., Greenlee Co., AZ). *Analytical data*: K_2O = 4.13, 4.15%; $^{40}Ar^*$ = 1.652 × 10^{-10} mol/gm; $^{40}Ar^*/\Sigma^{40}Ar$ = 69%. *Comment*: Rhyolite plug or dome is part of the volcanic sequence in the Big Lue Mountains. Analyzed material is a separate of subvitreous groundmass.

(whole-rock) 27.5 ± 1.0 m.y.

24. *Ratté and Hedlund, 1981* Fission-track
(USGS(D)–BL–148a–79)
Rhyolitic flow (33°02′10″N, 109°00′10″W; sec. 34, T14S, R21W; North Sawmill Creek, Big Lue Mountains quad., Grant Co., NM). *Analytical data*: (6 zircons) P_s = 1.07 × 10^6 tracks/cm² (178); P_i = 2.82 × 10^6 tracks/cm² (235); ϕ = 1.22 × 10^{15} n/cm²; U = 67 ppm. *Comment*: Flow correlates with porphyritic rhyodacite and rhyolite lava flows (unit Tsr) of Ratté and Brooks (1983).

(zircon) 27.6 ± 5.5 m.y.

25. *USGS(D)–BL–20–80* Fission-track
Tuff (33°13′58″N, 109°10′11″W; along jeep trail east of Salt Ground Canyon, Big Lue Mountains quad., Greenlee Co., AZ). *Analytical data*: (6 zircons) P_s = 2.76 × 10^6 tracks/cm² (472); P_i = 5.81 × 10^6 tracks/cm² (498); ϕ = 1.01 × 10^{15} n/cm²; U = 180 ppm. *Comment*: Bedded, pumiceous tuff, which may be partly reworked, is interlayered with mafic flows and volcaniclastic rocks. The zircon age is questionable because the sequence in which the tuff is interlayered is believed to be several million years younger than indicated by the fission-track age.

(zircon) 28.6 ± 3.7 m.y.

26. *USGS(D)–BL–321–81* K–Ar
Rhyodacite (33°13′16″N, 109°14′29″W; T2S, R30E; about 1 km west of Pat Creek and northwest of hill 4949, Big Lue Mountains quad., Greenlee Co., AZ). *Analytical data*: K_2O = 0.90, 0.91%; $^{40}Ar^*$ = 0.3654 × 10^{-10} mol/gm; $^{40}Ar^*/\Sigma^{40}Ar$ = 72%. *Comment*: Biotite-bearing dome–flow complex is part of the volcanic rocks of Bird Canyon. These rocks form a deeply eroded composite volcano north of the San Francisco River in the northwestern part of the Big Lue Mountains quad. (Ratté, unpubl. mapping 1981). Mafic phenocrysts are oxidized and altered. Dated plagioclase separate was treated with nitric acid to dissolve secondary carbonate.

(plagioclase) 27.8 ± 1.6 m.y.

27. *USGS(D)–BL–322–81* K–Ar
Rhyodacite (33°13′13″N, 109°14′27″W; T2S, R30E; about 1 km west of Pat Creek and northwest of hill 4949, Big Lue Mountains quad., Greenlee Co., AZ). *Analytical data*: (biotite) K_2O = 7.64, 7.61%; $^{40}Ar^*$ = 3.366 × 10^{-10} mol/gm; $^{40}Ar^*/\Sigma^{40}Ar$ = 87%; (plagioclase) K_2O = 0.60, 0.65, 0.61, 0.57%; $^{40}Ar^*$ = 0.2264 × 10^{-10} mol/gm; $^{40}Ar^*/\Sigma^{40}Ar$ = 67%. *Comment*: Biotite-bearing rhyodacitic dome–flow complex is part of the volcanic rocks of Bird Canyon. Sample represents a fresher, more biotite-rich facies than sample BL–321–81 (Entry 26).

(biotite) 30.4 ± 1.1 m.y.
(plagioclase) 25.7 ± 1.6 m.y.

28. *USGS(D)–BL–333–81* K–Ar
Rhyolitic tuff (33°11′35″N, 109°14′19″W; sec. 10, T3S, R30E; east side of Orejana Canyon, Big Lue Mountains quad., Greenlee Co., AZ). *Analytical data*: K_2O = 8.23, 8.22%; $^{40}Ar^*$ = 3.340 × 10^{-10} mol/gm; $^{40}Ar^*/\Sigma^{40}Ar$ = 76%. *Comment*: Tuff is interlayered with flows and breccias of the volcanic rocks of Bird Canyon.

(biotite) 28.0 ± 1.0 m.y.

29. *USGS(D)–BL–102–80* Fission-track
Rhyolite pumice (33°06′57″N, 109°00′11″W; roadcut on NM–78, east of junction with Harden Cienega Road to Traynor Ranch, Big Lue Mountains quad., Grant Co., NM). *Analytical data*: (4 zircons) P_s = 4.64 × 10^6 tracks/cm² (451); P_i = 10.57 ± 10^6 tracks/cm² (514); ϕ = 1.01 × 10^{15} n/cm²; U = 330 ppm. *Comment*: Pumice is out of a pyroclastic flow believed to be related to the rhyolite of Mule Creek (Ratté and Hedlund, 1981), but age is discordant with other ages obtained from that rhyolite (Entries 34, 35, and 36). Pyroclastic flow is same as Trp unit of Rhodes and Smith (1972).

(zircon) 26.5 ± 3.4 m.y.

30. *USGS(D)–BL–95–82* K–Ar
Intrusive andesite (33°02′22″N, 109°08′15″W; SE¼ sec. 34, T4S, R31E; Rustlers Canyon, Big Lue Mountains quad., Greenlee Co., AZ). *Analytical data*: (upgraded plagioclase) K_2O = 1.90, 1.85%; $^{40}Ar^*$ = 0.8039 × 10^{-10} mol/gm; $^{40}Ar^*/\Sigma^{40}Ar$ = 73%; (plagioclase) K_2O = 2.14, 2.12%; $^{40}Ar^*$ = 0.8876 × 10^{-10} mol/gm; $^{40}Ar^*/\Sigma^{40}Ar$ = 66%. *Comment*: The geologic relationships of this coarsely porphyritic andesite, which intrudes the rhyolite of Hells Hole, and its petrographic character suggest a correlation with the intrusive andesite of Tillie Hall Canyon (Entry 43), even though the plagioclase ages of the andesites are decidedly discordant.

(upgraded plagioclase) 29.5 ± 1.1 m.y.
(plagioclase) 28.7 ± 1.1 m.y.

31. *USGS(D)–BL–375–81* K–Ar
Andesite (33°07′18″N, 109°11′20″W; sec. 6, T4S,

R31E; north end of Brushy Mountain, Big Lue Mountains quad., Greenlee Co., AZ). *Analytical data*: K_2O = 1.10, 1.08%; $^{40}Ar^*$ = 0.3941 × 10^{-10} mol/gm; $^{40}Ar^*/\Sigma^{40}Ar$ = 63%. *Comment*: This coarsely porphyritic andesite flow was probably fed by dikes such as the one described in Entry 32.

(plagioclase) 25.0 ± 0.9 m.y.

32. *USGS(D)–BL–389–81* K–Ar
Andesite (33°06′12″N, 109°08′33″W; sec. 10, T4S, R31E; about 1.6 km northwest of 6-Shooter Gap, Big Lue Mountains quad., Greenlee Co., AZ). *Analytical data*: K_2O = 1.12, 1.14%; $^{40}Ar^*$ = 0.4293 × 10^{-10} mol/gm; $^{40}Ar^*/\Sigma^{40}Ar$ = 44%. *Comment*: One of several northwest-trending porphyritic andesitic dikes that mark a probable feeder rift zone for andesitic lava flows in this area.

(plagioclase) 26.2 ± 1.0 m.y.

33. *Ratté and Hedlund, 1981* K–Ar
(USGS(D)–BL–88–79)
Porphyritic hornblende dacite of Tennessee Creek (33°06′05″N, 109°02′00″W; sec. 8, T14S, R21W; north side of Tennessee Creek, Big Lue Mountains quad., Grant Co., NM). *Analytical data*: K_2O = 0.72, 0.73%; $^{40}Ar^*$ = 0.2291 × 10^{-10} mol/gm; $^{40}Ar^*/\Sigma^{40}Ar$ = 58%. *Comment*: Dacite forms domal flows that are overlain by the rhyolite of Mule Creek. Domal flows correlate with the pyroxene-bearing quartz-latite domes and flows of Rhodes and Smith (1972). Also see plagioclase age (21.3 ± 1.8 m.y.) from same dacite (Entry 195).

(hornblende) 21.8 ± 1.4 m.y.

34. *Weber and Bassett, 1963, no. 2* K–Ar
Weber, 1971, no. B/NMBM–361C–KA1
Obsidian (33°06′29″N, 109°02′44″W; SE1/4 sec. 6, T14S, R21W; Big Lue Mountains quad., Grant Co., NM). *Analytical data*: K_2O = 4.98%; $^{40}Ar^*$ = 1.366 × 10^{-10} mol/gm; $^{40}Ar^*/\Sigma^{40}Ar$ = 60%. *Comment*: The obsidian occurs as Apache tear nodules (marekanites) in the rhyolite of Mule Creek (Ratté and Brooks, 1983), which is the same as Mule Mountain Rhyolite of Rhodes and Smith (1972).

(glass) 19.0 ± 0.9 m.y.

35. *USGS(D)–BL–202–82* K–Ar
Obsidian (33°04′00″N, 109°01′25″W; SW1/4 sec. 21, T14S, R21W; head of Mule Creek, Big Lue Mountains quad., Grant Co., NM). *Analytical data*: K_2O = 4.67, 4.66%; $^{40}Ar^*$ = 1.233 × 10^{-10} mol/gm; $^{40}Ar^*/\Sigma^{40}Ar$ = 81%. *Comment*: Obsidian nodules (marekanites) are from the base of the rhyolite of Mule Creek, near vent at the head of Mule Creek (Ratté and Hedlund, 1981).

(glass) 18.3 ± 0.7 m.y.

36. *Ratté, 1982, table 2, no. 1 (no. BL–2–77)* K–Ar
Obsidian (33°10′48″N, 109°00′10″W; sec. 10, T13S, R21W; 1 km south of tank on Antelope Creek, Big Lue Mountains quad., Grant Co., NM). *Analytical data*: K_2O = 4.79, 4.83%; $^{40}Ar^*$ = 1.230 × 10^{-10} mol/gm; $^{40}Ar^*/\Sigma^{40}Ar$ = 93%. *Comment*: This age was mistakenly listed as a zircon fission-track age (Ratté, 1982). The ages of obsidian nodules (marekanites, Apache tears) in the rhyolite of Mule Creek (Ratté and Brooks, 1983) from separate vents in the Traynor Ranch area (this Entry and Entry 34), the vent at the head of Mule Creek (Entry 35), and the domal center in the Mule Mountains (Entry 44) indicate that all three eruptive centers were essentially contemporaneous.

(glass) 17.7 ± 0.6 m.y.

37. *USGS(D)–BL–209–81* K–Ar
Rhyolite at Coal Creek (33°10′01″N, 109°07′04″W; sec. 14, T3S, R31E; west side of Coal Creek at about 4,900-ft elevation, Big Lue Mountains quad., Greenlee Co., AZ). *Analytical data*: K_2O = 5.15, 5.13%; $^{40}Ar^*$ = 1.411 × 10^{-10} mol/gm; $^{40}Ar^*/\Sigma^{40}Ar$ = 87%. *Comment*: Sparsely porphyritic rhyolite from a plug that fed a local rhyolite flow and pyroclastic rocks exposed in the northeast slopes of Dix Mesa.

(whole-rock) 19.0 ± 0.7 m.y.

38. *USGS(D)–BL–253B–81* K–Ar
Basalt (33°08′54″N, 109°03′45″W; on ridge northeast of Grassy Mountain, southwest of hill 6186 at end of jeep trail, Big Lue Mountains quad., Greenlee Co., AZ). *Analytical data*: K_2O = 1.71, 1.66%; $^{40}Ar^*$ = 0.4644 × 10^{-10} mol/gm; $^{40}Ar^*/\Sigma^{40}Ar$ = 70%. *Comment*: Dike-fed hawaiite flow overlying the pyroclastic rocks of the rhyolite of Mule Creek.

(whole-rock) 19.0 ± 1.2 m.y.

39. *USGS(D)–BL–204A–82* K–Ar
Olivine basalt (33°11′00″N, 109°02′43″W; sec. 7, T13S, R21W; south side of Antelope Creek, Big Lue Mountains quad., Catron Co., NM). *Analytical data*: K_2O = 0.88, 0.87%; $^{40}Ar^*$ = 0.2414 × 10^{-10} mol/gm; $^{40}Ar^*/\Sigma^{40}Ar$ = 74%. *Comment*: Fine-grained olivine basalt (sparse olivine phenocrysts) overlying rhyolitic pyroclastic rocks associated with domes of the rhyolite of Mule Creek.

(whole-rock) 19.1 ± 1.1 m.y.

40. *Ratté and Brooks, 1983,* Fission-track
map locality no. 5 (USGS(D)–MC–164–80)
Rhyolite of Hells Hole (33°00′54″N, 108°56′28″W; sec. 7, T15S, R20W; head of Racetrack Canyon, Mule Creek quad., Grant Co., NM). *Analytical data*: (6 zircons) P_s = 2.10 × 10^6 tracks/cm^2 (427);

P_i = 4.73 × 10^6 tracks/cm^2 (482); ϕ = 1.01 × 10^{15} n/cm^2; U = 150 ppm. *Comment*: Fine-grained rhyolite with minor sodic-plagioclase and sanidine phenocrysts exposed in an erosional window in Racetrack Canyon.

(zircon) 26.7 ± 3.5 m.y.

41. *Ratté and Hedlund, 1981* K–Ar, Fission-track *(USGS(D)–MC–16–79)*
Ratté and Brooks, 1983, map locality no. 2 (USGS(D)–MC–16–79)
Rhyodacite vitrophyre (33°02′59″N, 108°59′06″W; SW1/4 sec. 26, T14S, R31W; south side of North Sawmill Creek at junction with Sawmill Creek, Mule Creek quad., Grant Co., NM). *Analytical data*: (biotite) K_2O = 8.18, 8.22%; $^{40}Ar^*$ = 3.022 × 10^{-10} mol/gm; $^{40}Ar^*/\Sigma^{40}Ar$ = 90%; (7 zircons) P_s = 0.800 × 10^6 tracks/cm^2 (100); P_i = 2.40 × 10^6 tracks/cm^2 (148); ϕ = 0.946 × 10^{15} n/cm^2; U = 73 ppm. *Comment*: Vitrophyre, consisting of about 20% phenocrysts of andesine, biotite, hornblende, and pyroxene, is from the rhyodacite and rhyolite of Sawmill Creek (Ratté and Brooks, 1983). Discordant K–Ar and fission-track ages probably indicate that the zircon fission-track age was reset by the subsequent volcanic event that produced the rhyolite of Mule Creek. Other ages for this unit (see Entry 42) are consistent with the biotite age reported here.

K–Ar (biotite) 25.4 ± 0.9 m.y.
Fission-track (zircon) 19.0 ± 5.0 m.y.

42. *Ratté and Hedlund, 1981* K–Ar, Fission-track *(USGS(D)–MC–74–79)*
Ratté and Brooks, 1983, map locality no. 3 (USGS(D)–MC–74–79)
Rhyolite dike (33°00′05″N, 108°58′20″W; between the forks of Pine Cienega Creek, Mule Creek quad., Grant Co., NM). *Analytical data*: (biotite) K_2O = 8.11, 8.16%; $^{40}Ar^*$ = 2.979 × 10^{-10} mol/gm; $^{40}Ar^*/\Sigma^{40}Ar$ = 71%; (6 zircons) P_s = 2.12 × 10^6 tracks/cm^2 (354); P_i = 5.22 × 10^6 tracks/cm^2 (435); ϕ = 1.00 × 10^{15} n/cm^2; U = 170 ppm. *Comment*: Dike is a probable feeder of rhyodacite and rhyolite flows of Sawmill Creek (Entry 41).

K–Ar (biotite) 25.3 ± 0.9 m.y.
Fission-track (zircon) 24.3 ± 3.5 m.y.

43. *Ratté and Hedlund, 1981* K–Ar, Fission-track *(USGS(D)–MC–27–79)*
Ratté and Brooks, 1983, map locality no. 1 (USGS(D)–MC–27–79)
Intrusive andesite of Tillie Hall Canyon (33°00′19″N, 108°59′28″W; NW1/4 sec. 15, T15S, R21W; on northeast side of Sawmill Creek below stock pond, Mule Creek quad., Grant Co., NM). *Analytical data*: (plagioclase) K_2O = 1.93, 1.99, 1.97, 2.00%; $^{40}Ar^*$ = 0.7086, 0.6861 × 10^{-10} mol/gm; $^{40}Ar^*/\Sigma^{40}Ar$ = 76, 67%; (apatite) P_s = 0.032 × 10^6 tracks/cm^2 (67); P_i = 0.578 × 10^6 tracks/cm^2 (260); ϕ = 1.10 × 10^{15} n/cm^2; U = 3.3 ppm. *Comment*: Stock of coarsely porphyritic andesite with turkey-track type texture of randomly oriented plagioclase phenocrysts as much as 3–6 cm long. Apatite age suggests that fission tracks were annealed during eruption of rhyolite of Mule Creek about 18 m.y. ago.

K–Ar (plagioclase) 24.5 ± 0.8 m.y.
Fission-track (apatite) 16.9 ± 4.3 m.y.

44. *Ratté and Brooks, 1983,* Fission-track *map locality no. 4 (USGS(D)–E–27–80)*
Rhyolite, Mule Mountains member, rhyolite of Mule Creek (33°06′42″N, 108°53′12″W; sec. 3, T14S, R20W; Mule Creek quad., Grant Co., NM). *Analytical data*: (6 zircons) P_s = 5.26 × 10^6 tracks/cm^2 (511); P_i = 18.99 × 10^6 tracks/cm^2 (923); ϕ = 1.07 × 10^{15} n/cm^2; U = 560 ppm. *Comment*: Rhyolite correlates with Mule Mountains Rhyolite of Rhodes and Smith (1972).

(zircon) 17.7 ± 1.9 m.y.

45. *Ratté, 1982, table 2, no. IV* K–Ar, Fission-track *(no. W–209D–80)*
Dacite of Mineral Spring Canyon (33°11′23″N, 108°53′13″W; sec. 10, T13S, R20W; south side of Outlaw Mountain, north of Mineral Spring Canyon, Wilson Mountain quad., Grant Co., NM). *Analytical data*: (biotite) K_2O = 7.45, 7.42%; $^{40}Ar^*$ = 2.814 × 10^{-10} mol/gm; $^{40}Ar^*/\Sigma^{40}Ar$ = 78%; (4 zircons) P_s = 3.54 × 10^6 tracks/cm^2 (460); P_i = 8.21 × 10^6 tracks/cm^2 (532); ϕ = 1.01 × 10^{15} n/cm^2; U = 260 ppm.

K–Ar (biotite) 26.1 ± 0.9 m.y.
Fission-track (zircon) 26.1 ± 3.3 m.y.

46. *USGS(D)–W–153A–80* Fission-track
Dacite of Mineral Spring Canyon (Ratté, 1982) (33°09′26″N, 108°54′18″W; SE1/4 sec. 21, T13S, R20W; northeast flank of Wilson Mountain, Wilson Mountain quad., Catron Co., NM). *Analytical data*: (6 zircons) P_s = 4.34 × 10^6 tracks/cm^2 (824); P_i = 10.48 × 10^6 tracks/cm^2 (995); ϕ = 1.01 × 10^{15} n/cm^2; U = 330 ppm. *Comment*: Dacitic lavas of Mineral Spring Canyon underlie and may be interlayered with Bearwallow Mountain Andesite.

(zircon) 25.0 ± 2.3 m.y.

47. *USGS(D)–W–41C–80* K–Ar
Andesite at Wilson Mountain (33°09′11″N, 108°54′48″W; SW1/4 sec. 21, T13S, R20W; west side of Wilson Mountain, Wilson Mountain quad., Grant Co., NM). *Analytical data*: K_2O = 3.44, 3.45%; $^{40}Ar^*$ = 1.233 × 10^{-10} mol/gm; $^{40}Ar^*/\Sigma^{40}Ar$ = 50%. *Comments*: Hypersthene andesite

represents the outflow from the small Wilson Mountain shield volcano.

(whole-rock) 24.7 ± 0.8 m.y.

48. *USGS(D)–W–59–80* K–Ar, Fission-track
Rhyolite at The Box (33°07′53″N, 108°55′25″W; sec. 32, T13S, R20W; along Pine Cienega Creek, Wilson Mountain quad., Grant Co., NM). *Analytical data*: (biotite) K_2O = 7.81, 7.87%; $^{40}Ar^*$ = 2.186 × 10^{-10} mol/gm; $^{40}Ar^*/\Sigma^{40}Ar$ = 64%; (plagioclase) K_2O = 3.01, 3.06%; $^{40}Ar^*$ = 0.8200 × 10^{-10} mol/gm; $^{40}Ar^*/\Sigma^{40}Ar$ = 81%; (6 zircons) P_s = 2.94 × 10^6 tracks/cm² (503); P_i = 10.04 × 10^6 tracks/cm² (860); ϕ = 1.08 × 10^{15} n/cm²; U = 290 ppm. *Comment*: Porphyritic domal rhyolite was included in "quartz latite domes" of Rhodes and Smith (1972).

K–Ar (biotite) 19.3 ± 0.7 m.y.
K–Ar (plagioclase) 18.7 ± 0.9 m.y.
Fission-track (zircon) 18.9 ± 2.1 m.y.

49. *Ratté, 1982, table 2, no. II (W–50–79)* K–Ar, Fission-track
Vitrophyre, rhyolite of Potholes Country (33°11′34″N, 108°56′49″W; sec. 7, T13S, R20W; top of ridge on north side of Mule Creek, Wilson Mountain quad., Grant Co., NM). *Analytical data*: (biotite) K_2O = 8.60, 8.56%; $^{40}Ar^*$ = 2.619 × 10^{-10} mol/gm; $^{40}Ar^*/\Sigma^{40}Ar$ = 42%; (6 zircons) P_s = 8.75 × 10^6 tracks/cm² (1,134); P_i = 27.63 × 10^6 tracks/cm² (1,791); ϕ = 1.00 × 10^{15} n/cm²; U = 880 ppm. *Comment*: Vitrophyre is about 15% phenocrysts—quartz, sanidine, plagioclase, biotite, and accessory sphene, zircon, and apatite—in contrast to nearly aphyric rhyolite of Mule Creek.

K–Ar (biotite) 21.1 ± 0.7 m.y.
Fission-track (zircon) 18.9 ± 1.4 m.y.

50. *Ratté, 1982, table 2, no. III (W–93–79)* Fission-track
Rhyolite of Potholes Country (33°10′47″N, 108°55′47″W; NW¼ sec. 17, T13S, R20W; on top of ridge south of Lost Grave Canyon, Wilson Mountain quad., Grant Co., NM). *Analytical data*: (6 zircons) P_s = 8.80 × 10^6 tracks/cm² (489); P_i = 28.58 × 10^6 tracks/cm² (794); ϕ = 1.00 × 10^{15} n/cm²; U = 910 ppm. *Comment*: Rhyolite is one of a series of porphyritic rhyolite plugs, domes, breccia pipes, and tuff rings within the west–northwest trending Potholes Country graben (Ratté, 1982).

(zircon) 18.4 ± 2.1 m.y.

51. *USGS(D)–W–105–80* K–Ar
Basalt (33°09′45″N, 108°59′47″W; NE¼ sec. 22, T13S, R21W; Wilson Mountain quad., Grant Co., NM). *Analytical data*: K_2O = 1.15, 1.21, 1.16, 1.16%; $^{40}Ar^*$ = 0.3097 × 10^{-10} mol/gm; $^{40}Ar^*/\Sigma^{40}Ar$ = 75%. *Comments*: Basalt flow, 6–7 m thick, lies beneath rhyolite of Mule Creek.

(whole-rock) 18.3 ± 0.7 m.y.

52. *USGS(D)–MN–7–80* K–Ar
Porphyritic andesite (33°10′58″N, 108°52′30″W; NE¼ sec. 14, T13S, R20W; in Burnt Stump Canyon above junction with Mineral Spring Canyon, Moon Ranch quad., Grant Co., NM). *Analytical data*: K_2O = 3.98, 3.95%; $^{40}Ar^*$ = 1.470 × 10^{-10} mol/gm; $^{40}Ar^*/\Sigma^{40}Ar$ = 85%. *Comment*: Coarsely porphyritic andesite overlies the rhyolite tuffs of Angel Roost and is overlain by the fine-grained andesite flows of Outlaw Mountain (Ratté, 1982).

(plagioclase) 25.6 ± 1.3 m.y.

53. *USGS(D)–HM–5–82* K–Ar
Quartz–alunite rock (33°15′59″N, 108°48′42″W; on hill 6881, north of Silted-Up tank, about 100 m inside Gila Wilderness boundary, Holt Mountain quad., Catron Co., NM). *Analytical data*: (alunite) K_2O = 4.29, 4.29%; $^{40}Ar^*$ = 2.104 × 10^{-10} mol/gm; $^{40}Ar^*/\Sigma^{40}Ar$ = 69%; (quartz–alunite concentrate) K_2O = 1.76, 1.76%; $^{40}Ar^*$ = 0.8182 × 10^{-10} mol/gm; $^{40}Ar^*/\Sigma^{40}Ar$ = 53%. *Comment*: A quartz–alunite–dickite rock (altered rhyolite?) from plug or dike is associated with gold–silver–molybdenum mineralization (Ratté et al., 1979) in southwest wall of Bursum caldera.

(alunite) 33.8 ± 1.2 m.y.
(quartz–alunite) 32.0 ± 1.7 m.y.

54. *USGS(D)–HM–8–80* K–Ar, Fission-track
Dacitic lava flow (33°16′47″N, 108°47′55″W; sec. 10, T12S, R19W; nose of ridge about 300 m west of Blue Jay Spring, Holt Mountain quad., Catron Co., NM). *Analytical data*: (biotite) K_2O = 7.43, 7.38%; $^{40}Ar^*$ = 3.209 × 10^{-10} mol/gm; $^{40}Ar^*/\Sigma^{40}Ar$ = 75%; (6 zircons) P_s = 2.63 × 10^6 tracks/cm² (572); P_i = 4.40 × 10^6 tracks/cm² (479); ϕ = 0.80 × 10^{15} n/cm²; U = 170 ppm. *Comment*: Porphyritic lava flow in the wall of the Bursum caldera correlates with lava flows of Gila Flat (Ratté and Gaskill, 1975), Entry 98.

K–Ar (biotite) 29.9 ± 1.1 m.y.
Fission-track (zircon) 28.5 ± 3.5 m.y.

55. *USGS(D)–HM–16–80* K–Ar, Fission-track
Ash-flow tuff (33°15′46″N, 108°47′57″W; sec. 15, T12S, R19W; ridge on west side of Dugway Canyon, Holt Mountain quad., Catron Co., NM). *Analytical data*: (biotite) K_2O = 7.78, 7.73%; $^{40}Ar^*$ = 3.212 × 10^{-10} mol/gm; $^{40}Ar^*/\Sigma^{40}Ar$ = 77%; (6 zircons) P_s = 2.06 × 10^6 tracks/cm² (372); P_i = 3.70 × 10^6 tracks/cm² (334); ϕ = 0.80 × 10^{15} n/cm²; U = 150 ppm. *Comment*: Crystal-rich, dacitic or rhyolitic ash-flow tuff may correlate

with Cooney Tuff or Shelley Peak Tuff, but alteration makes correlation and age uncertain.

K–Ar (biotite) 28.5 ± 1.0 m.y.
Fission-track (zircon) 26.7 ± 4.0 m.y.

56. *Smith et al., 1976, no. R131* Fission-track
Nabours Mountain Quartz Latite of Rhodes (1976a) (approx. 33°19′50″N, 108°47′50″W; sec. 22, T11S, R19W; Holt Mountain quad., Catron Co., NM). *Analytical data*: P_s = 251 tracks; P_i = 1,544 tracks; $\phi = 2.77 \times 10^{15}$ n/cm². *Comment*: Rhyolite lava flows, capping Nabours Mountain, overlie the Fanney Rhyolite along the ring-fracture zone of the Bursum caldera.

(sphene) 28.3 ± 3.9 m.y.

57. *UP–G84* K–Ar
Rhyolite flow (approx. 33°17′02″N, 105°47′05″W; along Holt–Apache Trail on Holt Mountain, Holt Mountain quad., Catron Co., NM). *Analytical data*: K_2O = 7.46%; $^{40}Ar^*$ = 3.0725×10^{-10} mol/gm; $^{40}Ar^*/\Sigma^{40}Ar$ = 74%. *Comment*: Dated vitrophyre is at the base of the lava flows, which, in this paper, are correlated with the Nabours Mountain Quartz Latite of Rhodes (1976a).

(sanidine) 28.4 ± 0.8 m.y.

58. *Bikerman, 1972, no. UP–G9* K–Ar
Cooney Tuff (approx. 33°22′30″N, 108°48′31″W; Power Plant Road, Holt Mountain quad., Catron Co., NM). *Analytical data*: K_2O = 8.61%; $^{40}Ar^*$ = 4.1403×10^{-10} mol/gm; $^{40}Ar^*/\Sigma^{40}Ar$ = 87%. *Comment*: Sample is from the Cooney Canyon Member of the Cooney Tuff (Ratté, 1981) as redefined from the Cooney Quartz Latite (Ferguson, 1927).

(biotite) 33.1 ± 1.5 m.y.

59. *Ratté, 1982, table 2, no. V* K–Ar, Fission-track
(no. GL–10–80)
Hornblende dacite of Goat Basin volcano (33°16′13″N, 108°58′46″W; in outcrops along road west of Holliman Camp, Glenwood quad., Catron Co., NM). *Analytical data*: (hornblende) K_2O = 0.73, 0.72%; $^{40}Ar^*$ = 0.2772×10^{-10} mol/gm; $^{40}Ar^*/\Sigma^{40}Ar$ = 56%; (plagioclase) K_2O = 0.50, 0.50%; $^{40}Ar^*$ = 0.2074×10^{-10} mol/gm; $^{40}Ar^*/\Sigma^{40}Ar$ = 47%; (6 zircons) $P_s = 2.86 \times 10^6$ tracks/cm² (437); $P_i = 6.95 \times 10^6$ tracks/cm² (531); $\phi = 1.08 \times 10^{15}$ n/cm²; U = 200 ppm. *Comment*: Hornblende dacite is from the flanks of a steep-sided cone, Goat Basin volcano, the eroded center of which forms Goat Basin. The dacite in the center of the cone is propylitically altered and is intruded by altered and weakly mineralized rhyolite dikes.

K–Ar (hornblende) 26.4 ± 1.6 m.y.
K–Ar (plagioclase) 28.6 ± 2.0 m.y.
Fission-track (zircon) 26.5 ± 3.4 m.y.

60. *USGS(D)–GL–4–82* K–Ar
Rhyolite dike (33°15′40″N, 108°57′43″W; east side of Goat Basin, Glenwood quad., Catron Co., NM). *Analytical data*: K_2O = 2.92, 2.94%; $^{40}Ar^*$ = 1.217×10^{-10} mol/gm; $^{40}Ar^*/\Sigma^{40}Ar$ = 73%. *Comment*: Sample represents an unaltered facies of small, mineralized rhyolite intrusives exposed in the deeply eroded central part of the Goat Basin volcano (Ratté, 1982). Plagioclase age indicates possible correlation with rhyolite of Hells Hole.

(plagioclase) 28.5 ± 1.0 m.y.

61. *Strangway et al., 1976, table 1, no. GB3B* K–Ar
Basaltic andesite (approx. 33°16′40″N, 108°53′20″W; NE¼ sec. 10, T12S, R20W; Brushy Mountain area, Glenwood quad., Catron Co., NM). *Comment*: Faulted andesite flows lie low along the west side of the San Francisco River where their stratigraphic position is uncertain. Age indicates that flows probably correlate with those that underlie the rhyolite dome lavas and pyroclastic rocks at Glenwood Brushy Mountain (Entry 62).

(whole-rock) 25.9 ± 0.5 m.y.

62. *USGS(D)–GL–1–82* K–Ar
Rhyolite flow (33°18′40″N, 108°53′53″W; west of the San Francisco River and the Glenwood Ranger Station, Glenwood quad., Catron Co., NM). *Analytical data*: K_2O = 4.82, 4.83%; $^{40}Ar^*$ = 1.627×10^{-10} mol/gm; $^{40}Ar^*/\Sigma^{40}Ar$ = 74%. *Comment*: Nearly aphyric, perlitic obsidian is from a rhyolite dome, which, with associated pyroclastic rocks, is sandwiched between andesite flow sequences.

(whole-rock) 23.3 ± 0.8 m.y.

63. *Ratté and Finnell, 1978* K–Ar
(USGS(D)–GL–2–74)
Olivine basalt (33°21′30″N, 108°53′52″W; sec. 11, T11S, R20W; lower part of Harve Gulch, Glenwood quad., Grant Co., NM). *Analytical data*: K_2O = 0.95, 0.94%; $^{40}Ar^*$ = 0.0762×10^{-10} mol/gm; $^{40}Ar^*/\Sigma^{40}Ar$ = 35%. *Comment*: Olivine basalt is interlayered with Gila Conglomerate.

(whole-rock) 5.6 ± 0.3 m.y.

64. *Ratté, 1981, table 2, no. 1* Fission-track
(MR–4B–76)
Whitewater Creek Member, Cooney Tuff (33°22′33″N, 108°50′04″W; sec. 5, T11S, R19W; Mogollon quad., Catron Co., NM). *Analytical data*: $P_s = 3.91 \times 10^6$ tracks/cm² (995); $P_i = 8.07 \times 10^6$ tracks/cm² (1,027); $\phi = 1.10 \times 10^{15}$ n/cm²; U = 210 ppm. *Comment*: Zircons for fission-track dating were obtained from a lithophysal zone in the lower part of a thick, simple-cooling unit of rhyolite ash-flow tuff. The Whitewater Creek

Member formerly was called Whitewater Creek Rhyolite by Ferguson (1927).

(zircon) 31.8 ± 2.8 m.y.

65. *Elston et al., 1968, table 1, no. MB–12–66* K–Ar
Cooney Tuff (sec. 4, T11S, R19W; near boundary between Mogollon and Holt Mountain quadrangles, Catron Co., NM). *Analytical data*: K_2O = 4.52%; $^{40}Ar^*$ = 1.59 × 10^{-10} mol/gm; $^{40}Ar^*/\Sigma^{40}Ar$ = 50%. *Comment*: Calculated age is too young to be the age of the tuff; it is undoubtedly related to the hydrothermal alteration of the Cooney Tuff in the vicinity of the southern margins of the Mogollon mining district.

(biotite) 24.3 ± 0.8 m.y.

66. *Damon and Assoc., 1966, table 14, no. PED–12–65* K–Ar
Livingston et al., 1968, table 3, no. 8
Cooney Tuff (approx. 33°03′20″N, 109°17′59″W; SE1/4 sec. 30, T4S, R30E; cliff outcrops behind old jailhouse in Clifton, north side of San Francisco River, Clifton quad., Greenlee Co., AZ). *Analytical data*: K_2O = 8.43, 8.46%; $^{40}Ar^*$ = 4.13 × 10^{-10} mol/gm; $^{40}Ar^*/\Sigma^{40}Ar$ = 55%. *Comment*: Outcrops are bleached and mineralized, but the bronze-colored biotite phenocrysts seem reasonably fresh. This rock was called the tuff at Clifton or Clifton tuff, an informal term by Livingston et al. (1968) and by Wahl (1980). In this paper, the tuff is correlated with the Cooney Tuff on the basis of age and mineralogy of nearby fresher outcrops to the east in the Big Lue Mountains quadrangle.

(biotite) 33.7 ± 1.0 m.y.

67. *Wahl, 1980, no. TF–4A* Fission-track
Cooney Tuff (approx. 33°03′20″N, 109°17′59″W; SE1/4 sec. 30, T4S, R30E; outcrops behind old Clifton jail, Clifton quad., Greenlee Co., AZ). *Analytical data*: P_s = 1,135 tracks; P_i = 2,132 tracks; ϕ = 1.04 × 10^{15} n/cm^2. *Comment*: Sample is from the same outcrops reported by Livingston et al. (1968); see Entry 66.

(zircon) 33.1 ± 2.8 m.y.

68. *Ratté, 1981, table 2, no. 2 (no. MR–2B–76)* Fission-track
Fall Canyon Tuff (33°23′35″N, 108°49′42″W; SW1/4 sec. 32, T11S, R19W; west side of Houston Canyon, Mogollon mining district, Mogollon quad., Catron Co., NM). *Analytical data*: P_s = 3.93 × 10^6 tracks/cm^2 (655); P_i = 8.80 × 10^6 tracks/cm^2 (733); ϕ = 1.10 × 10^{15} n/cm^2; U = 230 ppm. *Comment*: Tuff is interlayered with the Cranktown Sandstone in outcrops above the Bursum Road a few kilometers southwest of Mogollon and is correlated with the Fall Canyon Tuff (Ratté et al., 1979) on the basis of mineralogy and stratigraphic sequence. Other dated tuffs correlated with Fall Canyon Tuff are listed in Entries 95, 171, and 172. The Fall Canyon Tuff at the type locality has not been dated.

(zircon) 29.4 ± 3.1 m.y.

69. *Ratté, 1981, table 2, no. 6 (no. MR–40–74)* Fission-track
Shelley Peak Tuff (33°26′35″N, 108°48′25″W; from outcrop in north wall of Copper Creek, southwest of Negro Hill, Mogollon quad., Catron Co., NM). *Analytical data*: P_s = 3.19 × 10^6 tracks/cm^2 (974); P_i = 7.25 × 10^6 tracks/cm^2 (1,108); ϕ = 1.08 × 10^{15} n/cm^2; U = 220 ppm. *Comment*: Shelly Peak Tuff is overlain by Bloodgood Canyon Tuff at this locality.

(zircon) 28.4 ± 2.4 m.y.

70. *Ratté, 1981, table 2, no. 7 (no. MR–48E–74)* K–Ar, Fission-track
Shelley Peak Tuff (33°29′40″N, 108°45′30″W; sec. 25, T10S, R19W; north side of upper Devils Creek, north of Lost Lake Mountain, Mogollon quad., Catron Co., NM). *Analytical data*: (biotite) K_2O = 7.84, 7.84%; $^{40}Ar^*$ = 2.722, 2.662 × 10^{-10} mol/gm; $^{40}Ar^*/\Sigma^{40}Ar$ = 44, 47%; (zircon) P_s = 3.32 × 10^6 tracks/cm^2 (830); P_i = 7.59 × 10^6 tracks/cm^2 (949); ϕ = 1.05 × 10^{15} n/cm^2; U = 230 ppm. *Comment*: The Shelley Peak Tuff in these outcrops appears to be cut by a hornblende-andesite intrusive (see Entry 71), but the geologic relationships are uncertain. The discordant biotite and zircon ages listed for this sample suggest that the K–Ar system in the biotite was affected by the thermal regime accompanying the intrusion of the andesite; the zircons apparently were not so greatly affected.

K–Ar (biotite) 24.4 ± 0.8 m.y.
23.4 ± 0.8 m.y.
Fission-track (zircon) 27.3 ± 2.6 m.y.

71. *Ratté, 1981, table 2, no. 8 (no. MR–48D–74)* K–Ar
Hornblende-bearing andesite dome or intrusive (33°29′40″N, 108°45′17″W; sec. 25, T10S, R19W; north side of Devils Creek, Mogollon quad., Catron Co., NM). *Analytical data*: K_2O = 0.57, 0.59%; $^{40}Ar^*$ = 0.2556 × 10^{-10} mol/gm; $^{40}Ar^*/\Sigma^{40}Ar$ = 69%. *Comment*: The age and geologic relationships of this andesite, which forms a more extensive body to the north around Apache Peak in the O Block Canyon quadrangle (Ratté, unpubl. mapping 1976, 1977), are uncertain. As the geology is presently interpreted, the calculated age is too old, perhaps related to excess argon in the hornblende.

(hornblende) 30.4 ± 1.9 m.y.

72. *USGS(D)–MR–1–82* K–Ar
Fanney Rhyolite (33°24′25″N, 108°45′10″W; north side of Mineral Creek, elevation 6,600 ft, Mogollon quad., Catron Co., NM). *Analytical data*: K_2O = 5.09, 5.09%; $^{40}Ar^*$ = 1.983 × 10^{-10} mol/gm; $^{40}Ar^*/\Sigma^{40}Ar$ = 84%. *Comment*: Rhyolite vitrophyre at chilled contact between rhyolite intrusive and Mineral Creek Andesite contains about 10% phenocrysts of quartz and sanidine plus rare sodic plagioclase, biotite, and accessory zircon.

(sanidine) 26.9 ± 1.0 m.y.

73. *Strangway et al., 1976, table 1, no. MO1A* K–Ar
Mineral Creek Andesite (approx. 33°23′53″N, 108°49′29″W; SW1/4 sec. 32, T10S, R19W; above road to Mogollon along Houston Gulch, about 6,560-ft elevation, Mogollon quad., Catron Co., NM). *Comment*: At this locality, Mineral Creek Andesite laps onto the topographic wall of the Bursum caldera. This sample was identified as Last Chance Andesite by Strangway et al. (1976) following usage of Ferguson (1927, pl. 1); the volcanic stratigraphy was revised by Ratté (1981).

(whole-rock) 25.7 ± 0.5 m.y.

74. *Ratté, 1981, table 2, no. 4 (no. MR–81A–75)* K–Ar
Last Chance Andesite (33°25′07″N, 108°47′22″W; sec. 21, T10S, R19W; north side of Mineral Creek, about 200 m east of Queen fault at 6,400-ft elevation, Mogollon quad., Catron Co., NM). *Analytical data*: K_2O = 2.20, 2.20, 2.18, 2.14%; $^{40}Ar^*$ = 0.7895 × 10^{-10} mol/gm; $^{40}Ar^*/\Sigma^{40}Ar$ = 76%. *Comment*: Sample is from the lower part of the Last Chance Andesite where it is separated from the upper part by as much as 30 m of volcaniclastic sandstone.

(whole-rock) 25.0 ± 0.8 m.y.

75. *Ratté, 1981, table 2, no. 5 (no. MR–11C–76)* K–Ar
Last Chance Andesite (33°25′46″N, 108°48′02″W; north side of Mineral Creek, east of Queen fault at 6,600-ft elevation, Mogollon quad., Catron Co., NM). *Analytical data*: K_2O = 2.98, 2.94, 2.93, 2.87%; $^{40}Ar^*$ = 0.9852 × 10^{-10} mol/gm; $^{40}Ar^*/\Sigma^{40}Ar$ = 76%. *Comment*: Sample is from the upper part of the Last Chance Andesite, above a volcaniclastic sandstone lens that separates it from andesite described in Entry 73.

(whole-rock) 23.2 ± 0.8 m.y.

76. *Strangway et al., 1976, table 1, no. MO4B* K–Ar
Andesite (33°23′50″N, 108°45′05″W; center of sec. 36, T10S, R19W; south of Mineral Creek, Mogollon quad., Catron Co., NM). *Comment*: The location and rock description given by Strangway et al. (1976, pp. 121, 123) strongly suggest that the dated andesite probably is from the Last Chance Andesite, which caps the ridge between Mineral Creek and Spring Canyon. The calculated ages, which are much younger than the age of the Last Chance Andesite, may reflect the approximate time of hydrothermal activity, which left the rocks visibly altered. Another possibility is that the andesite is an outlier of the nearby andesite on the top of Cooney Peak, which gave an age of 15 m.y. (Entry 79).

(whole-rock) 17.7 ± 0.3 m.y.
17.6 ± 0.3 m.y.

77. *Ratté, 1981, table 2, no. 3 (no. MR–58C–74)* K–Ar, Fission-track
Andesite (33°23′46″N, 108°47′08″W; T10S, R19W; along Silver Creek, east of Mogollon, Mogollon quad., Catron Co., NM). *Analytical data*: (biotite) K_2O = 8.22, 8.18%; $^{40}Ar^*$ = 3.222 × 10^{-10} mol/gm; $^{40}Ar^*/\Sigma^{40}Ar$ = 76%; (zircon) P_s = 2.98 × 10^6 tracks/cm^2 (505); P_i = 7.04 × 10^6 tracks/cm^2 (597); ϕ = 0.930 × 10^{15} n/cm^2; U = 220 ppm; (50 apatite grains) P_s = 0.052 x 10^6 tracks/cm^2; P_i = 0.203 x 10^6 tracks/cm^2; ϕ = 0.961 × 10^{15} n/cm^2; U = 6.1 ppm. *Comment*: Andesite apparently intrudes rocks as young as Last Chance Andesite. The listed radiometric ages for this sample are not easily interpreted. The apatite age suggests that there has been a thermal event at this locality subsequent to the intrusion of the andesite. However, whether the intrusive andesite is about 23.5 m.y. old, which might be geologically acceptable, or 27.1 m.y. old, which would indicate that it is unconformably beneath the Last Chance Andesite, remains a problem.

K–Ar (biotite) 27.1 ± 0.9 m.y.
Fission-track (zircon) 23.5 ± 2.8 m.y.
Fission-track (apatite) 14.7 ± 2.7 m.y.

78. *USGS(D)–MR–34–76, MR–1A–81* K–Ar
Vein gangue (33°23′35″N, 108°48′07″W; dump of Last Chance mine, Mogollon mining district, Mogollon quad., Catron Co., NM). *Analytical data*: MR–34–76(1): K_2O = 1.08, 1.07%; $^{40}Ar^*$ = 0.2876 × 10^{-10} mol/gm; $^{40}Ar^*/\Sigma^{40}Ar$ = 48%; MR–34–76(2): K_2O = 1.48, 1.51%; $^{40}Ar^*$ = 0.3463 × 10^{-10} mol/gm; $^{40}Ar^*/\Sigma^{40}Ar$ = 48%; MR–1A–81: K_2O = 9.67, 9.63%; $^{40}Ar^*$ = 2.450 × 10^{-10} mol/gm; $^{40}Ar^*/\Sigma^{40}Ar$ = 84%. *Comment*: Vein gangue is an intimate intergrowth of quartz and adularia, in which quartz predominates. Mineralization apparently occurred about 17.5 m.y. ago at Mogollon.

MR–34–76 **(quartz–adularia)(1) 18.5 ± 0.7 m.y.**
(quartz–adularia)(2) 16.5 ± 0.6 m.y.
MR–1A–81 **(impure adularia) 17.5 ± 0.6 m.y.**

79. *Ratté, 1981 (USGS(D)–BR–10–74)* K–Ar
Basalt (33°24′56″N, 108°44′45″W; sec. 25, T1N, R19W; top of Cooney Peak, Bearwallow Mountain quad., Catron Co., NM). *Analytical data*: K_2O = 1.68, 1.60, 1.57, 1.54%; $^{40}Ar^*$ = 0.3526 × 10^{-10} mol/gm; $^{40}Ar^*/\Sigma^{40}Ar$ = 29%. *Comment*: Basalt rests on the Dog Gulch Formation, which overlies Last Chance Andesite. Whole-rock minimum age needs confirmation.
(whole-rock) 15.2 ± 0.4 m.y.

80. *USGS(D)–BW–1–82* K–Ar
Bearwallow Mountain Andesite (33°27′01″N, 108°40′03″W; along road to Bearwallow Mountain Lookout Tower, 9,840-ft elevation, Bearwallow Mountain quad., Catron Co., NM). *Analytical data*: K_2O = 2.86, 2.88%; $^{40}Ar^*$ = 0.9616 × 10^{-10} mol/gm; $^{40}Ar^*/\Sigma^{40}Ar$ = 84%. *Comment*: A finely amygdaloidal, hypersthene andesite with sparse small olivine microphenocrysts. Together with other Bearwallow Mountain andesites (Entries 81, 100, and 110), the age of this andesite from the type locality confirms the contention that the formation is older than the 20–21 m.y. age formerly assigned to it (Elston, 1976, pp. 132, 133).
(whole-rock) 23.1 ± 0.8 m.y.

81. *USGS(D)–N–1A–82* K–Ar
Bearwallow Mountain Andesite (33°27′56″N, 108°33′59″W; along road to Negrito Mountain Lookout Tower, about 1 km west of tower, 8,400-ft elevation, Negrito Mountain quad., Catron Co., NM). *Analytical data*: K_2O = 3.29, 3.29%; $^{40}Ar^*$ = 1.220 × 10^{-10} mol/gm; $^{40}Ar^*/\Sigma^{40}Ar$ = 89%. *Comment*: Fine-grained, gray, olivine-rich andesite or basaltic andesite from an eruptive center near Negrito Mountain (Coney, 1976, fig. 1).
(whole-rock) 25.6 ± 0.9 m.y.

82. *Weber and Bassett, 1963, table 1, no. 4* K–Ar
Weber, 1971, no. B/NMBM–338A–KA1
Rhyolitic vitrophyre (33°28′50″N, 108°30′52″W; W1/2 sec. 32, T9S, R16W; trail crossing at Ewe Canyon, Negrito Mountain quad., Catron Co., NM). *Analytical data*: K_2O = 4.84%; $^{40}Ar^*$ = 1.942 × 10^{-10} mol/gm (calculated from data listed by Weber, 1971); $^{40}Ar^*/\Sigma^{40}Ar$ = 79, 79%. *Comment*: Mapped as Jerky Mountains Rhyolite by Coney (1976, fig. 1).
(glass) 27.6 ± 1.8 m.y.

83. *Bikerman and New, 1982, no. UP–G81* K–Ar
Dacite (33°26′06″N, 108°35′26″W; SE1/4 sec. 16, T10S, R17W; crops out northeast of junction of NM–78 and Forest Road 142, Negrito Mountain quad., Catron Co., NM). *Analytical data*: (bronze biotite) K_2O = 7.51%; $^{40}Ar^*$ = 3.0471 × 10^{-10} mol/gm; $^{40}Ar^*/\Sigma^{40}Ar$ = 63%; (black biotite) K_2O = 8.25% (avg. of 2 runs); $^{40}Ar^*$ = 3.284 × 10^{-10} mol/gm (avg. of 2 runs); $^{40}Ar^*/\Sigma^{40}Ar$ = 51%. *Comment*: Dacite has large sanidine phenocrysts with plagioclase cores; also present are biotite, quartz, apatite, rare green hornblende, and corroded pyroxene crystals in a devitrified matrix. Black biotite contains significantly more potassium and magnesium than the coexisting bronze biotite. Dacite is correlated with porphyritic latite of Willow Creek (Coney, 1976, pp. 31–32).
(bronze biotite) 27.9 ± 0.5 m.y.
(black biotite) 27.5 ± 0.5 m.y.

84. *Elston et al., 1973, table 1, no. 6* K–Ar
Apache Spring Tuff (33°22′12″N, 108°43′25″W; sec. 5, T11S, R18W; NM–78 roadcut, Grouse Mountain quad., Catron Co., NM). *Analytical data*: K_2O = 7.35%; $^{40}Ar^*$ = 2.98 × 10^{-10} mol/gm; $^{40}Ar^*/\Sigma^{40}Ar$ = 63%. *Comment*: Densely welded ash-flow tuff from within the Bursum caldera.
(biotite) 27.9 ± 0.8 m.y.

85. *Ratté et al., 1984, table 6, no. 30 (MR–5–76)* K–Ar, Fission-track
Apache Spring Tuff (33°22′17″N, 108°43′09″W; sec. 5, T11S, R18W; switchback roadcut on NM–78, about 1.6 km west of Silver Divide, Grouse Mountain quad., Catron Co., NM). *Analytical data*: (biotite) K_2O = 7.65, 7.64%; $^{40}Ar^*$ = 3.118 × 10^{-10} mol/gm; $^{40}Ar^*/\Sigma^{40}Ar$ = 67%; (zircon) P_s = 1.84 × 10^6 tracks/cm^2 (478); P_i = 4.13 × 10^6 tracks/cm^2 (535); ϕ = 1.10 × 10^{15} n/cm^2; U = 110 ppm. *Comment*: Densely welded ash-flow tuff from within the Bursum caldera.
K–Ar (biotite) 28.1 ± 1.0 m.y.
Fission-track (zircon) 29.3 ± 3.6 m.y.

86a. *Ratté et al., 1984, table 6, no. 28 (GR–225)* Fission-track
Apache Spring Tuff (33°22′12″N, 108°43′24″W; NM–78 (Bursum Road), Grouse Mountain quad., Catron Co., NM). *Analytical data*: See Table 9.
(sphene) 29.9 ± 4.6 m.y.

86b. *Ratté et al., 1984, table 6, no. 29 (MO–11–67)* Fission-track
Apache Spring Tuff (33°22′12″N, 108°43′24″W; NM–78 (Bursum Road), Grouse Mountain quad., Catron Co., NM). *Analytical data*: See Table 9.
(sphene) 28.5 ± 5.6 m.y.

86c. *Ratté et al., 1984, table 6, no. 31 (MO–13–67)* Fission-track
Apache Spring Tuff (33°22′26″N, 108°38′25″W; NM–78 (Bursum Road), Grouse Mountain quad., Catron Co., NM). *Analytical data*: See Table 9.
(sphene) 30.0 ± 4.8 m.y.

TABLE 9—Fission-track data for sphenes from four samples of Apache Spring Tuff from within Bursum caldera (Entries 86a, 86b, 86c, and 86d). The low uranium content of the sphene grains analyzed (4–5 grains per sample) accounts for the large uncertainty in age.

Sample no.	P_s tracks/cm² (tracks counted)	P_i tracks/cm² (tracks counted)	ϕ n/cm²	U ppm	Age m.y.
GR–225	0.197×10^6 (213)	1.44×10^6 (779)	3.66×10^{15}	12	29.9 ± 4.6
MO–11–67	0.157×10^6 (131)	1.27×10^6 (482)	3.66×10^{15}	11	28.5 ± 5.6
MO–13–67	0.209×10^6 (200)	1.52×10^6 (729)	3.66×10^{15}	13	30.0 ± 4.8
MO–14–67	0.186×10^6 (202)	1.53×10^6 (731)	3.66×10^{15}	13	30.2 ± 4.8

86d. *Ratté et al., 1984, table 6, no. 32 (MO–14–67)* Fission-track
Apache Spring Tuff (33°22′55″N, 108°38′00″W; NM–78 (Bursum Road), Bearwallow Mountain quad., Catron Co., NM). *Analytical data*: See Table 9.

(sphene) 30.2 ± 4.8 m.y.

87. *Ratté et al., 1984, table 7, no. 6 (GR–194)* Fission-track
Quartz-porphyry dike (33°11′02″N, 108°40′13″W; at bend in Rain Creek, about 300 m up creek from Gold Spar mine, Rice Ranch quad., Grant Co., NM). *Analytical data*: (4 sphenes) $P_s = 0.504 \times 10^6$ tracks/cm² (294); $P_i = 2.32 \times 10^6$ tracks/cm² (678); $\phi = 2.05 \times 10^{15}$ n/cm²; U = 35 ppm. *Comment*: A 10–15-m-thick dike, trending N60°W and dipping about 55°SW, is in northwest-trending structural zone along southwest front of Mogollon Mountains, adjacent to ring-fracture zone of Bursum caldera.

(sphene) 26.6 ± 3.7 m.y.

88. *Bikerman, 1972, no. UP–G2* K–Ar
Cooney Tuff (33°10′53″N, 108°40′02″W; S½ sec. 11, T13S, R18W; east side of Rain Creek above Gold Spar mine, Rice Ranch quad., Grant Co., NM). *Analytical data*: K_2O = 1.01%; $^{40}Ar^*$ = 0.4966×10^{-10} mol/gm; $^{40}Ar^*/\Sigma^{40}Ar$ = 79%. *Comment*: Dark, crystal-rich, highly propylitized ash-flow tuff correlated with the Cooney Tuff (Ratté, 1981) by stratigraphic position, phenocryst mineralogy, and chemical composition.

(plagioclase) 34 ± 2 m.y.

89. *Ratté and Gaskill, 1975, map locality SA–5* K–Ar, Fission-track
Marvin and Dobson, 1979, entry no. 209 (GR–162DD)
Quartz-porphyry dike (33°08′06″N, 108°33′21″W; north edge of sec. 36, T13S, R17W; at the head of Davis Canyon, Shelley Peak quad., Grant Co., NM). *Analytical data*: (biotite) K_2O = 6.70, 6.62%; $^{40}Ar^*$ = 2.728×10^{-10} mol/gm; $^{40}Ar^*/\Sigma^{40}Ar$ = 67%; (sanidine) K_2O = 7.84, 7.75%; $^{40}Ar^*$ = 3.034×10^{-10} mol/gm; $^{40}Ar^*/\Sigma^{40}Ar$ = 84%; (sphene) $P_s = 0.259 \times 10^6$ tracks/cm² (195); $P_i = 1.354 \times 10^6$ tracks/cm² (507); $\phi = 2.41 \times 10^{15}$ n/cm²; U = 18 ppm. *Comment*: Dike, about 3 km long, extends out from a rhyolite dome–flow complex in the Diablo Range.

K–Ar (biotite) 28.2 ± 1.0 m.y.
K–Ar (sanidine) 26.8 ± 0.9 m.y.
Fission-track (sphene) 27.8 ± 2.7 m.y.

90. *Ratté and Gaskill, 1975, map locality SA–3* K–Ar
Marvin and Dobson, 1979, entry no. 211 (GR–185)
Dacite or latite, volcanic complex of Brock Canyon (33°02′18″N, 108°30′05″W; SW¼ sec. 33, T14S, R16W; about 50 m northwest of Clum shaft, Canteen Canyon quad., Grant Co., NM). *Analytical data*: K_2O = 7.72, 7.79%; $^{40}Ar^*$ = 3.575×10^{-10} mol/gm; $^{40}Ar^*/\Sigma^{40}Ar$ = 60%. *Comment*: Porphyritic dacitic to latitic lavas of this complex are host to the quartz–fluorite veins of the Gila fluorspar district and molybdenum mineralization associated with an elliptical alteration halo about 3 km long, along the Gila River at the south edge of the Gila Wilderness. The dated biotite of this sample may have been affected by the thermal regime accompanying the hydrothermal event that produced the alteration and mineralization.

(biotite) 31.7 ± 0.8 m.y.

91. *Ratté and Gaskill, 1975, map locality SA–4* K–Ar
Marvin and Dobson, 1979, entry no. 212 (GR–186)
Dacite or latite, volcanic complex of Brock Canyon (33°02′18″N, 108°30′06″W; SW¼ sec. 33, T14S, R6W; about 200 m west of Clum shaft, Canteen Canyon quad., Grant Co., NM). *Analytical data*: K_2O = 8.15, 8.11%; $^{40}Ar^*$ = 3.956×10^{-10} mol/gm; $^{40}Ar^*/\Sigma^{40}Ar$ = 74%. *Comment*: Porphyritic dacite or latite is another sample of the flows of the volcanic complex (see Entry 90). This sample is farther from the Clum quartz–

fluorite vein than sample GR–185 (Entry 90), and the dated biotite grains vary from fresh to quite altered.

(biotite) 33.5 ± 0.8 m.y.

92. *USGS(D)–GR–190* Fission-track
Dacite or latite, volcanic complex of Brock Canyon (33°04′33″N, 108°30′16″W; NW¼ sec. 21, T14S, R16W; Canteen Canyon quad., Grant Co., NM). *Analytical data*: $P_s = 1.50 \times 10^6$ tracks/cm^2 (180); $P_i = 3.17 \times 10^6$ tracks/cm^2 (191); $\phi = 1.10 \times 10^{15}$ n/cm^2; U = 83 ppm. *Comment*: Dacitic to latitic porphyry in gulch south of Watson Canyon on west side of Gila River is overlain by Fall Canyon Tuff and younger ash-flow tuffs.

(zircon) 31.0 ± 6.4 m.y.

93a. *Ratté and Gaskill, 1975 (GR–95)* Fission-track
Marvin and Dobson, 1979, entry no. 210
Altered dacite or latite, volcanic complex of Brock Canyon (33°03′17″N, 108°30′12″W; SW¼ sec. 28, T14S, R16W; from dump at adit on west side of lower Brushy Canyon, Canteen Canyon quad., Grant Co., NM). *Analytical data*: $P_s = 1.01 \times 10^6$ tracks/cm^2 (247); $P_i = 2.16 \times 10^6$ tracks/cm^2 (265); $\phi = 1.06 \times 10^{15}$ n/cm^2; U = 65 ppm. *Comment*: Sample is a pyritic, argillically altered rock, which is probably the altered and mineralized equivalent of samples GR–185, GR–186, and GR–190 (Entries 90, 91, and 92). This zircon date of an altered rock is not appreciably different from the zircon date of a less altered rock (sample GR–190, Entry 92) suggesting (1) that mineralization took place soon after the formation of the volcanic complex or (2) that the temperature regime of the hydrothermal solutions did not cause significant annealing of zircon fission tracks.

(zircon) 31.2 ± 5.5 m.y.

93b. *USGS(D)–GR–191* Fission-track
Altered dacite or latite, volcanic complex of Brock Canyon (33°03′17″N, 108°30′12″W; SW¼ sec. 28, T14S, R16W; from dump at adit on west side of lower Brushy Canyon, Canteen Canyon quad., Grant Co., NM). *Analytical data*: $P_s = 1.36 \times 10^6$ tracks/cm^2 (221); $P_i = 2.80 \times 10^6$ tracks/cm^2 (226); $\phi = 0.94 \times 10^{15}$ n/cm^2; U = 88 ppm. *Comment*: see "Comment" for Entry 93a.

(zircon) 27.8 ± 5.3 m.y.

94. *Ratté et al., 1979, p. 23 (GR–92C)* Fission-track
Dacitic intrusive(?) of Holt Gulch (33°17′36″N, 108°49′28″W; north side of Holt Gulch northwest of Gold Hill, Holt Mountain quad., Catron Co., NM). *Analytical data*: $P_s = 1.91 \times 10^6$ tracks/cm^2 (664); $P_i = 5.32 \times 10^6$ tracks/cm^2 (923); $\phi = 1.03 \times 10^{15}$ n/cm^2; U = 273 ppm. *Comment*: Zircon age indicates that the propylitically altered intrusive(?) may be younger than the adjacent Fanney Rhyolite and Mineral Creek Andesite, contrary to preliminary interpretation of Ratté and Gaskill (1975). This zircon age is similar to zircon age of andesitic intrusive at Silver Creek (Entry 77).

(zircon) 22.7 ± 2.3 m.y.

95. *USGS(D)–CH–1–74* K–Ar
Fall Canyon Tuff (33°04′39″N, 108°29′56″W; sec. 21, T14S, R16W; near mouth of Watson Canyon, Canyon Hill quad., Grant Co., NM). *Analytical data*: K_2O = 12.79, 12.87, 13.07, 13.08%; $^{40}Ar^*$ = 3.053 and 2.868 × 10^{-10} mol/gm; $^{40}Ar^*/\Sigma^{40}Ar$ = 74, 74%. *Comment*: Sanidine age for the Fall Canyon Tuff appears to have been reset, possibly by a thermal event associated with intrusion of an adjacent undated quartz-porphyry dike.

(sanidine) 15.8 ± 1.0 m.y.

96. *Ratté et al., 1984, table 6, no. 19* Fission-track
(GR–129A)
Bloodgood Canyon Tuff (33°05′58″N, 108°18′59″W; near top of Granny Mountain, Granny Mountain quad., Grant Co., NM). *Analytical data*: (4 sphenes) $P_s = 0.177 \times 10^6$ tracks/cm^2 (96); $P_i = 1.55 \times 10^6$ tracks/cm^2 (421); $\phi = 3.66 \times 10^{15}$ n/cm^2; U = 13 ppm. *Comment*: Low uranium content of the sphene grains accounts for the large estimated analytical uncertainty.

(sphene) 24.9 ± 5.6 m.y.

97. *Ratté et al., 1984, table 6, no. 18* Fission-track
(DG–449)
Bloodgood Canyon Tuff (33°11′52″N, 108°19′59″W; north side of Bloodgood Canyon at about 7,000-ft elevation, Little Turkey Park quad., Grant Co., NM). *Analytical data*: (8 sphenes) $P_s = 0.192 \times 10^6$ tracks/cm^2 (272); $P_i = 1.43 \times 10^6$ tracks/cm^2 (1,010); $\phi = 3.66 \times 10^{15}$ n/cm^2; U = 12 ppm.

(sphene) 29.4 ± 4.0 m.y.

98. *Ratté and Gaskill, 1975,* K–Ar
map locality SA–1
Marvin and Dobson, 1979, entry no. 214 (GR–197)
Quartz latite of the latitic lava flows of Gila Flat (33°02′24″N, 108°13′28″W; SE¼ NE¼ sec. 31, T14S, R13W; hilltop west of NM–255 and south of Sapillo Creek, Copperas Peak quad., Grant Co., NM). *Analytical data*: (biotite) K_2O = 8.71, 8.75%; $^{40}Ar^*$ = 3.838 × 10^{-10} mol/gm; $^{40}Ar^*/\Sigma^{40}Ar$ = 84%; (sanidine) K_2O = 9.52, 9.58%; $^{40}Ar^*$ = 4.157 × 10^{-10} mol/gm; $^{40}Ar^*/\Sigma^{40}Ar$ = 92%. *Comment*: Biotite-rich quartz-latite lava flows overlap the altered and mineralized rocks of the volcanic complex of Alum Mountain and

are therefore apparently younger than the mineralizing event at that volcanic center.

(biotite) 30.3 ± 0.7 m.y.
(sanidine) 30.0 ± 0.7 m.y.

99. *Ratté and Gaskill, 1975, map locality SA–2* K–Ar
Marvin and Dobson, 1979, entry no. 213 (GR–220A)
Granitic dike (33°04′31″N, 108°12′26″W; SE1/4 SW1/4 sec. 17, T14S, R13W; dike crops out in gulch about 0.4 km west of NM–15, Copperas Peak quad., Grant Co., NM). *Analytical data*: K_2O = 8.66, 8.61%; $^{40}Ar^*$ = 3.814 × 10^{-10} mol/gm; $^{40}Ar^*/\Sigma^{40}Ar$ = 74%. *Comment*: Fine-grained granitic dike intrudes the volcanic complex of Alum Mountain, which appears to be about 30 m.y. old or older. The age of unaltered lava flows of Gila Flat (see Entry 98), which unconformably overlap the altered rocks of the Alum Mountain center, also suggests that the mineralization along Copperas Creek and at Alum Mountain is probably 30 m.y. old or older.

(K-feldspar) 30.4 ± 0.7 m.y.

100. *Elston et al., 1973, table 1, no. 13* K–Ar
Basalt (33°01′50″N, 108°09′48″W; NW1/4 sec. 2, T15S, R13W; Roberts Lake Dam, Copperas Peak quad., Grant Co., NM). *Analytical data*: K_2O = 2.49%; $^{40}Ar^*$ = 0.761 × 10^{-10} mol/gm; $^{40}Ar^*/\Sigma^{40}Ar$ = 74.7%. *Comment*: Basalt or basaltic andesite from the upper part of the Bearwallow Mountain Formation (Elston, 1976, p. 132). Lavas of this age are more mafic and have more primitive Sr-isotopic ratios than older andesites of the Bearwallow Mountain Andesite and should be separated from the Bearwallow Mountain Andesite.

(whole-rock) 21.1 ± 0.5 m.y.

101. *Smith et al., 1976, no. 75–20* Fission-track
Granite of North Star Mesa (approx. 33°03′30″N, 108°01′50″W; SE1/4 sec. 24, T14S, R12W; North Star Mesa quad., Grant Co., NM). *Analytical data*: (zircon) P_s = 576 tracks; P_i = 1,025 tracks; ϕ = 1.27 × 10^{15} n/cm²; (apatite) P_s = 396 tracks; P_i = 743 tracks; ϕ = 1.27 × 10^{15} n/cm². *Comment*: Granite occurs as cobbles on a hilltop along the trace of the Santa Rita–Hanover axis (Aldrich, 1976, 1974).

(zircon) 42.6 ± 5.2 m.y.
(apatite) 42.7 ± 5.3 m.y.

102. *Bikerman, 1972, no. UP–M675* K–Ar
Bloodgood Canyon Tuff (33°11′22″N, 108°10′45″W; sec. 3, T13S, R13W; Lyons Lodge area, Gila Hot Springs quad., Grant Co., NM). *Analytical data*: (biotite) K_2O = 7.73%; $^{40}Ar^*$ = 3.0134 × 10^{-10} mol/gm; $^{40}Ar^*/\Sigma^{40}Ar$ = 83%; (sanidine) K_2O = 6.22%; $^{40}Ar^*$ = 2.3429 × 10^{-10} mol/gm; $^{40}Ar^*/\Sigma^{40}Ar$ = 96%. *Collected by*: W. E. Elston, 1968. *Comment*: The Bloodgood Canyon Tuff along the East Fork of the Gila River is believed to be part of the outflow sheet whose eruption caused the initial collapse of the Bursum caldera; this Bloodgood Canyon Tuff locality is also beyond the area of collapse of the earlier Gila Cliff Dwellings caldera (Ratté et al., 1984).

(biotite) 26.9 ± 1.5 m.y.
(sanidine) 26.0 ± 1.5 m.y.

103. *Ratté et al., 1984, table 6, no. 26 (WL–1–79)* K–Ar
Bloodgood Canyon Tuff (33°22′15″N, 108°03′42″W; NW1/4 sec. 2, T11S, R21W; west side of Whitewater Canyon of Taylor Creek, Wall Lake quad., Catron Co., NM). *Analytical data*: K_2O = 6.26, 6.28%; $^{40}Ar^*$ = 2.543 × 10^{-10} mol/gm; $^{40}Ar^*/\Sigma^{40}Ar$ = 68%. *Comment*: Ash-flow tuff overlies Taylor Creek Rhyolite and is correlated with Bloodgood Canyon Tuff on the basis of petrographic composition and age (Richter, 1986).

(sanidine) 28.0 ± 1.0 m.y.

104. *Ratté et al., 1984, table 7, no. 8 (WL–2A–79)* K–Ar
Taylor Creek Rhyolite (33°21′51″N, 108°03′30″W; center of sec. 2, T11S, R12W; east side of Whitewater Canyon of Taylor Creek, Wall Lake quad., Catron Co., NM). *Analytical data*: K_2O = 7.16, 7.12%; $^{40}Ar^*$ = 2.874 × 10^{-10} mol/gm; $^{40}Ar^*/\Sigma^{40}Ar$ = 65%. *Comment*: At this locality, the Taylor Creek Rhyolite is overlain by poorly welded Bloodgood Canyon Tuff (Richter, 1986). Taylor Creek Rhyolite was interpreted to be part of the caldera fill of the Gila Cliff Dwellings caldera and the defluidized equivalent of the Bloodgood Canyon Tuff by Rhodes (1976b). That interpretation is the primary basis for the size and extent of the Gila Cliff Dwellings caldera as shown by Elston (1984, fig. 2 and elsewhere). These interpretations are considered to be incompatible with the distribution of outflow facies and age relationships of the Bloodgood Canyon Tuff (Ratté et al., 1984).

(sanidine) 27.7 ± 0.9 m.y.

105. *Elston et al., 1973, table 1, no. 8* K–Ar
Taylor Creek Rhyolite (33°23′N, 108°02′W; NE 1/4 sec. 1, T11S, R12W; Taylor Creek, Spring Canyon quad., Catron Co., NM). *Analytical data*: K_2O = 7.87%; $^{40}Ar^*$ = 2.80 × 10^{-10} mol/gm; $^{40}Ar^*/\Sigma^{40}Ar$ = 95%. *Comment*: This age is shown to be too young by stratigraphic constraints imposed by $^{40}Ar/^{39}Ar$ ages of the underlying La Jencia Tuff (28.76 m.y.) and the overlying Bloodgood Canyon Tuff (28.36 m.y.) (McIntosh et al., 1986; this paper, Table 2) and by comparison with other conventional K–Ar ages cited here

(Entries 103 and 104) and new ages listed by Maxwell et al. (1986, table 2) and Eggleston and Norman (1986, p. 174).

(sanidine) 24.6 ± 0.5 m.y.

106. *Elston et al., 1973, table 1, no. 12* K–Ar
Rhyolite ash-flow tuff (33°29′N, 108°08′W; SE 1/4 NW1/4 sec. 36, T9S, R13W; NM–61 roadcut, Black Mountain quad., Catron Co., NM). *Analytical data*: K_2O = 6.10%; $^{40}Ar^*$ = 1.96 × 10^{-10} mol/gm; $^{40}Ar^*/\Sigma^{40}Ar$ = 82%. *Comment*: Tuff correlated with the Jordan Canyon Formation by Elston et al. (1973); called tuff of Slash Ranch by Richter (1978).

(sanidine) 22.2 ± 0.7 m.y.

107. *UP–ARS* K–Ar
Rhyolite (33°23′48″N, 108°22′32″W; sec. 34, T10S, R15W; Canyon Creek, Loco Mountain quad., Catron Co., NM). *Analytical data*: (biotite) K_2O = 8.36%; $^{40}Ar^*$ = 3.359 × 10^{-10} mol/gm; $^{40}Ar^*/\Sigma^{40}Ar$ = 83%; (groundmass) K_2O = 1.88%; $^{40}Ar^*$ = 0.676 × 10^{-10} mol/gm; $^{40}Ar^*/\Sigma^{40}Ar$ = 69%. *Collected by*: R. C. Rhodes, E. I. Smith, and M. J. Aldrich in 1970. *Analyzed by*: M. Bikerman, Univ. of Pittsburgh. *Comment*: Rhyolite crops out near the projected intersection of the Gila Cliff Dwellings and Bursum calderas (Ratté and Gaskill, 1975). It correlates with the Jerky Mountains Rhyolite of Elston (1976, p. 137).

(biotite) 27.7 ± 2.0 m.y.
(groundmass) 24.8 ± 2.0 m.y.

108. *Ratté et al., 1984, table 6, no. 15 (RR–1–75)* K–Ar, Fission-track
Bloodgood Canyon Tuff (33°36′05″N, 108°03′20″W; sec. 22, T8S, R12W; north side of Railroad Canyon near Whiskey tank, Indian Peaks West quad., Catron Co., NM). *Analytical data*: (sanidine) K_2O = 7.24, 7.31, 7.26, 7.27%; $^{40}Ar^*$ = 2.916 × 10^{-10} mol/gm; $^{40}Ar^*/\Sigma^{40}Ar$ = 40%; (zircon) P_s = 3.24 × 10^6 tracks/cm^2 (720); P_i = 6.86 × 10^6 tracks/cm^2 (762); ϕ = 0.920 × 10^{15} n/cm^2; U = 210 ppm. *Comment*: Sample was collected from the type locality of the former Railroad Canyon Tuff of Elston (1976). Tuff is now correlated with the Bloodgood Canyon Tuff (Ratté et al., 1984, p. 8721), and the name Railroad Canyon Tuff has been abandoned (Lawrence and Richter, 1986). Also see Entry 109.

K–Ar (sanidine) 27.7 ± 0.9 m.y.
Fission-track (zircon) 26.0 ± 2.7 m.y.

109. *Elston et al., 1973, table 1, no. 11* K–Ar
Bloodgood Canyon Tuff (approx. 33°35′55″N, 108°03′25″W; NE1/4 SE1/4 sec. 22, T8S, R12W; Railroad Canyon, Indian Peaks West quad., Catron Co., NM). *Analytical data*: K_2O = 7.26%; $^{40}Ar^*$ = 2.46 × 10^{-10} mol/gm; $^{40}Ar^*/\Sigma^{40}Ar$ = 88%. *Comment*: Sample is from the same outcrops as sample RR–1–75 (see Entry 108); tuff was designated as the Railroad Canyon Rhyolite Tuff by Elston (1976, pp. 133, 140)—a name now abandoned.

(sanidine) 23.4 ± 0.7 m.y.

110. *USGS(D)–PM–2–82* K–Ar
Andesite plug (33°40′56″N, 108°05′54″W; sec. 29, T7S, R12W; south side of stock pond on Pelona Mountain, south of San Agustin Plains, Pelona Mountain quad., Catron Co., NM). *Analytical data*: K_2O = 3.17, 3.11%; $^{40}Ar^*$ = 1.210 × 10^{-10} mol/gm; $^{40}Ar^*/\Sigma^{40}Ar$ = 84%. *Comment*: Hypersthene-andesite plug (SiO_2 = 61%, Na_2O = 3.4%, K_2O = 3.4%) represents the Pelona Mountain Andesite of the Bearwallow Mountain Formation of Elston (1976, p. 139). Although the rock contains patches of fine-grained granophyric quartz and orthoclase, it is not rhyolite as shown by Willard and Stearns (1971). Age of this plug and ages given by samples USGS(D)–BW–1–82, USGS(D)–N–1A–82, and USGS(D)–O–1B–82 (Entries 80, 81, and 111) require a revision of the age of the Bearwallow Mountain Andesite, previously assigned an age of about 21 m.y. (Elston, 1976, p. 132).

(whole-rock) 26.6 ± 1.0 m.y.

111. *USGS(D)–0–1B–82* K–Ar
Andesite plug (33°36′13″N, 108°18′50″W; sec. 20, T8S, R14W; about 300 m north of Redondo Springs on O Bar O Mountain, south of San Agustin Plains, O Bar O Canyon West quad., Catron Co., NM). *Analytical data*: K_2O = 2.66, 2.65%; $^{40}Ar^*$ = 0.9895 × 10^{-10} mol/gm; $^{40}Ar^*/\Sigma^{40}Ar$ = 50%. *Comment*: Andesite plug fills the feeder vent of a small andesitic shield volcano, which is virtually identical to the volcano at Pelona Mountain; see sample USGS(D)–PM–2–82 (Entry 110). Andesite was included in the Pelona Mountain Andesite Member of the Bearwallow Mountain Formation of Elston (1976, p. 139).

(whole-rock) 25.7 ± 0.9 m.y.

112. *UP–G46* K–Ar
Rhyolite of Shaw Canyon (33°45′35″N, 108°04′17″W; SW1/4 sec. 27, T6S, R12W; north side of Shaw Canyon at junction with Fullerton Spring Canyon, Shaw Mountain quad., Catron Co., NM). *Analytical data*: (sanidine: 40–60 mesh) K_2O = 5.77%; $^{40}Ar^*$ = 2.406 and 2.367 × 10^{-10} mol/gm; $^{40}Ar^*/\Sigma^{40}Ar$ = 90, 89%; (sanidine: 100–140 mesh) K_2O = 4.22%; $^{40}Ar^*$ = 1.818 × 10^{-10} mol/gm; $^{40}Ar^*/\Sigma^{40}Ar$ = 85%. Rb–Sr analytical data for whole-rock material: Rb = 221 ppm; Sr = 4.67 ppm; $^{87}Rb/^{86}Sr$ = 138.2; $^{87}Sr/^{86}Sr$ = 0.7842; calculated initial $^{87}Sr/^{86}Sr$ = 0.7283 ±

0.0006. *Collected and analyzed by*: M. Bikerman, Univ. of Pittsburgh. *Comment*: This sample represents the rhyolite-flow unit, Tdrf, of Stearns (1962).

(sanidine: 40–60 mesh) 28.7 ± 1.5 m.y.
28.3 ± 1.5 m.y.
(sanidine: 100–140 mesh) 29.7 ± 1.5 m.y.

113. *USGS(D)–H–9–77* K–Ar, Fission-track
Davis Canyon(?) Tuff (33°50′01″N, 108°00′45″W; sec. 30, T5S, R11W; low cliffs along the south side of the San Agustin Plains, northeast of Shaw Mountain, Shaw Mountain quad., Catron Co., NM). *Analytical data*: (sanidine) K_2O = 4.72, 4.67%; $^{40}Ar^*$ = 1.986 × 10^{-10} mol/gm; $^{40}Ar^*/\Sigma^{40}Ar$ = 76%; (zircon) P_s = 3.59 × 10^6 tracks/cm² (608); P_i = 7.46 × 10^6 tracks/cm² (632); ϕ = 0.950 × 10^{15} n/cm²; U = 230 ppm. *Comment*: Phenocryst-poor rhyolite ash-flow tuff has petrographic characteristics and stratigraphic position beneath the Bloodgood Canyon Tuff that suggest it correlates with the Davis Canyon Tuff (Ratté, et al., 1984). However, preliminary paleomagnetic analysis indicates that it may be Vicks Peak Tuff, which is similar in age and composition to the Davis Canyon Tuff (McIntosh, pers. comm. 1985).

K–Ar (sanidine) 29.2 ± 1.0 m.y.
Fission-track (zircon) 27.3 ± 3.1 m.y.

114. *USGS(D)–H–7–77* K–Ar, Fission-track
Rhyolite (33°58′43″N, 108°06′50″W; about 8,920-ft elevation, west of saddle on Horse Mountain, Horse Mountain East quad., Catron Co., NM). *Analytical data*: (plagioclase) K_2O = 0.45, 0.41, 0.56, 0.53%; $^{40}Ar^*$ = 0.08478 × 10^{-10} mol/gm; $^{40}Ar^*/\Sigma^{40}Ar$ = 35%; (hornblende) K_2O = 0.17, 0.17%; $^{40}Ar^*$ = 0.0871 × 10^{-10} mol/gm; $^{40}Ar^*/\Sigma^{40}Ar$ = 35%; (6 zircons) P_s = 2.18 × 10^6 tracks/cm² (318); P_i = 11.91 × 10^6 tracks/cm² (868); ϕ = 0.952 × 10^{15} n/cm²; U = 360 ppm. *Comment*: These are the first reported K–Ar ages on rocks from the composite Horse Mountain volcano, described by Stearns (1962). Bornhorst (1980) estimated the age to be about 22.5 m.y. and designated the rocks as the member of Horse Mountain of the Bearwallow Mountain Formation. Jones (1980) reported a zircon fission-track age of 13.7 m.y. in an M.S. thesis, University of New Mexico, an age similar to the plagioclase and zircon ages listed here. The spurious hornblende age is probably due to the presence of excess radiogenic argon.

K–Ar (plagioclase) 12.0 ± 3.0 m.y.
K–Ar (hornblende) 35.3 ± 6.1 m.y.
Fission-track (zircon) 10.4 ± 1.3 m.y.

115. *USGS(D)–HW–1A–82* K–Ar
Blue Canyon Tuff (33°55′23″N, 108°14′41″W; sec. 36, T4S, R14W; roadcut on north side of NM–12, Horse Mountain West quad., Catron Co., NM). *Analytical data*: (impure sanidine) K_2O = 7.51, 7.18, 8.02, 7.16%; $^{40}Ar^*$ = 3.546 × 10^{-10} mol/gm; $^{40}Ar^*/\Sigma^{40}Ar$ = 81%; (sanidine) K_2O = 10.22, 10.36%; $^{40}Ar^*$ = 4.978 × 10^{-10} mol/gm; $^{40}Ar^*/\Sigma^{40}Ar$ = 91%. *Comment*: Crystal-rich, vitroclastic tuff was correlated with the Blue Canyon Tuff by Bornhorst (1976).

(sanidine) 33.3 ± 1.0 m.y.
(impure sanidine) 32.7 ± 4.6 m.y.

116. *USGS(D)–HW–3C–82* K–Ar
Datil Well Tuff (33°54′57″N, 108°11′38″W; SE¼ sec. 33, T4S, R13W; about 200 m south of Davis well, south of NM–12, Horse Mountain West quad., Catron Co., NM). *Analytical data*: K_2O = 6.36, 6.29%; $^{40}Ar^*$ = 3.373 × 10^{-10} mol/gm; $^{40}Ar^*/\Sigma^{40}Ar$ = 88%. *Comment*: Tuff containing about 15% phenocrysts, mostly sanidine with some clinopyroxene and biotite, is the oldest of five ash-flow tuffs exposed at this locality.

(sanidine) 36.7 ± 1.3 m.y.

117. *UP–G38* K–Ar
Datil Well(?) Tuff (33°58′59″N, 108°09′18″W; SW ¼ sec. 1, T4S, R13W; about 8,300-ft elevation on ridge extending northwest from Horse Mountain, Horse Mountain West quad., Catron Co., NM). *Analytical data*: K_2O = 8.75%; $^{40}Ar^*$ = 4.505 × 10^{-10} mol/gm; $^{40}Ar^*/\Sigma^{40}Ar$ = 82%. *Collected and analyzed by*: M. Bikerman, Univ. of Pittsburgh. *Comment*: Tuff is part of unit Tdrp–1 of Stearns (1962). Sample location indicates that this tuff should be correlated with the Blue Canyon Tuff, as mapped by Bornhorst (1976, fig. 4), but the listed radiometric age for this tuff and its sanidine-dominant phenocryst mineralogy suggest that it represents the Datil Well Tuff (Bornhorst, 1976), which underlies the Blue Canyon Tuff.

(biotite) 35.4 ± 2.0 m.y.

118. *USGS(D)–P–5–78* K–Ar
Tuff breccia of Horse Springs Canyon (Bornhorst, 1976) (33°55′16″N, 108°15′32″W; sec. 36, T4S, R14W; north side of NM–12, Bell Peak quad., Catron Co., NM). *Analytical data*: (biotite) K_2O = 6.85, 6.62, 6.98, 6.69%; $^{40}Ar^*$ = 3.507 × 10^{-10} mol/gm; $^{40}Ar^*/\Sigma^{40}Ar$ = 76%; (plagioclase) K_2O = 2.88, 2.82%; $^{40}Ar^*$ = 1.405 × 10^{-10} mol/gm; $^{40}Ar^*/\Sigma^{40}Ar$ = 86%. *Comment*: Sample is from approximately the same outcrops that provided the cognate(?) quartz-monzonite clast, dated by Bornhorst et al. (1982, sample no. 77T20). See Entry 119.

(biotite) 35.5 ± 2.2 m.y.
(plagioclase) 33.9 ± 1.2 m.y.

119. *Bornhorst et al., 1982, entry 4, no. 77T20* Fission-track
Quartz-monzonite clast (33°55′09″N, 108°15′56″W; NW1/4 sec. 35, T4S, R14W; Bell Peak quad., Catron Co., NM). *Analytical data*: P_s = 806 tracks; P_i = 1,276 tracks; $\phi = 0.855 \times 10^{15}$ n/cm². *Comment*: Cognate(?) quartz-monzonite clast in the tuff breccia of Horse Springs Canyon. (Sample locality is probably in sec. 35, not sec. 31, as published by Bornhorst et al., 1982.)
(zircon) 32.4 ± 3.4 m.y.

120. *Bornhorst et al., 1982, entry 9, no. T–384A* Fission-track
Rhyolite of Wye Hill (Bornhorst, 1976) (33°55′55″N, 108°15′37″W; sec. 25, T4S, R14W; north of NM–12, Bell Peak quad., Catron Co., NM). *Analytical data*: P_s = 187 tracks; P_i = 388 tracks; $\phi = 1.05 \times 10^{15}$ n/cm². *Comment*: The rhyolite of Wye Hill is the same as the latite (Tdl) of Stearns (1962). It forms flow–dome complexes beneath Squirrel Springs Canyon Andesite (Bornhorst, 1976, fig. 4) both north and south of the San Agustin Plains in the Bell Peak and Fullerton quadrangles and elsewhere (Stearns, 1962, pl. 1; Ratté, unpubl. mapping 1985).
(zircon) 30.3 ± 6.1 m.y.

121. *Bornhorst et al., 1982, entry 10, no. 76T4* K–Ar
Rhyolite of Wye Hill (Bornhorst, 1976) (33°54′45″N, 108°16′W; S1/2 sec. 35, T4S, R14W; south of NM–12, Bell Peak quad., Catron Co., NM). *Analytical data*: K_2O = 6.453, 6.412%; $^{40}Ar^*$ = 2.548, 2.544, 2.541 × 10^{-10} mol/gm; $^{40}Ar^*/\Sigma^{40}Ar$ = 82.9, 82.5, 82.7%. *Comment*: Bornhorst et al. (1982) published an age of 28.0 m.y., an age they consider to be too young on the basis of stratigraphic evidence. The age calculated from their published analytical data (shown above) is 27.3 m.y., not 28.0 m.y.
sanidine 27.3 ± 0.6 m.y.

122. *USGS(D)–P–3–78* K–Ar
Rhyolite of Wye Hill (Bornhorst, 1976) (33°54′46″N, 108°15′52″W; sec. 35, T4S, R14W; northeast flank of hill 8012 at about 7,900-ft elevation, south of NM–12, Bell Peak quad., Catron Co., NM). *Analytical data*: K_2O = 5.29, 5.40, 5.21, 5.12%; $^{40}Ar^*$ = 2.459 × 10^{-10} mol/gm; $^{40}Ar^*/\Sigma^{40}Ar$ = 72%. *Comment*: Sample is from same outcrop area as sample T–384A (Entry 120).
(sanidine) 32.2 ± 2.0 m.y.

123. *UP–G31* K–Ar
Biotite-bearing tuff (33°55′10″N, 108°15′29″W; NW1/4 sec. 36, T4S, R14W; south of NM–12, Bell Peak quad., Catron Co., NM). *Analytical data*: (biotite: 40–60 mesh) K_2O = 8.10%; $^{40}Ar^*$ = 4.261 × 10^{-10} mol/gm; $^{40}Ar^*/\Sigma^{40}Ar$ = 79%; (biotite: 60–100 mesh) K_2O = 8.58%; $^{40}Ar^*$ = 4.007 and 3.882 × 10^{-10} mol/gm; $^{40}Ar^*/\Sigma^{40}Ar$ = 62, 69%. Whole-rock Rb–Sr data: Rb = 177 ppm; Sr = 217 ppm; $^{87}Rb/^{86}Sr$ = 2.361; $^{87}Sr/^{86}Sr$ meas. = 0.711; $^{87}Sr/^{86}Sr$ initial = 0.7099 ± 0.0005. *Collected and analyzed by*: M. Bikerman, Univ. of Pittsburgh. *Comment*: Sample probably represents either the Blue Canyon Tuff or the tuff breccia of Horse Springs Canyon, mapped as the lower rhyolite pyroclastic unit (Tdrp–1) of Stearns (1962).
(biotite: 40–60 mesh) 36.2 ± 2.0 m.y.
(biotite: 60–100 mesh) 32.2 ± 1.0 m.y.
31.2 ± 1.0 m.y.

124. *UP–G26* K–Ar
Shelley Peak Tuff (33°52′48″N, 108°29′13″W; SE 1/4 sec. 8, T5S, R14W; west side of Bursum Road, about 4 km south of junction with NM–12, Bell Peak quad., Catron Co., NM). *Analytical data*: (biotite) K_2O = 7.35%; $^{40}Ar^*$ = 2.920 × 10^{-10} mol/gm; $^{40}Ar^*/\Sigma^{40}Ar$ = 47%; (feldspar) K_2O = 2.95%; $^{40}Ar^*$ = 1.126 × 10^{-10} mol/gm; $^{40}Ar^*/\Sigma^{40}Ar$ = 42%. *Collected and analyzed by*: M. Bikerman, Univ. of Pittsburgh. *Comment*: Petrography and stratigraphic position of the tuff—beneath the Bloodgood Canyon Tuff in nearby outcrops—indicates correlation with the Shelley Peak Tuff.
(biotite) 27.4 ± 1.3 m.y.
(feldspar) 31.7 ± 1.5 m.y.

125. *UP–G24* K–Ar
Bloodgood Canyon Tuff (33°56′00″N, 108°25′20″W; NE1/4 sec. 29, T4S, R15W; along NM–12 at Continental Divide, Tularosa Canyon quad., Catron Co., NM). *Analytical data*: (biotite) K_2O = 7.68%; $^{40}Ar^*$ = 3.201 × 10^{-10} mol/gm; $^{40}Ar^*/\Sigma^{40}Ar$ = 85%; (sanidine) K_2O = 5.65%; $^{40}Ar^*$ = 2.308 × 10^{-10} mol/gm; $^{40}Ar^*/\Sigma^{40}Ar$ = 98%. *Collected and analyzed by*: M. Bikerman, Univ. of Pittsburgh.
(biotite) 28.8 ± 1.0 m.y.
(sanidine) 28.2 ± 1.0 m.y.

126a. *Smith, 1976; Smith et al., 1976, no. J59–81* Fission-track
John Kerr Peak Quartz Latite (sec. 24, T6S, R16W; Cottonwood Canyon dome (Smith, 1976, fig. 3), John Kerr Peak quad., Catron Co., NM). *Analytical data*: From Smith (1976, table 2) (sphene) P_s = 129 tracks; P_i = 456 tracks; $\phi = 1.29 \times 10^{15}$ n/cm²; (apatite) P_s = 89 tracks; P_i = 316 tracks; $\phi = 1.29 \times 10^{15}$ n/cm²; (zircon) P_s = 539 tracks; P_i = 1,977 tracks; $\phi = 1.29 \times 10^{15}$ n/cm². *Comment*: Analytical data and location for this sample differ between Smith et al.

(1976, table 1) and Smith (1976, tables 2 and 3), but ages listed are virtually the same in both articles.

(sphene) 22.7 ± 4.8 m.y.
(apatite) 22.7 ± 5.2 m.y.
(zircon) 21.4 ± 2.2 m.y.

126b. *Smith, 1976; Smith et al., 1976, no. J40* Fission-track
John Kerr Peak Quartz Latite (SE¼ sec. 10, T6S, R16W; base of the John Kerr Peak dome (Smith, 1976, fig. 3), John Kerr Peak quad., Catron Co., NM). *Analytical data*: From Smith (1976, table 2) (sphene) P_s = 107 tracks; P_i = 408 tracks; ϕ = 1.29×10^{15} n/cm^2; (zircon) P_s = 475 tracks; P_i = 1,892 tracks; $\phi = 1.29 \times 10^{15}$ n/cm^2. *Comment*: Analytical data and location for this sample differ between Smith et al. (1976, table 1) and Smith (1976, tables 2 and 3), but the ages are virtually the same in both articles. However, the ages in Entries 126a and 126b differ significantly from the age from another sample also identified as John Kerr Peak Quartz Latite; see sample USGS(D)–JKP–1–76 (Entry 127).

(sphene) 20.6 ± 4.8 m.y.
(zircon) 19.9 ± 2.2 m.y.

127. *USGS(D)–JKP–1–76* K–Ar, Fission-track
John Kerr Peak Quartz Latite (Smith, 1976) (33°47′17″N, 108°29′11″W; west side of road near Willow Spring, southwest of John Kerr Peak, John Kerr Peak quad., Catron Co., NM). *Analytical data*: (biotite) K_2O = 5.33, 5.37%; $^{40}Ar^*$ = 1.051×10^{-10} mol/gm; $^{40}Ar^*/\Sigma^{40}Ar$ = 81%; (6 zircons) $P_s = 2.10 \times 10^6$ tracks/cm^2 (356); $P_i = 9.88 \times 10^6$ tracks/cm^2 (837); $\phi = 0.947 \times 10^{15}$ n/cm^2; U = 300 ppm. *Comment*: The agreement between the K–Ar and fission-track ages indicates that 13 m.y. is the approximate age of this rock. The reason for the discordance between these ages and those reported for John Kerr Peak Quartz Latite for samples J59–81 and J40 (Entries 126a and 126b) is not known. If the much younger ages reported in this paper are correct, the description of the John Kerr Peak Quartz Latite as intercalated in the lower part of the Bearwallow Mountain Andesite (Elston, 1976, p. 137) is untenable.

K–Ar (biotite) 13.6 ± 0.5 m.y.
Fission-track (zircon) 12.0 ± 1.6 m.y.

128. *Bikerman, 1972, no. UP–G5* K–Ar
Basalt (33°44′04″N, 108°28′35″W; NE¼ sec. 3, T7S, R16W; Cox Canyon Road near Dutchman Spring, Collins Park quad., Catron Co., NM). *Analytical data*: K_2O = 2.73%; $^{40}Ar^*$ = 0.8082×10^{-10} mol/gm; $^{40}Ar^*/\Sigma^{40}Ar$ = 80%. Rb–Sr whole-rock data: Rb = 64.7 ppm; Sr = 643 ppm; $^{87}Rb/^{86}Sr$ = 0.2908; $^{87}Sr/^{86}Sr$ = 0.7078; calculated initial $^{87}Sr/^{86}Sr$ = 0.7077 (Bikerman, 1976). *Comment*: Basalt was mapped as Bearwallow Mountain Formation by Rhodes and Smith (1976, fig. 2), and its initial strontium isotopic ratio is consistent with most other rocks here correlated with the Bearwallow Mountain Andesite. Whole-rock age is probably a minimum age.

(whole-rock) 20.4 ± 1.5 m.y.

129. *Bikerman, 1972, no. UP–G6* K–Ar
Rhyolite (approx. 33°39′40″N, 108°23′24″W; NW ¼ sec. 33, T7S, R15W; along Bursum Road in Y Canyon, Collins Park quad., Catron Co., NM). *Analytical data*: K_2O = 6.72%; $^{40}Ar^*$ = 2.554×10^{-10} mol/gm; $^{40}Ar^*/\Sigma^{40}Ar$ = 98%. Rb–Sr whole-rock data: Rb = 270 ppm; Sr = 6.17 ppm; $^{87}Rb/^{86}Sr$ = 127.2; $^{87}Sr/^{86}Sr$ = 0.7622; calculated initial $^{87}Sr/^{86}Sr$ = 0.7154. *Collected by*: R. C. Rhodes, E. I. Smith, and M. Bikerman. *Comment*: Argon value is revised from that reported by Bikerman (1972). This flow-banded rhyolite is correlated with Jerky Mountains Rhyolite by Rhodes and Smith (1976, fig. 2).

(sanidine) 26.2 ± 1.2 m.y.

130. *Bikerman, 1972, no. UP–G7* K–Ar
Bloodgood Canyon Tuff (33°40′27″N, 108°21′20″W; NE¼ sec. 26, T7S, R15W; north side of Bursum Road about 2 km northeast of Y Canyon well, Y Canyon, Salvation Peak quad., Catron Co., NM). *Analytical data*: (biotite) K_2O = 7.64%; $^{40}Ar^*$ = 3.029×10^{-10} mol/gm; $^{40}Ar^*/\Sigma^{40}Ar$ = 83%; (sanidine) K_2O = 5.41%; $^{40}Ar^*$ = 2.073×10^{-10} mol/gm; $^{40}Ar^*/\Sigma^{40}Ar$ = 96%. Rb–Sr whole-rock data: Rb = 230 ppm; Sr = 80.1 ppm; $^{87}Rb/^{86}Sr$ = 8.307; $^{87}Sr/^{86}Sr$ = 0.7132; calculated initial $^{87}Sr/^{86}Sr$ = 0.7100. *Comment*: Argon values listed above are revised from those reported by Bikerman (1972). The tuff, mapped as Railroad Canyon Tuff by Rhodes and Smith (1976, fig. 2), is now correlated with Bloodgood Canyon Tuff (Ratté et al., 1984).

(biotite) 27.3 ± 1.5 m.y.
(sanidine) 26.4 ± 1.5 m.y.

131. *UP–G15b* K–Ar
Shelley Peak Tuff (33°45′58″N, 108°32′30″W; SE ¼ sec. 24, T6S, R17W; west of junction of Cold Springs Canyon and Cox Canyon Roads, Squirrel Springs Canyon quad., Catron Co., NM). *Analytical data*: (Univ. of Pittsburgh) K_2O = 7.86%; $^{40}Ar^*$ = 2.924×10^{-10} mol/gm; $^{40}Ar^*/\Sigma^{40}Ar$ = 79%; (USGS) K_2O = 7.90, 7.45%; $^{40}Ar^*$ = 3.200×10^{-10} mol/gm; $^{40}Ar^*/\Sigma^{40}Ar$ = 71%. *Collected by*: M. Bikerman, Univ. of Pittsburgh. *Comment*: Tuff was mapped as Apache Spring Tuff by Rhodes and Smith (1976, fig.2), but in this paper, it is correlated with the Shelley Peak Tuff, which is overlain at this locality by the

Bloodgood Canyon Tuff. The noticeable difference in the calculated ages for the same biotite concentrate is due to variations in both the potassium and argon content as determined by each laboratory; the age difference is slightly more than the analytical uncertainties.

Univ. of Pittsburgh **(biotite) 25.7 ± 1.7 m.y.**
USGS **(biotite) 28.7 ± 1.0 m.y.**

132. *Bikerman, 1972, no. UP–G4* K–Ar
Basalt at Apache Creek (33°49′35″N, 108°37′15″W; SW1/4 sec. 33, T5S, R17W; mesa-capping flow on south side of NM–12 at Apache Creek store, Squirrel Springs Canyon quad., Catron Co., NM). *Analytical data*: K_2O = 1.10%; $^{40}Ar^*$ = 0.01485 × 10^{-10} mol/gm; $^{40}Ar^*/\Sigma^{40}Ar$ = 39%. Rb–Sr whole-rock data: Rb = 11.8 ppm; Sr = 283 ppm; $^{87}Rb/^{86}Sr$ = 0.1208; $^{87}Sr/^{86}Sr$ = 0.70363; calculated initial $^{87}Sr/^{86}Sr$ = 0.7036 (Bikerman, 1976). *Comment*: Basalt flow is underlain by Gila Conglomerate.

(whole-rock) 0.9 ± 0.2 m.y.

133. *USGS(D)–SS–1–77* K–Ar
Basalt at Apache Creek (33°49′38″N, 108°37′14″W; sec. 33, T5S, R17W; mesa-capping flow, Squirrel Springs Canyon quad., Catron Co., NM). *Analytical data*: K_2O = 1.04, 1.03%; $^{40}Ar^*$ = 0.0150 × 10^{-10} mol/gm; $^{40}Ar^*/\Sigma^{40}Ar$ = 16%. *Comment*: Same basalt flow dated by Bikerman (1972); see Entry 132 (this paper).

(whole-rock) 1.0 ± 0.1 m.y.

134. *USGS(D)–SS–2–77* K–Ar
Basalt (33°49′32″N, 108°37′15″W; sec. 33, T5S, R17W; outcrop is at road level on north side of Cold Springs Canyon Road, Squirrel Springs Canyon quad., Catron Co., NM). *Analytical data*: K_2O = 0.33, 0.36%; $^{40}Ar^*$ = 0.0681 × 10^{-10} mol/gm; $^{40}Ar^*/\Sigma^{40}Ar$ = 53%. *Comment*: This amygdaloidal basalt flow contains plagioclase phenocrysts nearly 1 cm long; thus, it is petrographically distinct from the much younger, fine-grained basalt flow that caps the mesa; see samples UP–G4 and USGS(D)–SS–1–77 (Entries 132 and 133). The two flows are separated by 60–70 m of Gila Conglomerate. The plagioclase age is geologically reasonable.

(plagioclase) 13.7 ± 1.4 m.y.

135. *USGS(D)–LR–1–75* K–Ar, Fission-track
Rhyolite ash-flow tuff of Luna (33°51′14″N, 108°55′55″W; sec. 21, T5S, R20W; north side of the road to Centerfire Creek, Luna quad., Catron Co., NM). *Analytical data*: (biotite) K_2O = 5.22, 5.24%; $^{40}Ar^*$ = 2.776 × 10^{-10} mol/gm; $^{40}Ar^*/\Sigma^{40}Ar$ = 78%; (sanidine) K_2O = 10.58, 10.50%; $^{40}Ar^*$ = 4.880 × 10^{-10} mol/gm; $^{40}Ar^*/\Sigma^{40}Ar$ = 93%; (6 zircons) P_s = 3.49 × 10^6 tracks/cm² (776); P_i = 6.49 × 10^6 tracks/cm² (721); ϕ = 1.01 × 10^{15} n/cm²; U = 200 ppm. *Comment*: This light-colored, welded, vitroclastic tuff contains small plagioclase, sanidine, quartz, and biotite phenocrysts (20–30% of total volume) plus accessory hornblende, pyroxene, zircon, sphene, apatite, and opaque oxides in a glassy matrix of compacted shards. The tuff has been mapped in the Luna, Centerfire Bog, Bull Basin, and Reserve quadrangles by T. L. Finnell and Ratté. Its greatest thickness, less than 30 m, is in the Luna quadrangle. Petrography and age suggest that the tuff may correlate with the Fall Canyon Tuff and/or Hells Mesa Tuff. Preliminary paleomagnetic analysis indicates correlation with Hells Mesa Tuff (McIntosh, pers. comm. 1985).

Tuff is probably 32–33 m.y. old as indicated by the sanidine and zircon ages. The older age given by the biotite is not as reliable because impurities in the biotite concentrate (visible and inferred from the low potassium content) increase the uncertainty of obtaining accurate analytical measurements. A similar sanidine age has been obtained for a correlative tuff in the Centerfire Bog quadrangle, sample USGS(D)–CF–1–79 (Entry 136).

K–Ar (biotite) 36.5 ± 1.3 m.y.
K–Ar (sanidine) 31.9 ± 0.7 m.y.
Fission-track (zircon) 32.5 ± 3.4 m.y.

136. *USGS(D)–CF–1–79* K–Ar, Fission-track
Rhyolite ash-flow tuff of Luna (33°54′41″N, 108°51′18″W; sec. 31, T4S, R19W; nose of ridge on north side of road, northwest of Deadman tank, Centerfire Bog quad., Catron Co., NM). *Analytical data*: (biotite) K_2O = 6.12, 6.25%; $^{40}Ar^*$ = 3.171 × 10^{-10} mol/gm; $^{40}Ar^*/\Sigma^{40}Ar$ = 79%; (sanidine) K_2O = 10.68, 10.72%; $^{40}Ar^*$ = 4.948 × 10^{-10} mol/gm; $^{40}Ar^*/\Sigma^{40}Ar$ = 87%; (6 zircons) P_s = 3.83 × 10^6 tracks/cm² (887); P_i = 5.84 × 10^6 tracks/cm² (676); ϕ = 1.01 × 10^{15} n/cm²; U = 180 ppm. *Comment*: Tuff is probably 32–33 m.y. old; see ages obtained for a correlative tuff in Luna quadrangle, USGS(D)–LR–1–75 (Entry 135). The ages given by zircon and biotite appear to be too old. The biotite age may be the result of sample inhomogeneity (visible impurities and low K_2O content), which could produce an apparent age that is either too young or too old. Petrography and the sanidine age suggest that this tuff may correlate with the Fall Canyon Tuff and/or Hells Mesa Tuff. Preliminary paleomagnetic analysis indicates correlation with Hells Mesa Tuff (McIntosh, pers. comm. 1985).

K–Ar (biotite) 35.3 ± 1.3 m.y.
K–Ar (sanidine) 31.8 ± 0.7 m.y.
Fission-track (zircon) 39.5 ± 4.0 m.y.

137. *USGS(D)–T–4–81* K–Ar
Basalt (33°50′51″N, 108°57′24″W; NW1/4 NW1/4 sec. 29, T5S, R20W; along Trout Creek, west of bridge about 4 km north of Luna, Luna quad., Catron Co., NM). *Analytical data*: K_2O = 1.49, 1.51%; $^{40}Ar^*$ = 0.05729 × 10^{-10} mol/gm; $^{40}Ar^*/\Sigma^{40}Ar$ = 27%. *Comment*: Holocrystalline basalt with sparse olivine phenocrysts is representative of flows and related cinder cones in the Luna–Underwood Lake area.

(whole-rock) 2.65 ± 0.10 m.y.

138. *USGS(D)–T–14–81* K–Ar
Tuff of Bishop Peak (33°58′25″N, 108°58′53″W; NE1/4 sec. 12, T4S, R21W; cut on new road, west side of Smith Creek Canyon, Underwood Lake quad., Catron Co., NM). *Analytical data*: (biotite) K_2O = 8.16, 8.15%; $^{40}Ar^*$ = 4.404 × 10^{-10} mol/gm; $^{40}Ar^*/\Sigma^{40}Ar$ = 86%; (sanidine) K_2O = 6.84, 6.82%; $^{40}Ar^*$ = 3.408 × 10^{-10} mol/gm; $^{40}Ar^*/\Sigma^{40}Ar$ = 78%. *Comment*: Rhyolitic ash-flow tuff contains about 15% phenocrysts, mainly plagioclase, minor biotite, and traces of sanidine, hornblende, pyroxene, zircon, and opaque oxides in a glassy matrix. The tuff of Bishop Peak is known only from the Underwood Lake, Luna, and Dillon Mountain quadrangles, where it has a maximum thickness of about 10 m. The dated biotite and sanidine concentrates are from a basal vitrophyre. The biotite age is tentatively accepted as the age of the tuff.

(biotite) 37.1 ± 1.3 m.y.
(sanidine) 34.3 ± 1.2 m.y.

139. *USGS(D)–BB–4E–76, Ratté, 1986* K–Ar, Fission-track
Tuff (33°39′22″N, 108°59′13″W; sec. 35, T7S, R21W; 0.8 km west of Black Bull Peak, Bull Basin quad., Catron Co., NM). *Analytical data*: (sanidine) K_2O = 7.12, 7.14%; $^{40}Ar^*$ = 3.527 × 10^{-10} mol/gm; $^{40}Ar^*/\Sigma^{40}Ar$ = 82%; (zircon) P_s = 5.85 × 10^6 tracks/cm² (704); P_i = 11.71 × 10^6 tracks/cm² (705); ϕ = 1.10 × 10^{15} n/cm²; U = 310 ppm. *Comment*: Thin, light-colored, pumiceous tuff is discontinuously interlayered with the pre-Davis Canyon andesitic complex of lava flows, mudflow breccia, and volcaniclastic rocks that extends into the Bull Basin quad. from the west and from the Saliz Pass quad. to the south (Ratté, 1980; 1986). The tuff contains less than 5% phenocrysts, mostly sanidine, minor plagioclase, and accessory biotite and brown hornblende in a glassy pumiceous matrix.

K–Ar (sanidine) 34.0 ± 1.2 m.y.
Fission-track (zircon) 32.8 ± 3.5 m.y.

140. *USGS(D)–BB–16E–76, Ratté, 1986* K–Ar, Fission-track
Quartz diorite (33°42′00″N, 108°53′40″W; sec. 15, T4N, R20W; Wet Leggett Spring, Bull Basin quad., Catron Co., NM). *Analytical data*: (biotite) K_2O = 2.42, 2.45%; $^{40}Ar^*$ = 0.6231 × 10^{-10} mol/gm; $^{40}Ar^*/\Sigma^{40}Ar$ = 47%; (hornblende) K_2O = 0.54, 0.57%; $^{40}Ar^*$ = 0.1114 × 10^{-10} mol/gm; $^{40}Ar^*/\Sigma^{40}Ar$ = 40%; (zircon) P_s = 2.13 × 10^6 tracks/cm² (414); P_i = 9.83 × 10^6 tracks/cm² (956); ϕ = 0.922 × 10^{15} n/cm²; U = 310 ppm. *Comment*: Hypabyssal quartz-diorite intrusive at Wet Leggett Spring forms a small body along the San Francisco Mountains fault zone (Ratté, 1986). Quartz diorite contains about 30% phenocrysts, mainly plagioclase, plus amethystine quartz, green hornblende, and biotite, in a finely granular to granophyric matrix of quartz and alkali feldspar. The biotite age is questionable because the low potassium content of the biotite suggests possible alteration, although such alteration was not visually evident.

K–Ar (biotite) 17.7 ± 0.6 m.y.
(hornblende) 13.9 ± 0.7 m.y.
Fission-track (zircon) 11.9 ± 1.4 m.y.

141. *USGS(D)–BB–3–82, Ratté, 1986* K–Ar
Rhyolite east of Maverick Peak (33°39′27″N, 108°55′34″W; NE1/4 sec. 32, T7S, R20W; about 1 km southwest of Lost Spring, Bull Basin quad., Catron Co., NM). *Analytical data*: K_2O = 6.49, 6.55%; $^{40}Ar^*$ = 1.318 × 10^{-10} mol/gm; $^{40}Ar^*/\Sigma^{40}Ar$ = 86%. *Comment*: Sanidine concentrate is from a marginal vitrophyre zone of a small rhyolite flow–dome, one of several intrusive–extrusive silicic- to intermediate-composition bodies along the San Francisco Mountains fault zone (Ratté, 1980; 1986). See also sample USGS(D)–BB–16E–76 (Entry 140).

(sanidine) 14.0 ± 0.5 m.y.

142. *Ratté, 1980, table 1, no. 2 (SP–5–74)* K–Ar, Fission-track
Ash-flow tuff (33°35′35″N, 108°54′26″W; SE1/4 sec. 21, T8S, R20W; roadcut on US–180, about 2 km north of Saliz Pass, Saliz Pass quad., Catron Co., NM). *Analytical data*: (sanidine) K_2O = 6.91, 6.91%; $^{40}Ar^*$ = 3.255 × 10^{-10} mol/gm; $^{40}Ar^*/\Sigma^{40}Ar$ = 92%; (biotite) K_2O = 6.78, 6.77%; $^{40}Ar^*$ = 2.923 × 10^{-10} mol/gm; $^{40}Ar^*/\Sigma^{40}Ar$ = 35% (redetermination, $^{40}Ar^*$ = 2.776 × 10^{-10} mol/gm; $^{40}Ar^*/\Sigma^{40}Ar$ = 32%); (7 zircons) P_s = 4.37 × 10^6 tracks/cm² (1,031); P_i = 9.65 × 10^6 tracks/cm² (1,139); ϕ = 1.19 × 10^{15} n/cm²; U = 260 ppm. *Comment*: Tuff occurs as an isolated lens interlayered in the pre-Davis Canyon Tuff andesite complex. Age given by the biotite is probably too young. The percentage of radiogenic argon obtained for biotite in both this sample and sample UP–G20 (Entry 143) is less than is commonly expected for biotites of this general age. Loss of radiogenic argon could have been

caused by strain or distortion of the biotite crystalline structure by ions not usually present in biotite—thus allowing diffusive loss of radiogenic argon. Or, the biotite may have been altered to some degree by ground water.

K–Ar (sanidine) 32.4 ± 1.1 m.y.
(biotite) 29.7 ± 1.0 m.y.
28.2 ± 1.0 m.y.
Fission-track (zircon) 32.3 ± 2.4 m.y.

143. *UP–G20* K–Ar
Ash-flow tuff lens interlayered in pre-Davis Canyon Tuff andesite complex (33°35′35″N, 108°54′26″W; SE1/4 sec. 21, T8S, R20W; roadcut on US–180, about 2 km north of Saliz Pass, Saliz Pass quad., Catron Co., NM). *Analytical data*: (sanidine) K_2O = 6.81%; $^{40}Ar^*$ = 2.987 and 3.149 × 10^{-10} mol/gm; $^{40}Ar^*/\Sigma^{40}Ar$ = 100, 100%; (biotite) K_2O = 6.05%; $^{40}Ar^*$ = 2.340 and 2.138 × 10^{-10} mol/gm; $^{40}Ar^*/\Sigma^{40}Ar$ = 29, 29%. *Collected and analyzed by*: M. Bikerman, Univ. of Pittsburgh. *Comment*: Ash-flow tuff sample is from same outcrop as sample SP–5–74 (Entry 142). Similarly, the biotite ages are apparently too young. See discussion under sample SP–5–74 (Entry 142).

(sanidine) 30.2 ± 2.0 m.y.
31.8 ± 2.0 m.y.
(biotite) 26.7 ± 2.0 m.y.
24.4 ± 2.0 m.y.

144. *Ratté, 1980, table 1, no. 3 (SP–62–75)* K–Ar
Davis Canyon Tuff (33°36′42″N, 108°53′21″W; sec. 15, T8S, R20W; outcrop on west side of US–180, about 1 km south of Cottonwood Campground, Saliz Pass quad., Catron Co., NM). *Analytical data*: (biotite) K_2O = 8.37, 8.41%; $^{40}Ar^*$ = 3.743 × 10^{-10} mol/gm; $^{40}Ar^*/\Sigma^{40}Ar$ = 81%; (sanidine) K_2O = 5.74, 5.72, 5.78%; $^{40}Ar^*$ = 2.415 × 10^{-10} mol/gm; $^{40}Ar^*/\Sigma^{40}Ar$ = 81%. *Comment*: The Davis Canyon Tuff at this sample locality is overlain successively by Shelley Peak Tuff; see sample UP–G73 (Entry 145) and Bloodgood Canyon Tuff.

(biotite) 30.7 ± 1.0 m.y.
(sanidine) 28.9 ± 1.0 m.y.

145. *UP–G73* K–Ar
Shelley Peak Tuff (33°36′34″N, 108°53′16″W; SE 1/4 sec. 15, T8S, R20W; roadcut west of US–180, about 1 km south of Cottonwood Campground, Saliz Pass quad., Catron Co., NM). *Analytical data*: K_2O = 7.80%; $^{40}Ar^*$ = 3.454 × 10^{-10} mol/gm; $^{40}Ar^*/\Sigma^{40}Ar$ = 63%. *Collected and analyzed by*: M. Bikerman, Univ. of Pittsburgh. *Comment*: Shelley Peak Tuff at this locality overlies Davis Canyon Tuff (SP–62–75, Entry 144). Both tuffs are part of a block between faults of the Brushy Mountains fault zone where it crosses US–180 (Ratté, 1980).

(biotite) 30.5 ± 1.5 m.y.

146. *Ratté, 1980, table 1, no. 4* K–Ar, Fission-track
(SP–3–74)
Shelley Peak Tuff (33°30′56″N, 108°52′42″W; sec. 23, T9S, R20W; east side of San Francisco River, Saliz Pass quad., Catron Co., NM). *Analytical data*: (biotite) K_2O = 7.46, 7.50%; $^{40}Ar^*$ = 3.146 × 10^{-10} mol/gm; $^{40}Ar^*/\Sigma^{40}Ar$ = 75%; (sanidine) K_2O = 6.40, 6.32%; $^{40}Ar^*$ = 2.585 × 10^{-10} mol/gm; $^{40}Ar^*/\Sigma^{40}Ar$ = 83%; (zircon) P_s = 2.29 × 10^6 tracks/cm² (953); P_i = 5.23 × 10^6 tracks/cm² (1,089); ϕ = 1.09 × 10^{15} n/cm²; U = 150 ppm. *Comment*: Shelley Peak Tuff at this sample locality is overlain by Bloodgood Canyon Tuff. See samples SP–4A–74, SP–4B–74, and SP–4C–74 (Entries 147a, 147b, and 147c).

K–Ar (biotite) 29.1 ± 1.0 m.y.
(sanidine) 28.1 ± 1.0 m.y.
Fission-track (zircon) 28.5 ± 2.4 m.y.

147a. *Ratté, 1980, table 1, no. 5 (SP–4A–74)* K–Ar
Bloodgood Canyon Tuff (33°30′36″N, 108°52′33″W; sec. 23, T9S, R20W; cliffs on east side of San Francisco River, Saliz Pass quad., Catron Co., NM). *Analytical data*:

Sample no.	K_20 %	$^{40}Ar^*$ × 10^{-10} mol/gm	$^{40}Ar^*/\Sigma^{40}Ar$
sanidine–1	6.18, 6.16, 6.13, 6.14	2.519	86%
sanidine–2	6.31, 6.28	2.555	90%
sanidine–3	9.07, 9.10, 9.02, 9.07	3.404	73%

Comment: Tuff samples SP–4A–74 (Entry 147a), SP–4B–74 (Entry 147b), and SP–4C–74 (Entry 147c) represent progressive welding of the Bloodgood Canyon Tuff, from a poorly welded vapor phase at the top to a densely welded vapor phase at the bottom. SP–4A–74 is from the poorly welded zone. Sanidine–1 and –2 contained 15–20% quartz; sanidine–3 was almost free of quartz. However, the K–Ar age given by sanidine–3 is too young. Bloodgood Canyon Tuff at this locality is 28–29 m.y. old.

K–Ar (sanidine–1) 28.2 ± 1.0 m.y.
(sanidine–2) 28.0 ± 1.0 m.y.
(sanidine–3) 25.9 ± 0.9 m.y.

147b. *Ratté, 1980, table 1, no. 5* Fission-track
(SP–4B–74)
Bloodgood Canyon Tuff (same location as sample SP–4A–74, Entry 147a). *Analytical data*: (zircon) P_s = 2.03 × 10^6 tracks/cm² (461); P_i = 4.69 × 10^6 tracks/cm² (532); ϕ = 1.06 × 10^{15} n/cm²; U = 140 ppm. *Comment*: Dated sample is from the top of the densely welded zone described under Entry 147a.

(zircon) 27.4 ± 3.4 m.y.

147c. *Ratté, 1980, table 1, no. 5 (SP–4C–74)* K–Ar
Bloodgood Canyon Tuff (same location as sample SP–4A–74, Entry 147a). *Analytical data*: (sanidine) K_2O = 6.84, 6.81, 6.84, 6.86%; $^{40}Ar^*$ =

2.739×10^{-10} mol/gm; $^{40}Ar^*/\Sigma^{40}Ar = 78\%$. *Comment*: Dated sample is from the bottom of the densely welded zone mentioned under Entry 147a.

(sanidine) 27.6 ± 0.9 m.y.

148. *Ratté, 1980, table 1, no. 1 (SP–7E–76)* K–Ar
Vitrophyre (33°34′09″N, 108°53′07″W; NE¼ sec. 34, T8S, R20W; east of Saliz Canyon, Saliz Pass quad., Catron Co., NM). *Analytical data*: K_2O = 6.93, 6.89%; $^{40}Ar^* = 3.368 \times 10^{-10}$ mol/gm; $^{40}Ar^*/\Sigma^{40}Ar = 71\%$. *Comment*: Vitrophyre is from vent breccia of the early andesite complex. Age is consistent with that of tuffs interlayered with the lava flows and volcaniclastic rocks of the pre-Davis Canyon Tuff andesitic volcanic complex at this locality and in adjacent quadrangles. See samples USGS(D)–BB–4E–76 (Entry 139) and SP–5–74 (Entry 142).

(biotite) 33.6 ± 1.1 m.y.

149. *USGS(D)–SP–1–82* K–Ar
Basalt of Saliz Hill (Ratté, 1980) (33°33′48″N, 108°55′15″W; sec. 32, T8S, R20W; outcrop on west side of US–180, about 1.5 km south of Saliz Pass, Saliz Pass quad., Catron Co., NM). *Analytical data*: K_2O = 1.85, 1.86%; $^{40}Ar^* = 0.3276 \times 10^{-10}$ mol/gm; $^{40}Ar^*/\Sigma^{40}Ar = 70\%$. *Comment*: The two-pyroxene andesitic basalt consists of nonaligned, stubby plagioclase and lesser pyroxene microphenocrysts in a partly glassy matrix. Even though this whole-rock age is a minimum age and may be only approximately correct, it indicates that the basalt of Saliz Pass is chronologically misplaced in the volcanic sequence shown by the map units on the geologic map of the Saliz Pass quadrangle (Ratté, 1980). The basalt should be higher in the volcanic sequence.

(whole-rock) 12.2 ± 0.5 m.y.

150. *Ratté, 1980, table 1, no. 6 (SP–50A–75)* K–Ar
Basalt of Pueblo Park (33°36′04″N, 108°56′55″W; NW¼ sec. 19, T8S, R20W; east of the bridge over Dangerous Park Canyon, Pueblo Park Road, Saliz Pass quad., Catron Co., NM). *Analytical data*: K_2O = 0.25, 0.21, 0.24, 0.25%; $^{40}Ar^* = 0.0668 \times 10^{-10}$ mol/gm; $^{40}Ar^*/\Sigma^{40}Ar = 7\%$. *Comment*: Olivine basalt contains clear plagioclase phenocrysts several centimeters long and near bytownite in composition (An_{67}). It overlies Bloodgood Canyon Tuff with or without intervening volcaniclastic sandstone beds and thus is comparable in stratigraphic position, if not in age, to the basalt of Saliz Hill, sample USGS(D)–SP–1–82 (Entry 149).

(plagioclase) 19.2 ± 2.7 m.y.

151. *USGS(D)–OB–100C–77* K–Ar, Fission-track
Rhyolite intrusive (33°31′06″N, 108°51′17″W; NE¼ sec. 24, T2N, R20W; north of Frying Pan Creek, O Block Canyon quad., Catron Co., NM). *Analytical data*: (whole-rock) K_2O = 4.93, 4.93%; $^{40}Ar^* = 2.183 \times 10^{-10}$ mol/gm; $^{40}Ar^*/\Sigma^{40}Ar$ = 84%; (6 zircons) $P_s = 3.80 \times 10^6$ tracks/cm² (296); $P_i = 8.05 \times 10^6$ tracks/cm² (314); $\phi = 0.945 \times 10^{15}$ n/cm²; U = 250 ppm. *Comment*: Small rhyolite intrusive cuts Davis Canyon, Shelley Peak, and Bloodgood Canyon Tuffs. Thus, the zircon age is in better agreement with the geologic field relations than the whole-rock age. The rhyolite seems to underlie a trapdoor-like fault block situated between Frying Pan Creek and the San Francisco River (Ratté, unpubl. mapping 1977).

K–Ar (whole-rock) 30.5 ± 1.0 m.y.
Fission-track (zircon) 26.6 ± 4.2 m.y.

152. *USGS(D)–OB–8C–76* K–Ar, Fission-track
Rhyolite tuff (33°31′00″N, 108°48′52″W; Black Mountain, west of Devil's Park, O Block Canyon quad., Catron Co., NM). *Analytical data*: (sanidine) K_2O = 7.63, 7.63%; $^{40}Ar^* = 7.500 \times 10^{-10}$ mol/gm; $^{40}Ar^*/\Sigma^{40}Ar = 96\%$; (zircon) $P_s = 4.78 \times 10^6$ tracks/cm² (841); $P_i = 11.99 \times 10^6$ tracks/cm² (1,055); $\phi = 1.10 \times 10^{15}$ n/cm²; U = 310 ppm. *Comment*: A white rhyolite-tuff lens, 1–2 m thick, occurring within a 5-m sandy-tuff sequence enclosed between thin andesitic flows and flow breccia (Ratté, unpubl. mapping 1977). The sanidine age is spurious.

K–Ar (sanidine) 67.0 ± 2.3 m.y.
Fission-track (zircon) 26.2 ± 2.4 m.y.

153. *Ratté et al., 1984, table 6, no. 6A & 6B (UP–G35)* K–Ar
Bloodgood Canyon Tuff (33°43′09″N, 108°47′11″W; SE¼ sec. 3, T7S, R19W; Starkweather Canyon, Reserve quad., Catron Co., NM). *Analytical data*: (Univ. of Pittsburgh) K_2O = 6.60%; $^{40}Ar^* = 2.327 \times 10^{-10}$ mol/gm; $^{40}Ar^*/\Sigma^{40}Ar$ = 91%; (USGS) K_2O = 6.57, 6.67%; $^{40}Ar^* = 2.616 \times 10^{-10}$ mol/gm; $^{40}Ar^*/\Sigma^{40}Ar = 92\%$. *Collected by*: M. Bikerman, Univ. of Pittsburgh. *Comment*: The significant difference (more than 10%) in calculated ages for the same sanidine concentrate is due to the difference in the radiogenic argon determined by the different laboratories.

The Bloodgood Canyon Tuff at this locality is separated from the underlying Shelley Peak Tuff by 20 m or more of reddish-brown volcaniclastic sandstone (Ratté, unpubl. mapping 1978).

Univ. of Pittsburgh **(sanidine) 24.3 ± 1.5 m.y.**
USGS **(sanidine) 27.3 ± 0.9 m.y.**

154. *Weber and Bassett, 1963, no. 5* K–Ar
Weber, 1971, no. B/NMBM–313A–KA1
Vitrophyre, Shelley Peak Tuff (33°39′46″N, 108°48′18″W; SE¼ sec. 28, T7S, R19W; east-facing slope of Saliz Mountains at about 6,800-ft

elevation, Reserve quad., Catron Co., NM). *Analytical data*: K_2O = 3.83%; $^{40}Ar^*$ = 1.606 × 10^{-10} mol/gm (calculated from data listed by Weber, 1971); $^{40}Ar^*/\Sigma^{40}Ar$ = 64, 64%. *Comment*: The latitude–longitude of the sample locality are consistent with its location in T7S, not T9S as published in Weber (1971). Sample location as described by Weber (1971) is not quite the same as the sample location described by Weber and Bassett (1963). The Shelley Peak Tuff in this area underlies the Bloodgood Canyon Tuff and overlies Davis Canyon Tuff (Ratté, unpubl. mapping 1978).

(glass) 28.9 ± 1.8 m.y.

155. *Elston et al., 1973, table 1, no. 10* K–Ar
Bloodgood Canyon Tuff (approx. 33°44′50″N, 108°43′20″W; sec. 29, T6S, R18W; roadcut along east side of NM–12, Milligan Mountain quad., Catron Co., NM). *Analytical data*: K_2O = 8.10%; $^{40}Ar^*$ = 2.78 × 10^{-10} mol/gm; $^{40}Ar^*/\Sigma^{40}Ar$ = 98%. *Comment*: The latitude–longitude listed above are slightly different from the latitude–longitude given by Elston et al. (1973) but are more consistent with the section, township, and range described by Elston et al. (1973).

Tuff was mapped as the Railroad Canyon Rhyolite Tuff of Elston (1976, p. 140) by Rhodes and Smith (1976, fig. 2), but in this paper it is correlated with the Bloodgood Canyon Tuff. See samples MM–1A–74, MM–2–74, MM–3–74, and MM–4–74 (Entries 156, 157a, 157b, and 157c).

(sanidine) 23.7 ± 0.7 m.y.

156. *Ratté et al., 1984, table 6, no. 8 (MM–1A–74)* K–Ar, Fission-track
Bloodgood Canyon Tuff (33°44′49″N, 108°43′20″W; sec. 29, T6S, R18W; roadcut along east side of NM–12, Milligan Mountain quad., Catron Co., NM). *Analytical data*: (biotite) K_2O = 7.42, 7.41%; $^{40}Ar^*$ = 3.016 × 10^{-10} mol/gm; $^{40}Ar^*/\Sigma^{40}Ar$ = 76%; (sanidine) K_2O = 7.00, 6.99%; $^{40}Ar^*$ = 2.746 × 10^{-10} mol/gm; $^{40}Ar^*/\Sigma^{40}Ar$ = 75%; (zircon) P_s = 1.35 × 10^6 tracks/cm^2 (625); P_i = 3.08 × 10^6 tracks/cm^2 (714); ϕ = 1.10 × 10^{15} n/cm^2; U = 90 ppm. *Comment*: Sample is from same outcrops as sample 10, Entry 155. The previously published fission-track age (Ratté et al., 1984) has been corrected in this paper.

K–Ar (biotite) 28.0 ± 1.0 m.y.
(sanidine) 27.1 ± 0.9 m.y.
Fission-track (zircon) 28.9 ± 3.0 m.y.

157a. *Ratté et al., 1984, table 6, no. 9 (MM–2–74)* K–Ar
Bloodgood Canyon Tuff (33°44′35″N, 108°41′48″W; NE corner of sec. 33, T6S, R18W; base of cliff along top of ridge west of Tularosa River, Milligan Mountain quad., Catron Co., NM). *Analytical data*: K_2O = 7.72, 7.80, 7.77, 7.82%; $^{40}Ar^*$ = 2.999 and 3.033 × 10^{-10} mol/gm; $^{40}Ar^*/\Sigma^{40}Ar$ = 89, 92%. *Comment*: Bloodgood Canyon Tuff is about 60 m thick at this locality. The dated sample is a densely welded vapor-phase tuff within about 1 m of the base of the formation. This tuff unit was mapped as Apache Spring Quartz Latite (Elston, 1976, p. 132) by Rhodes and Smith (1976, fig. 2), but in this paper it is considered to be the same unit that they mapped as Railroad Canyon Rhyolite Tuff (sample 10, Entry 155) 2 km to the west. In this paper, both units are correlated by petrographic, chemical, and regional stratigraphic relationships with the Bloodgood Canyon Tuff.

(sanidine) 26.6 ± 0.9 m.y.
26.9 ± 0.9 m.y.

157b. *Ratté et al., 1984, table 6, no. 10 (MM–3–74)* K–Ar, Fission-track
Bloodgood Canyon Tuff (same location as sample MM–2–74, Entry 157a). *Analytical data*: (sanidine) K_2O = 8.10, 8.06, 8.04, 8.05%; $^{40}Ar^*$ = 3.253 × 10^{-10} mol/gm; $^{40}Ar^*/\Sigma^{40}Ar$ = 82%; (sphene) P_s = 0.316 × 10^6 tracks/cm^2 (215); P_i = 4.743 × 10^6 tracks/cm^2 (1,614); ϕ = 6.98 × 10^{15} n/cm^2; U = 20 ppm. *Comment*: Dated sample is from the most densely welded crystal-rich zone in the formation. The stratigraphic information given for sample MM–2–74 (Entry 157a) also applies to this sample. Previously published ages for this sample (Ratté et al., 1984) have been corrected slightly in this paper.

K–Ar (sanidine) 27.8 ± 0.9 m.y.
Fission-track (sphene) 27.9 ± 4.0 m.y.

157c. *Ratté et al., 1984, table 6, no. 11 (MM–4–74)* K–Ar, Fission-track
Bloodgood Canyon Tuff (same location as sample MM–2–74, Entry 157a). *Analytical data*: (sanidine–1) K_2O = 6.99, 6.98%; $^{40}Ar^*$ = 2.781 × 10^{-10} mol/gm; $^{40}Ar^*/\Sigma^{40}Ar$ = 90%; (sanidine–2) K_2O = 7.59, 7.50, 7.52, 7.63%; $^{40}Ar^*$ = 3.075 × 10^{-10} mol/gm; $^{40}Ar^*/\Sigma^{40}Ar$ = 56%; (zircon) P_s = 2.99 × 10^6 tracks/cm^2 (691); P_i = 7.02 × 10^6 tracks/cm^2 (812); ϕ = 1.07 × 10^{15} n/cm^2; U = 210 ppm; (sphene) P_s = 0.313 × 10^6 tracks/cm^2 (165); P_i = 4.20 × 10^6 tracks/cm^2 (1,108); ϕ = 6.82 × 10^{15} n/cm^2; U = 20 ppm. *Comment*: Dated sample is a partially welded tuff near the top of the formation. Stratigraphic information given for sample MM–2–74 (Entry 157a) also applies to this sample. Previously published sphene fission-track age (Ratté et al., 1984) has been corrected in this paper.

K–Ar (sanidine–1) 27.4 ± 0.9 m.y.
(sanidine–2) 28.0 ± 1.0 m.y.
Fission-track (zircon) 27.3 ± 2.8 m.y.
(sphene) 30.4 ± 5.0 m.y.

158. *Ratté et al., 1984, table 5, no. 2 (UP–TTC)* K–Ar
Basal tuff, Tularosa Canyon Rhyolite (Elston, 1976, p. 143) (33°44′00″N, 108°42′15″W; sec. 33, T6S, R18W; Tularosa Canyon, Milligan Mountain quad., Catron Co., NM). *Analytical data*: (biotite) K_2O = 7.23%; $^{40}Ar^*$ = 3.116 × 10^{-10} mol/gm; $^{40}Ar^*/\Sigma^{40}Ar$ = 77%; (feldspar mixture) K_2O = 3.26%; $^{40}Ar^*$ = 1.279 × 10^{-10} mol/gm; $^{40}Ar^*/\Sigma^{40}Ar$ = 79%. *Collected by*: R. C. Rhodes. *Analyzed by*: M. Bikerman, Univ. of Pittsburgh. *Comment*: The volcanic sequence at this locality includes two thin (less than 50 m thick) crystal-poor ash-flow tuffs that underlie Bloodgood Canyon Tuff. Both crystal-poor tuffs were included in the Tularosa Canyon Rhyolite by Rhodes and Smith (1976), who considered eruption of the tuffs to have caused subsidence of the buried Squirrel Springs depression. Which tuff they dated is not known. Alternatively, the crystal-poor tuffs were tentatively considered to be separate cooling units of Davis Canyon Tuff by Ratté (unpubl. mapping 1978). However, preliminary paleomagnetic observations by McIntosh (pers. comm. 1985) suggest that only the lower tuff is Davis Canyon Tuff and that the upper tuff may be Vicks Peak Tuff. These correlations obviate the need for the Squirrel Springs depression because both the Davis Canyon and Vicks Peak Tuffs have probable sources elsewhere (Ratté et al., 1984; Osburn and Chapin, 1983).

(biotite) 29.7 ± 1.5 m.y.
(feldspar mixture) 27.1 ± 2.0 m.y.

159. *Smith et al., 1976, no. Ttc* Fission-track
Tularosa Canyon Rhyolite (Elston, 1976, p. 143) (approx. 33°44′00″N, 108°35′10″W; SW1/4 sec. 34, T6S, R17W (Rhodes and Smith, 1976, fig. 2); north of road to Eagle Peak, along upper Long Canyon, Eagle Peak quad., Catron Co., NM). *Analytical data*: P_s = 98 tracks; P_i = 492 tracks; ϕ = 2.51 × 10^{15} n/cm². *Comment*: The phenocryst-poor rhyolitic ash-flow tuff at this locality underlies the Bloodgood Canyon and Shelley Peak Tuffs (Ratté, unpubl. mapping 1983) and probably correlates either with Davis Canyon Tuff or Vicks Peak Tuff.

(sphene) 31.6 ± 2.0 m.y.

160. *Bikerman, 1972, no. UP–G3* K–Ar
Squirrel Springs Canyon Andesite (Rhodes and Smith, 1976, fig. 2) (approx. 33°43′54″N, 108°35′05″W; SW1/4 sec. 34, T6S, R17W; along Forest Road near head of Long Canyon, Eagle Peak quad., Catron Co., NM). *Analytical data*: K_2O = 0.524%; $^{40}Ar^*$ = 0.18487 × 10^{-10} mol/gm; $^{40}Ar^*/\Sigma^{40}Ar$ = 84%. *Collected by*: R. C. Rhodes, E. I. Smith, and M. Bikerman. *Analyzed by*: M. Bikerman, Univ. of Pittsburgh. *Comment*: Coarsely porphyritic andesite, which contains plagioclase phenocrysts 1–2 cm long, seems to underlie Shelley Peak and Bloodgood Canyon Tuffs at this locality. This is consistent with the volcanic sequence elsewhere south and west of the San Agustin Plains. If the sequence is the same here, the plagioclase age is 3–5 m.y. too young for Squirrel Springs Canyon Andesite.

(plagioclase) 24.3 ± 1.5 m.y.

161. *Ratté et al., 1984, table 6, no. 12 (UP–G48)* K–Ar
Bloodgood Canyon Tuff (approx. 33°43′39″N, 108°34′30″W; NE1/4 sec. 3, T7S, R17W; near head of Long Canyon, Forest Road 233 to Eagle Peak, Eagle Peak quad., Catron Co., NM). *Analytical data*: (Univ. of Pittsburgh) K_2O = 6.51%; $^{40}Ar^*$ = 2.582 × 10^{-10} mol/gm; $^{40}Ar^*/\Sigma^{40}Ar$ = 95%; (USGS) K_2O = 6.69, 6.68%; $^{40}Ar^*$ = 2.529 × 10^{-10} mol/gm; $^{40}Ar^*/\Sigma^{40}Ar$ = 91%. *Collected and analyzed by*: M. Bikerman, Univ. of Pittsburgh. *Comment*: This tuff was mapped as Railroad Canyon Tuff by Rhodes and Smith (1976, fig. 2), but in this paper, it is correlated with the Bloodgood Canyon Tuff.

Univ. of Pittsburgh **(sanidine) 27.3 ± 1.5 m.y.**
USGS **(sanidine) 26.1 ± 0.9 m.y.**

162. *UP–TDW* K–Ar
Deadwood Gulch Member, Fanney Rhyolite (33°22′14″N, 108°42′26″W; sec. 4, T11S, R18W; along Bursum Road at Silver Creek Divide, Grouse Mountain quad., Catron Co., NM). *Analytical data*: K_2O = 7.56%; $^{40}Ar^*$ = 2.672 × 10^{-10} mol/gm; $^{40}Ar^*/\Sigma^{40}Ar$ = 98%. *Collected by*: R. V. Fodor, W. R. Sigleo, and R. C. Rhodes. *Analyzed by*: M. Bikerman, Univ. of Pittsburgh. *Comment*: Pyroclastic member of the Fanney Rhyolite. Age is too young; compare with Fanney Rhyolite (Entry 72).

(sanidine) 24.4 ± 1.5 m.y.

163. *USGS(D)–SU–2–77* K–Ar, Fission-track
Rhyolitic ash-flow tuff (34°06′05″N, 107°56′05″W; S1/2 sec. 25, T2S, R11W; at 8,680-ft elevation on southeast slope of South Crosby Peak, Sugarloaf Mountain quad., Catron Co., NM). *Analytical data*: K_2O = 5.84, 5.84%; $^{40}Ar^*$ = 2.301 × 10^{-10} mol/gm; $^{40}Ar^*/\Sigma^{40}Ar$ = 89%; (6 zircons) P_s = 3.87 × 10^6 tracks/cm² (878); P_i = 9.51 × 10^6 tracks/cm² (1,080); ϕ = 0.943 × 10^{15} n/cm²; U = 290 ppm. *Comment*: A 2-m thick, partly welded, vapor-phase, phenocryst-poor tuff overlying the volcaniclastic rocks of South Crosby Peak was included in the A–L Peak Tuff of Lopez and Bornhorst (1979) but now is called Vicks

Peak Tuff (see Entry 187). Age and correlation of this dated unit remain uncertain.

K–Ar (sanidine) 27.2 ± 0.9 m.y.
Fission-track (zircon) 22.9 ± 2.1 m.y.

164. *USGS(D)–SU–3–77* K–Ar, Fission-track
Intrusive of Cerrito Viejo (Lopez and Bornhorst, 1979) (34°02′33″N, 107°56′45″W; sec. 14, T3S, R11W; Sugarloaf Mountain quad., Catron Co., NM). *Analytical data*: (biotite) K_2O = 2.91, 2.86%; $^{40}Ar^*$ = 1.264 × 10^{-10} mol/gm; $^{40}Ar^*/\Sigma^{40}Ar$ = 71%; (7 zircons) P_s = 3.18 × 10^6 tracks/cm² (582); P_i = 8.35 × 10^6 tracks/cm² (764); ϕ = 0.940 × 10^{15} n/cm²; U = 260 ppm. *Comment*: Age of this quartz-diorite intrusive is uncertain. Its actual age could be around 21 m.y. An age of 30 m.y. is not geologically unreasonable, but the low potassium content of the biotite separate suggests possible mineral contamination or biotite alteration; both possibilities could give rise to a spurious K–Ar age.

K–Ar (biotite) 30.2 ± 1.1 m.y.
Fission-track (zircon) 21.4 ± 2.3 m.y.

165. *USGS(D)–SU–4–77* $^{40}Ar/^{39}Ar$, K–Ar, Fission-track
Hells Mesa Tuff (Osburn and Chapin, 1983) (34°04′48″N, 107°54′26″W; sec. 5, T3S, R10W; roadcut on west side of NM–12, Sugarloaf Mountain quad., Catron Co., NM). *Analytical data*: (biotite) K_2O = 7.92, 7.88%; $^{40}Ar^*$ = 3.788 × 10^{-10} mol/gm; $^{40}Ar^*/\Sigma^{40}Ar$ = 70%; (impure biotite) K_2O = 5.64, 5.71%; $^{40}Ar^*$ = 2.735 × 10^{-10} mol/gm; $^{40}Ar^*/\Sigma^{40}Ar$ = 79%; (sanidine) K_2O = 7.24, 7.29%; $^{40}Ar^*$ = 3.255 × 10^{-10} mol/gm; $^{40}Ar^*/\Sigma^{40}Ar$ = 94%; (7 zircons) P_s = 5.67 × 10^6 tracks/cm² (1,231); P_i = 10.16 × 10^6 tracks/cm² (1,102); ϕ = 0.938 × 10^{15} n/cm²; U = 310 ppm. *Comment*: Rhyolite ash-flow tuff was originally mapped as tuff of Rock Tank (Lopez and Bornhorst, 1979). $^{40}Ar/^{39}Ar$ ages indicate that this tuff is 32 m.y. old (Kedzie, 1984, p. 44). See also sample USGS(D)–SU–5–77 (Entry 166).

$^{40}Ar/^{39}Ar$ (biotite) 32.11 ± 0.19 m.y.
K–Ar (biotite) 33.0 ± 1.1 m.y.
(impure biotite) 33.2 ± 1.1 m.y.
(sanidine) 30.9 ± 1.1 m.y.
Fission-track (zircon) 31.4 ± 2.6 m.y.

166. *USGS(D)–SU–5–77* $^{40}Ar/^{39}Ar$, K–Ar, Fission-track
Hells Mesa Tuff (Osburn and Chapin, 1983) (34°06′30″N, 107°53′17″W; sec. 28, T2S, R10W; roadcut on east side of NM–12, Sugarloaf Mountain quad., Catron Co., NM). *Analytical data*: (biotite) K_2O = 7.35, 7.50, 7.48%; $^{40}Ar^*$ = 3.489 × 10^{-10} mol/gm; $^{40}Ar^*/\Sigma^{40}Ar$ = 85%; (sanidine) K_2O = 6.94, 6.95%; $^{40}Ar^*$ = 2.886 × 10^{-10} mol/gm; $^{40}Ar^*/\Sigma^{40}Ar$ = 89%; (plagioclase) K_2O = 0.80, 0.81%; $^{40}Ar^*$ = 0.3633 × 10^{-10} mol/gm; $^{40}Ar^*/\Sigma^{40}Ar$ = 80%; (6 zircons) P_s = 4.96 × 10^6 tracks/cm² (790); P_i = 9.45 × 10^6 tracks/cm² (753); ϕ = 0.935 × 10^{15} n/cm²; U = 290 ppm. *Comment*: Rhyolite ash-flow tuff was originally mapped as tuff of Ary Ranch (Lopez and Bornhorst, 1979). The K–Ar biotite age of 32.3 m.y. is in excellent agreement with the $^{40}Ar/^{39}Ar$ plateau age of biotite from this sample determined by Kedzie (1984, p. 44). See sample USGS(D)–SU–4–77 (Entry 165).

$^{40}Ar/^{39}Ar$ (biotite) 32.09 ± 0.10 m.y.
(sanidine) 31.87 ± 0.07 m.y.
K–Ar (biotite) 32.3 ± 1.5 m.y.
(sanidine) 28.6 ± 1.0 m.y.
(plagioclase) 31.1 ± 1.9 m.y.
Fission-track (zircon) 29.3 ± 3.0 m.y.

167. *USGS(D)–DA–2A–76* Fission-track
Rock House Canyon Tuff (Osburn and Chapin, 1983)(34°09′43″N, 107°50′55″W; center of sec. 2, T1S, R10W; top of hill 7791, Datil quad., Catron Co., NM). *Analytical data*: (6 zircons) P_s = 4.31 × 10^6 tracks/cm² (585); P_i = 8.69 × 10^6 tracks/cm² (589); ϕ = 0.954 × 10^{15} n/cm²; U = 260 ppm. *Comment*: Tuff was originally mapped as tuff of Main Canyon (Lopez and Bornhorst, 1979). The calculated zircon age for this tuff is too young if the Blue Canyon Tuff (Entry 189), which overlies the Rock House Canyon Tuff elsewhere, is 32–33 m.y. old (Bornhorst et al., 1982).

(zircon) 28.3 ± 3.3 m.y.

168. *USGS(D)–DA–1B–82* K–Ar
Datil Well Tuff (Lopez and Bornhorst, 1979) (34°09′23″N, 107°51′01″W; SW¼ sec. 2, T2S, R10W; east of White House Canyon and NM–60, west of Datil, Datil quad., Catron Co., NM). *Analytical data*: K_2O = 6.96, 6.94%; $^{40}Ar^*$ = 3.603 × 10^{-10} mol/gm; $^{40}Ar^*/\Sigma^{40}Ar$ = 66%. *Comment*: Rhyolitic, crystal-rich tuff is part of the Datil Group (Osburn and Chapin, 1983). The sanidine age agrees remarkably well with a sanidine age—35.6 m.y.—reported by Bornhorst et al. (1982) for a sample of Datil Well Tuff from the same locality (see Entry 190).

(sanidine) 35.6 ± 1.3 m.y.

169. *USGS(D)–DU–1–79* K–Ar, Fission-track
Rhyolite ash-flow tuff (33°41′28″N, 107°43′34″W; NW¼ sec. 24, T7S, R9W; south side of Stone Canyon, Dusty quad., Catron Co., NM). *Analytical data*: (sanidine) K_2O = 6.98, 6.96%; $^{40}Ar^*$ = 2.726 × 10^{-10} mol/gm; $^{40}Ar^*/\Sigma^{40}Ar$ = 88%; (7 zircons) P_s = 1.4 × 10^6 tracks/cm² (156); P_i = 5.7 × 10^6 tracks/cm² (326); ϕ = 1.14 × 10^{15} n/cm²; U = 144 ppm. *Comment*: Phenocryst-poor tuff was mapped as tuff of Wahoo Canyon

(Fodor, 1976, fig. 2); it is now correlated with La Jencia Tuff or Vicks Peak Tuff (Osburn and Chapin, 1983). The sanidine age compares to $^{40}Ar/^{39}Ar$ ages of 28.46 and 28.78 m.y. for Vicks Peak and La Jencia Tuffs, respectively (Table 2).

K–Ar (sanidine) 27.0 ± 1.0 m.y.
Fission-track (zircon) 16.8 ± 3.2 m.y.

170. *Elston et al., 1973, table 1, no. 15* K–Ar
Olivine basalt (approx. 32°55′30″N, 107°59′45″W; sec. 9, T16S, R11W; San Lorenzo quad., Grant Co., NM). *Analytical data*: K_2O = 1.55%; $^{40}Ar^*$ = 0.145 × 10^{-10} mol/gm; $^{40}Ar^*/\Sigma^{40}Ar$ = 27%. *Comment*: Basalt flow is interlayered with the uppermost beds of Gila Conglomerate east of the Mimbres Valley, according to Elston et al. (1973). The township location of this sample (Elston et al., 1973) has been changed from T15S to T16S to be consistent with the approximate latitude–longitude cited here.

(whole-rock) 6.47 ± 0.41 m.y.

171. *Ratté et al., 1984, table 3, no. 2, (CM–1–77)* K–Ar, Fission-track
Fall Canyon(?) Tuff (32°51′55″N, 108°26′32″W; SE¼ sec. 36, T16S, R16W; about 1 km northeast of Circle Mesa, Circle Mesa quad., Grant Co., NM). *Analytical data*: K_2O = 7.54, 7.55%; $^{40}Ar^*$ = 3.812 × 10^{-10} mol/gm; $^{40}Ar^*/\Sigma^{40}Ar$ = 66%; (6 zircons) P_s = 3.96 × 10^6 tracks/cm² (698); P_i = 7.34 × 10^6 tracks/cm² (647); ϕ = 0.957 × 10^{15} n/cm²; U = 220 ppm. *Comment*: Phenocryst-rich tuff may correlate with the Fall Canyon Tuff (Ratté and Gaskill, 1975; Ratté, 1981). See sample USGS(D)–SR–10–81 (Entry 172).

K–Ar (biotite) 34.7 ± 1.2 m.y.
Fission-track (zircon) 30.8 ± 3.4 m.y.

172. *USGS(D)–SR–10–81* $^{40}Ar/^{39}Ar$, K–Ar
Fall Canyon(?) Tuff (32°47′30″N, 108°54′20″W; NE corner of sec. 33, T17S, R20W; Davenport Canyon, Steeple Rock quad., Grant Co., NM). *Analytical data*: (biotite) K_2O = 8.34, 8.34%; $^{40}Ar^*$ = 3.936 × 10^{-10} mol/gm; $^{40}Ar^*/\Sigma^{40}Ar$ = 86%; (sanidine) K_2O = 7.02, 7.03%; $^{40}Ar^*$ = 2.976 × 10^{-10} mol/gm; $^{40}Ar^*/\Sigma^{40}Ar$ = 80%. *Comment*: Crystal-rich ash-flow tuff contains quartz, sanidine, plagioclase, and biotite phenocrysts. Biotite gave a $^{40}Ar/^{39}Ar$ plateau age of 32.4 m.y. (Sutter, pers. comm. 1984), which is in good agreement with the conventional K–Ar biotite age and the accepted age for Hells Mesa Tuff. See Entries 165 and 166.

$^{40}Ar/^{39}Ar$ (biotite) 32.42 ± 0.14 m.y.
K–Ar (biotite) 32.5 ± 1.2 m.y.
(sanidine) 29.2 ± 1.1 m.y.

173a. *Ratté et al., 1984, table 6, no. 21 (SR–1C–81)* Fission-track
Bloodgood Canyon Tuff (32°48′22″N, 108°59′36″W; sec. 27, T17S, R21W; Steeple Rock quad., Grant Co., NM). *Analytical data*: See Table 10. *Comment*: Fission-track dating of five zircon samples from the Bloodgood Canyon Tuff in the Steeple Rock quad. indicates an average age of about 30 m.y. (Table 10). The fission-track age listed below is the average of three ages.

(zircon) 30.3 ± 1.9 m.y.

173b. *Ratté et al., 1984, table 6, no. 21 (SR–3D–81)* Fission-track
Bloodgood Canyon Tuff (32°49′45″N, 108°59′42″W; sec. 15, T17S, R21W; Steeple Rock quad., Grant Co., NM). *Analytical data*: See Table 10. *Comment*: See sample SR–1C–81 (Entry 173a).

(zircon) 31.0 ± 2.1 m.y.

173c. *Ratté et al., 1984, table 6, no. 21 (SR–5B–81)* Fission-track
Bloodgood Canyon Tuff (32°49′12″N, 108°54′40″W; NE¼ sec. 21, T17S, R20W; Steeple Rock quad., Grant Co., NM). *Analytical data*: See Table 10. *Comment*: See sample SR–1C–81 (Entry 173a).

(zircon) 27.4 ± 1.2 m.y.

173d. *Ratté et al., 1984, table 6, no. 21 (SR–6A–81)* Fission-track
Bloodgood Canyon Tuff (32°48′42″N, 108°55′20″W; SW¼ sec. 21, T17S, R20W; Steeple Rock quad., Grant Co., NM). *Analytical data*: See Table 10. *Comment*: See sample SR–1C–81 (Entry 173a).

(zircon) 30.0 ± 1.4 m.y.

173e. *Ratté et al., 1984, table 6, no. 21 (SR–7B–81)* Fission-track
Bloodgood Canyon Tuff (32°48′18″N, 108°55′05″W; sec. 28, T17S, R20W; Steeple Rock quad., Grant Co., NM). *Analytical data*: See Table 10. *Comment*: See sample SR–1C–81 (Entry 173a).

(zircon) 31.0 ± 1.5 m.y.

174. *Strangway et al., 1976, no. RB, no. RB9B* K–Ar
Andesite (approx. 32°59′20″N, 108°57′40″W; NE ¼ sec. 24, T15S, R21W; top of Brushy Mountain, Steeple Rock quad., Grant Co., NM). *Comment*: The andesitic lavas on Brushy Mountain known locally as Radar Brushy represent a major andesitic volcano of the Bearwallow Mountain Andesite.

Field no.	Whole-rock age (m.y.)
RB	23.7 ± 0.5
RB9B	25.6 ± 0.5

175. *USGS(D)–H77–NM–333* K–Ar
Quartz–alunite rock (32°53′14″N, 109°01′45″W; sec. 29, T16S, R21W; top of ridge west of Sad-

TABLE 10—Fission-track data for zircons from five samples of Bloodgood Canyon Tuff, Steeple Rock quadrangle. Fission-track counts were made on the same sample by three different investigators. The average fission-track age determined by each investigator for the five samples is as follows: 30.0 m.y. (investigator 1), 29.9 m.y. (investigator 2), 30.0 m.y. (investigator 3). The range in ages determined by each investigator is as follows: 13.0 m.y. (investigator 1), 1.6 m.y. (investigator 2), 2.8 m.y. (investigator 3). The age range can be related directly to the continuity of counting experience of each investigator—the smallest age span was obtained by the investigator with the most counting experience. $\phi = 3.46 \times 10^{15}$ n/cm².

Sample no.	P_s (tracks counted)	P_i (tracks counted)	U ppm	Age m.y.	Investigator
SR–1C–81	157	222	258–448	32.6 ± 2.8	1
SR–1C–81	344	361	avg. 359	29.0 ± 1.2	2
SR–1C–81	381	378		29.4 ± 1.2	3
				avg. 30.3 ± 1.9	
SR–3D–81	411	362	58–229	34.6 ± 2.8	1
SR–3D–81	576	586	avg. 88	29.9 ± 1.5	2
SR–3D–81	449	461		28.4 ± 1.8	3
				avg. 31.0 ± 2.1	
SR–5B–81	335	313	137–296	21.6 ± 1.1	1
SR–5B–81	563	581	avg. 200	29.5 ± 1.3	2
SR–5B–81	753	703		31.2 ± 1.2	3
				avg. 27.4 ± 1.2	
SR–6A–81	275	296	250–353	28.3 ± 1.5	1
SR–6A–81	470	468	avg. 283	30.6 ± 1.4	2
SR–6A–81	344	322		31.2 ± 1.2	3
				avg. 30.0 ± 1.4	
SR–7B–81	418	389	142–381	32.7 ± 2.0	1
SR–7B–81	500	502	avg. 260	30.3 ± 1.3	2
SR–7B–81	606	590		30.0 ± 1.2	3
				avg. 31.0 ± 1.5	

dleback Mountain, York Valley quad., Grant Co., NM). *Analytical data*: K_2O = 1.45, 1.48%; $^{40}Ar^*$ = 0.6649 × 10^{-10} mol/gm; $^{40}Ar^*/\Sigma^{40}Ar$ = 44%. *Collected by*: R. B. Hall, 1977. *Comment*: Quartz–alunite rock is from an extensive area of advanced argillic alteration west of Steeple Rock mining district (Hedlund, unpubl. mapping 1979). A similar age was obtained for an alunite rock in the Wilcox mining district, sample USGS(D)–HM–5–82 (Entry 53).

(whole-rock) 31.3 ± 1.1 m.y.

176. *Finnell, 1976a, no. T–13* K–Ar
Bloodgood Canyon Tuff (32°53′22″N, 108°10′06″W; boundary line between sec. 26 and 27, T16S, R13W; east of Twin Sisters Creek in the Pinos Altos Range, Twin Sisters quad., Grant Co., NM). *Analytical data*: (biotite) K_2O = 6.30, 6.34%; $^{40}Ar^*$ = 2.747 and 2.797 × 10^{-10} mol/gm; $^{40}Ar^*/\Sigma^{40}Ar$ = 71, 69%; (sanidine) K_2O = 4.72, 4.71%; $^{40}Ar^*$ = 1.805 × 10^{-10} mol/gm; $^{40}Ar^*/\Sigma^{40}Ar$ = 88%. *Comment*: These ages, inadvertently, were not recalculated as indicated in an earlier publication (Ratté et al., 1984, table 6, no. 22A).

(biotite) 30.0 ± 1.0 m.y.
30.5 ± 1.0 m.y.
(sanidine) 26.4 ± 0.9 m.y.

177. *Finnell, 1976a, no. T–35* K–Ar
Tadpole Ridge Quartz Latite (32°53′34″N, 108°13′48″W; NW¼ sec. 30, T16S, R13W; east side of Bear Creek, above NM–15, Twin Sisters quad., Grant Co., NM). *Analytical data*: K_2O = 8.11, 8.17%; $^{40}Ar^*$ = 3.771 × 10^{-10} mol/gm; $^{40}Ar^*/\Sigma^{40}Ar$ = 74%. *Comment*: Sample is from vitrophyre at base of lower cooling unit.

(biotite) 31.9 ± 1.0 m.y.

178. *Finnell, 1976a, no. T–48* K–Ar
Tadpole Ridge Quartz Latite (32°56′05″N, 108°10′39″W; N½ sec. 10, T16S, R13W; north side of Bear Canyon Road, about 1 km north of Signal Peak, Twin Sisters quad., Grant Co., NM). *Analytical data*: K_2O = 6.86, 6.86%; $^{40}Ar^*$ = 3.157 × 10^{-10} mol/gm; $^{40}Ar^*/\Sigma^{40}Ar$ = 87%.

Comment: Sample is from the upper cooling unit.
(biotite) 31.7 ± 1.0 m.y.

179. *Ratté et al., 1984, table 3, no. 2 (T–2–73)* $^{40}Ar/^{39}Ar$, K–Ar, Fission-track
Kneeling Nun(?) Tuff (32°52′45″N, 108°18′17″W; NE¼ sec. 32, T16S, R14W; hill 6602, about 2 km south–southwest of Preacher's Point, Reading Mountain quad., Grant Co., NM). *Analytical data*: (biotite) K_2O = 8.36, 8.36, 8.36%; $^{40}Ar^*$ = 4.264×10^{-10} mol/gm; $^{40}Ar^*/\Sigma^{40}Ar$ = 74%; (sanidine) K_2O = 7.51, 7.45%; $^{40}Ar^*$ = 3.556×10^{-10} mol/gm; $^{40}Ar^*/\Sigma^{40}Ar$ = 90%; (6 zircons) P_s = 2.91×10^6 tracks/cm² (620); P_i = 5.38×10^6 tracks/cm² (573); $\phi = 1.07 \times 10^{15}$ n/cm²; U = 140 ppm. *Comment*: The biotite age is in fair agreement with the K–Ar recalculated biotite age of 34.2 m.y. obtained by McDowell (1971) for the Kneeling Nun Tuff (Entry 191). The biotite $^{40}Ar/^{39}Ar$ plateau age of 35.88 m.y. was obtained by Sutter (pers. comm. 1984). The K–Ar ages reported by Ratté et al. (1984, table 3, no. 2) were not recalculated, as intended, and are, therefore, slightly different than the ages listed here.
$^{40}Ar/^{39}Ar$ (biotite) 35.88 ± 0.11 m.y.
K–Ar (biotite) 35.1 ± 0.8 m.y.
(sanidine) 32.7 ± 0.8 m.y.
Fission-track (zircon) 34.6 ± 4.0 m.y.

180. *Hedlund, 1977 (USGS(D)–SL–57–73)* K–Ar
Rhyolite porphyry intrusive (32°54′15″N, 107°50′50″W; T16S, R10W; Dry Gallinas Campground, San Lorenzo quad., Grant Co., NM). *Analytical data*: (biotite) K_2O = 7.58, 7.49%; $^{40}Ar^*$ = 3.908×10^{-10} mol/gm; $^{40}Ar^*/\Sigma^{40}Ar$ = 84%; (sanidine) K_2O = 7.36, 7.48%; $^{40}Ar^*$ = 3.593 and 3.746×10^{-10} mol/gm; $^{40}Ar^*/\Sigma^{40}Ar$ = 87, 93%. *Comment*: Since the rhyolite probably intrudes the lower part of the Kneeling Nun Tuff, it conditionally provides a minimum age for the Kneeling Nun Tuff. The 35.7 m.y. biotite age is compatible with the $^{40}Ar/^{39}Ar$ plateau age of 35.88 m.y. for the Kneeling Nun(?) Tuff in Reading Mountain quadrangle, sample USGS(D)–T–2–73 (Entry 179).
(biotite) 35.7 ± 1.2 m.y.
(sanidine) 33.3 ± 1.2 m.y.
34.7 ± 1.2 m.y.

181. *Hedlund, 1978 (USGS(D)–CB–268B–75)* $^{40}Ar/^{39}Ar$, K–Ar
Kneeling Nun(?) Tuff (32°29′55″N, 108°28′45″W; SE¼ NW¼ sec. 10, T21S, R16W; along highline right-of-way, north of NM–90, C Bar Ranch quad., Grant Co., NM). *Analytical data*: K_2O = 7.94, 7.99%; $^{40}Ar^*$ = 4.001×10^{-10} mol/gm; $^{40}Ar^*/\Sigma^{40}Ar$ = 79%. *Comment*: The $^{40}Ar/^{39}Ar$ plateau age of 34.1 m.y. (Sutter, pers. comm. 1984) is in good agreement with the conventional K–Ar biotite age reported here. The latter age was not recalculated, as intended, when it was listed by Ratté et al. (1984, table 3, no. 3).
$^{40}Ar/^{39}Ar$ (biotite) 34.13 ± 0.11 m.y.
K–Ar (biotite) 34.6 ± 0.8 m.y.

182. *Elston et al., 1973, table 1, no. 7* K–Ar
Bloodgood Canyon Tuff (32°52′N, 108°37′W; sec. 32, T16S, R17W; Cliff quad., Grant Co., NM). *Analytical data*: K_2O = 6.66, 6.72%; $^{40}Ar^*$ = 2.62 and 2.63×10^{-10} mol/gm; $^{40}Ar^*/\Sigma^{40}Ar$ = 74, 84%. *Comment*: Sanidine was dated in 1962 and again in 1967. These ages were not recalculated, as intended, when listed by Ratté et al. (1984, table 6, no. 25A and 25B).
1962 analysis **(sanidine) 27.1 ± 1.2 m.y.**
1967 analysis **(sanidine) 27.0 ± 0.8 m.y.**

183. *Aldrich and Laughlin, 1984* K–Ar
Basaltic andesite (33°57′00″N, 108°40′54″W; NE ¼ sec. 23, T4S, R17W; roadcut on new alignment of NM–32, which is not shown on the 1965 quadrangle map, Queens Head quad., Catron Co., NM). *Analytical data*: Geochron Laboratories: K_2O = 2.27%; $^{40}Ar^*$ = 0.9800×10^{-10} mol/gm. *Comment*: Sample is from a basaltic-andesite flow that may correlate with the andesite of Dry Leggett Canyon (Ratté, 1986). The andesite of Dry Leggett Canyon underlies the tuff of Luna (Entries 135 and 136). If this is the andesite of Dry Leggett Canyon, the whole-rock age is too young.
(whole-rock) 29.6 ± 1.4 m.y.

184. *Elston et al., 1973, table 1, no. 2* K–Ar
Tadpole Ridge Quartz Latite (32°53′50″N, 108°14′36″W; sec. 24, T16S, R14W; Twin Sisters quad., Grant Co., NM). *Analytical data*: K_2O = 7.35%; $^{40}Ar^*$ = 3.41×10^{-10} mol/gm; $^{40}Ar^*/\Sigma^{40}Ar$ = 56%. *Comment*: This ash-flow tuff was correlated with the Cooney Quartz Latite (Cooney Tuff, Entries 58, 64, 65, 66, 67, and 88) by Elston et al. (1973, table 2, no. 7), but thickness distribution of the two tuffs indicates that they are different tuffs from different source areas (Finnell, 1976a, 1976b; Ratté et al., 1984).
(biotite) 31.9 ± 1.0 m.y.

185. *Bornhorst et al., 1982, entry no. 6, no. T6T3* K–Ar
Hells Mesa Tuff (34°05′14″N, 107°56′07″W; NE ¼ SW¼ sec. 36, T2S, R11W; Sugarloaf Mountain quad., Catron Co., NM). *Analytical data*: K_2O = 8.343, 8.323, 8.318, 8.403%; $^{40}Ar^*$ = 3.761 and 3.794×10^{-10} mol/gm; $^{40}Ar^*/\Sigma^{40}Ar$ = 83.5, 84%. *Comment*: Tuff was originally designated by Lopez and Bornhorst (1979) as the rhyolite tuff of Rock Tank, but now it is correlated with

the Hells Mesa Tuff (Osburn and Chapin, 1983).
(sanidine) 32.1 ± 0.7 m.y.

186. *Bornhorst et al., 1982, entry no. 5, no. J–218* Fission-track
Tuff breccia of Horse Springs Canyon (Bornhorst, 1976) (34°00′04″N, 108°12′43″W; SE¼ NW ¼ sec. 29, T3S, R13W; Wallace Mesa quad., Catron Co., NM). *Analytical data*: P_s = 596 tracks; P_i = 1,170 tracks; ϕ = 1.0700 × 10^{15} n/cm². *Comment*: Tuff breccia sample is from outcrops in White Rock Canyon; published sample locality in Bornhorst et al. (1982) is in error, but correct location was obtained from Bornhorst (pers. comm. 1985). Zircons were separated from the matrix material of the breccia.
(zircon) 32.7 ± 3.8 m.y.

187. *Bornhorst et al., 1982, entry no. 7, no. T417* Fission-track
Vicks Peak(?) Tuff (Farkas, 1969) (34°06′47″N, 107°56′20″W; SW¼ SW¼ sec. 24, T2S, R11W; Sugarloaf Mountain quad., Catron Co., NM). *Analytical data*: P_s = 325 tracks; P_i = 556 tracks; ϕ = 0.894 × 10^{15} n/cm². *Comments*: Tuff was correlated with the A–L Peak Rhyolite Tuff by Lopez and Bornhorst (1979) but is now correlated with the Vicks Peak Tuff (Osburn and Chapin, 1983); this dated tuff likely is the same unit as that listed for Entry 163 (this paper). The age and correlation of this unit remain uncertain.
(zircon) 31.3 ± 5.0 m.y.

188. *Bornhorst et al., 1982, entry no. 8, no. J–53* Fission-track
Tularosa Canyon Rhyolite (Smith and Rhodes, 1974) (34°08′45″N, 108°11′20″W; NW¼ SW¼ sec. 10, T2S, R13W; south end of Alegres Mountain, Alegres Mountain quad., Catron Co., NM). *Analytical data*: P_s = 480 tracks; P_i = 1,028 tracks; ϕ = 1.09 × 10^{15} n/cm². *Comment*: Correlation of this dated tuff is uncertain. The Tularosa Canyon Rhyolite of Elston (1976, p. 143), where first described, is now known to consist of two separate ash-flow sheets believed to correlate with Vicks Peak Tuff and Davis Canyon Tuff on the basis of paleomagnetic analysis by McIntosh (pers. comm. 1985) and unpublished geologic mapping by Ratté (1985). The tuff dated at Alegres Mountain could be any one of several tuffs that occur in the stratigraphic interval between Blue Canyon Tuff and Bearwallow Mountain Andesite.
(zircon) 30.5 ± 3.8 m.y.

189. *Bornhorst et al., 1982, entry no. 3, no. 76T193* Fission-track
Blue Canyon Tuff (Lopez and Bornhorst, 1979) (34°04′21″N, 108°02′50″W; SW¼ sec. 1, T3S, R12W; Log Canyon quad., Catron Co., NM). *Analytical data*: P_s = 896 tracks; P_i = 1,420 tracks; ϕ = 0.878 × 10^{15} n/cm². *Comment*: Tuff was apparently sampled in sec. 1, not sec. 2, as published (Bornhorst, pers. comm. 1985). Compare with $^{40}Ar/^{39}Ar$ sanidine age of 33.93 m.y. (Table 2).
(zircon) 33.2 ± 3.2 m.y.

190. *Bornhorst et al., 1982, entry no. 2, no. 76T5* K–Ar, Fission-track
Datil Well Tuff (Lopez and Bornhorst, 1979) (34°09′22″N, 107°51′00″W; SW¼ sec. 2, T2S, R10W; Datil quad., Catron Co., NM). *Analytical data*: (sanidine) K_2O = 7.761, 7.640, 7.632, 7.638%; $^{40}Ar^*$ = 3.829, 3.836, and 3.869 × 10^{-10} mol/gm; $^{40}Ar^*/\Sigma^{40}Ar$ = 96.4, 96.5, 96.6%; (zircon) P_s = 1,090 tracks; P_i = 1,530 tracks; ϕ = 0.88393 × 10^{15} n/cm². *Comment*: Tuff sample is from the same locality as sample for Entry 168 (USGS(D)–DA–1B–82). Note very good agreement of independent sanidine ages.
K–Ar (sanidine) 35.6 ± 0.7 m.y.
Fission-track (zircon) 37.7 ± 3.8 m.y.

191. *McDowell, 1971, entry no. 60A, no. L–1111* K–Ar
Kneeling Nun Tuff (32°46′40″N, 108°06′00″W; NW¼ sec. 9, T18S, R12W; Lucky Bill Canyon, 2.5 km south of Santa Rita open-pit copper mine, Santa Rita quad., Grant Co., NM). *Analytical data*: K_2O = 8.50%; $^{40}Ar^*$ = 4.22 × 10^{-10} mol/gm; $^{40}Ar^*/\Sigma^{40}Ar$ = 73%. *Comment*: K–Ar age reported by Ratté et al. (1984, table 3, no. 1) was not recalculated as had been intended.
(biotite) 34.2 ± 1.0 m.y.

192. *Bornhorst, 1980* K–Ar
Andesite on Black Mountain (Black Mountain quad., Catron Co., NM). *Comment*: Age is cited by Bornhorst (1980, pp. 964–971) as an unpublished age from Stinnett and Damon. Location is uncertain. Andesite correlates with Bearwallow Mountain Andesite.
(whole-rock)(?) 23.9 m.y.

193. *Wahl, 1980, table 4, no. TF–1* Fission-track
Bloodgood Canyon Tuff (southeast end of Noeh Mesa, York Valley quad., Grant Co., NM). *Analytical data*: P_s = 1,119 tracks; P_i = 2,196 tracks; ϕ = 0.825 × 10^{15} n/cm². *Comment*: Wahl's suggestion that the tuff on Noeh Mesa of his thesis area correlates with the Bloodgood Canyon Tuff has been confirmed by subsequent studies (Ratté and Hedlund, 1981).
(zircon) 25.7 ± 2.1 m.y.

194. *Wahl, 1980, table 4, no. TF–2* Fission-track

Bloodgood Canyon Tuff (north side of dirt road into Soapbox Canyon, west edge of Big Lue Mountains quad., Greenlee Co., AZ). *Analytical data*: P_s = 826 tracks; P_i = 1,728 tracks; ϕ = 0.820 × 10^{15} n/cm². *Comment*: The tuff in these outcrops correlates with Bloodgood Canyon Tuff as suggested by Wahl and confirmed by Ratté (unpubl. mapping 1982).

(zircon) 24.0 ± 2.3 m.y.

195. *USGS(D)–BL–59–83* K–Ar
Dacite of Tennessee Creek (33°06′26″N, 109°02′09″W; N½ sec. 8, T14S, R21W; roadcut on north side of NM–78, Big Lue Mountains quad., Grant Co., NM). *Analytical data*: K_2O = 0.44, 0.41, 0.40, and 0.39%; $^{40}Ar^*$ = 0.1264 × 10^{-10} mol/gm; $^{40}Ar^*/\Sigma^{40}Ar$ = 49%. *Comment*: Plagioclase age is in good agreement with previously determined hornblende age of 21.8 m.y. (see Entry 33).

(plagioclase) 21.3 ± 1.8 m.y.

196. *USGS(D)–BL–292–82* K–Ar
Dacite (33°04′46″N, 109°06′25″W; sec. 13, T4S, R31E; near head of south fork of Seep Spring Canyon, Big Lue Mountains quad., Greenlee Co., AZ). *Analytical data*: K_2O = 3.27, 3.26%; $^{40}Ar^*$ = 1.146 × 10^{-10} mol/gm; $^{40}Ar^*/\Sigma^{40}Ar$ = 83%. *Comment*: Dacite probably is related to a volcanic center between Seep Spring Canyon and Cold Spring Mountain (USGS, unpubl. mapping 1982).

(whole-rock) 24.2 ± 0.9 m.y.

197. *USGS(D)–BL–90B–83* K–Ar
Porphyritic dacite flow (33°05′31″N, 109°12′08″W; NW corner of sec. 18, T4S, R31E; head of southeast fork of Limestone Gulch, about 2 km north of Chalk Peak, Big Lue Mountains quad., Greenlee Co., AZ). *Analytical data*: (hornblende) K_2O = 0.89, 0.80%; $^{40}Ar^*$ = 0.3153 × 10^{-10} mol/gm; $^{40}Ar^*/\Sigma^{40}Ar$ = 64%; (plagioclase) K_2O = 0.59, 0.59%; $^{40}Ar^*$ = 0.1719 × 10^{-10} mol/gm; $^{40}Ar^*/\Sigma^{40}Ar$ = 51%. *Comment*: The hornblende age is compatible with the age of the volcanic sequence in this part of the Big Lue Mountains quad., but the plagioclase age is younger than expected. These hornblendic flows are part of a complex intrusive–extrusive center whose relationship to the surrounding sequence needs further clarification.

(hornblende) 27.2 ± 1.0 m.y.
(plagioclase) 20.1 ± 1.1 m.y.

198. *USGS(D)–BL–241–82* K–Ar
Basalt (33°11′20″N, 109°10′04″W; SE¼ sec. 8, T3S, R31E; west of right prong of Dix Creek, Big Lue Mountains quad., Greenlee Co., AZ). *Analytical data*: K_2O = 2.23, 2.22%; $^{40}Ar^*$ = 0.5692 × 10^{-10} mol/gm; $^{40}Ar^*/\Sigma^{40}Ar$ = 69%. *Comments*: Basalt flow is one of the interlayered lavas in the Gila Conglomerate; basalt is a dense, fine-grained rock with sparse, large plagioclase phenocrysts.

(whole-rock) 17.7 ± 0.6 m.y.

199. *USGS(D)–BL–271–82* K–Ar
Andesite (33°01′17″N, 109°11′14″W; SE¼ sec. 6, T5S, R31E; in right fork of Buzzard Roost Canyon, Big Lue Mountains quad., Greenlee Co., AZ). *Analytical data*: K_2O = 3.11, 3.13%; $^{40}Ar^*$ = 1.246 × 10^{-10} mol/gm; $^{40}Ar^*/\Sigma^{40}Ar$ = 82%. *Comment*: Fine-grained amygdaloidal andesite flow overlying Bloodgood Canyon Tuff in Big Lue Mountains volcanic sequence.

(whole-rock) 27.5 ± 1.0 m.y.

200. *USGS(D)–BB–1–82, Ratté, 1986* K–Ar
Basalt (33°07′54″N, 108°53′36″W; NW¼ sec. 10, T8S, R20W; top of small hill east of US–180, Bull Basin quad., Catron Co., NM). *Analytical data*: K_2O = 0.94, 0.95%; $^{40}Ar^*$ = 0.2100 × 10^{-10} mol/gm; $^{40}Ar^*/\Sigma^{40}Ar$ = 57%. *Comment*: A gray, fine- to medium-grained olivine basalt with a few plagioclase phenocrysts (~1 cm long). Basalt flow is separated from underlying Bloodgood Canyon Tuff by 50 m or more of volcaniclastic Gila Conglomerate.

(whole-rock) 15.4 ± 0.6 m.y.

201. *USGS(D)–BL–117–82* K–Ar
Rhyolite of Hells Hole(?) (Ratté and Hedlund, 1981) (33°02′33″N, 109°09′56″W; sec. 33, T4S, R31E; west of AZ–78 in east fork of Buzzard Roost Canyon, Big Lue Mountains quad., Greenlee Co., AZ). *Analytical data*: K_2O = 0.762% by isotope dilution; $^{40}Ar^*$ = 0.3263 × 10^{-10} mol/gm; $^{40}Ar^*/\Sigma^{40}Ar$ = 40%. *Comment*: Fine-grained lithophysal rhyolite.

(hornblende) 29.5 ± 0.9 m.y.

202. *USGS(D)–345ALME84* K–Ar
Andesite (33°26′24″N, 109°01′18″W; T10S, R21W; along road on east side of Keller Canyon, Alma Mesa quad., Catron Co., NM). *Analytical data*: K_2O = 3.69, 3.69%; $^{40}Ar^*$ = 1.347 × 10^{-10} mol/gm; $^{40}Ar^*/\Sigma^{40}Ar$ = 87%. *Comment*: Fine-grained, porphyritic andesite flows in this area (Houser, unpubl. mapping 1985) correlate with the Bearwallow Mountain Andesite.

(whole-rock) 25.2 ± 0.9 m.y.

203. *USGS(D)–C–7–82* K–Ar
Rhyolite at Enebro Mountain (33°10′44″N, 109°22′48″W; NE¼ sec. 17, T3S, R29E; west of US–666 at about 7,000-ft elevation on the northeast flanks of Enebro Mountain, Clifton quad., Greenlee Co., AZ). *Analytical data*: K_2O = 4.63,

4.57%; $^{40}Ar^*$ = 1.393, 1.373 × 10^{-10} mol/gm; $^{40}Ar^*/\Sigma^{40}Ar$ = 88, 60%. *Comment*: Rhyolite is part of a flow–dome complex adjacent to the Morenci mining district. The rhyolite is similar in age to other high-silica rhyolites in adjacent areas, such as the rhyolite of Mule Creek (see Table 7).

(whole-rock) 20.9 ± 0.8 m.y.
20.6 ± 0.7 m.y.

204. *EP–2–83* K–Ar
Dacite at Eagle Peak (33°41′11″N, 108°34′30″W; secs. 15–22, T7S, R17W; roadcut on Long Canyon Road to Eagle Peak at Eagle Peak tank, Eagle Peak quad., Catron Co., NM). *Analytical data*: K_2O = 3.02, 2.99%; $^{40}Ar^*$ = 0.3726, 0.4334, 0.4289 × 10^{-10} mol/gm; $^{40}Ar^*/\Sigma^{40}Ar$ = 74, 76, 80%. *Comment*: Dacite was previously considered to be a member of the Bearwallow Mountain Formation of Elston (1976, p. 132) with an age estimated by Bornhorst (1980, pp. 1016–1019) at 22.5 m.y. Ages reported here indicate that dacite at Eagle Peak is similar in age to other composite volcanoes adjacent to the Morenci–Reserve fault zone, such as John Kerr Peak (Entry 127) and Horse Mountain (Entry 114).

(whole-rock) 8.6 ± 0.3 m.y.
9.9 ± 0.4 m.y.
10.0 ± 0.4 m.y.

205. *Kress et al., 1985, entry no. 14, no. GW–2* K–Ar
Rhyolite dike (33°12′18″N, 108°41′24″W; N1/2 sec. 3, T13S, R18W; Rice Ranch quad., Grant Co., NM). *Analytical data*: K_2O = 4.543%; $^{40}Ar^*$ = 1.523 × 10^{-10} mol/gm; $^{40}Ar^*/\Sigma^{40}Ar$ = 38.5%. *Analyzed by*: Geochron Laboratories, Inc. *Comment*: Northwest-trending dike cuts Cooney Tuff in mineralized zone bordering southern margin of Bursum caldera.

(K-feldspar) 23.1 ± 1.0 m.y.

206. *Leopoldt and Kortemeier, 1984, entry no. 2, no. A8–9* Fission-track
Vitric ash in Gila Conglomerate (33°05′N, 108°35′W; SE1/4 sec. 21, T14S, R17W; elevation about 1,720 m, east slope of mesa just west of Wild Horse Mesa, Canteen Canyon quad., Grant Co., NM). *Analytical data*: 4.5 fossil tracks counted; 118 induced tracks counted; ϕ = 0.914 × 10^{15} n/cm^2; P_s/P_i = 0.0356. Decay constant for spontaneous fission of ^{238}U = 6.85 × 10^{17}/yr.

(zircon) 2.01 ± 0.97 m.y.

207. *B–1–84* K–Ar
Andesite at Saddle Mountain (33°38′71″N, 109°01′00″W; sec. 4, T8S, R21W; outcrop along road to Saddle Mountain Lookout, Blue quad., Catron Co., NM). *Analytical data*: K_2O = 1.29, 1.30%; $^{40}Ar^*$ = 0.6259 × 10^{-10} mol/gm; $^{40}Ar^*/\Sigma^{40}Ar$ = 74%. *Comment*: The plagioclase age shows the andesitic eruptive center at Saddle Mountain to be part of the older andesite complex that is now included in the formation of Pueblo Creek (Ratté, 1986) and is largely equivalent to the Spears Formation (Osburn and Chapin, 1983).

(plagioclase) 33.3 ± 1.2 m.y.

208. *USGS(D)–MN–117–84* K–Ar
Rhyolite at Sheridan Mountain (33°14′56″N, 108°46′33″W; sec. 14, T12S, R19W; vitrophyre at base of cliffs near 7,400-ft elevation, southeast flank of Sheridan Mountain, Moon Ranch quad., Catron Co., NM). *Analytical data*: K_2O = 3.31, 3.32%; $^{40}Ar^*$ = 1.242 × 10^{-10} mol/gm; $^{40}Ar^*/\Sigma^{40}Ar$ = 91%. *Comment*: Rhyolite is part of younger rhyolite flow–dome complex along southwest ring-fracture zone of Bursum caldera (Ratté and Gaskill, 1975). Plotted as Fanney Rhyolite in Fig. 4A.

(plagioclase) 25.9 ± 0.9 m.y.

209. *USGS(D)–GR–85A* K–Ar
Rhyolite of the Mogollon Mountains (33°12′37″N, 108°31′38″W; secs. 31 and 32, T12S, R16W; at elevation of 7,700 ft on nose of ridge on south side of Mogollon Creek, Shelley Peak quad., Catron Co., NM). *Analytical data*: K_2O = 4.35, 4.31%; $^{40}Ar^*$ = 1.769 × 10^{-10} mol/gm; $^{40}Ar^*/\Sigma^{40}Ar$ = 83%. *Comment*: Rhyolite is part of flow–dome complex (Ratté and Gaskill, 1975) inside Bursum caldera at its southeast margin. Flows were called Jerky Mountains Rhyolite by Rhodes (1976a, fig. 3).

(sanidine) 28.2 ± 1.0 m.y.

210. *USGS(D)–GR–131D* K–Ar
Rhyolite of the Diablo Range (33°11′15″N, 108°26′50″W; sec. 6, T13S, R15W; at elevation of 8,600 ft just west of 8,700-ft summit about 1 km west of White Pinnacle, Diablo Range quad., Grant Co., NM). *Analytical data*: K_2O = 6.61, 5.57, 6.47%; $^{40}Ar^*$ = 2.635 × 10^{-10} mol/gm; $^{40}Ar^*/\Sigma^{40}Ar$ = 88%. *Comment*: This rhyolite was interpreted to be part of the Bursum caldera wall and older than compositionally similar rhyolite (Entry 209) within the caldera (Ratté and Gaskill, 1975), but the age relationship between the two rhyolites has not been resolved by conventional K–Ar dating. Sanidine ages agree within the analytical uncertainty.

(sanidine) 27.7 ± 1.5 m.y.

211. *USGS(D)–BL–130–83* K–Ar
Rhyodacite of the Big Lue Mountains (33°04′17″N, 109°07′24″W; sec. 23, T4S, R31E; at

elevation about 5,680 ft, north of Rustlers Springs, Big Lue Mountains quad., Greenlee Co., AZ). *Analytical data:* (biotite) K_20 = 7.34, 7.42%; $^{40}Ar^*$ = 3.004 x 10^{-10} mol/gm; $^{40}Ar^*/\Sigma^{40}Ar$ = 72%; (plagioclase) K_20 = 0.60, 0.61%; $^{40}Ar^*$ = 0.2110 x 10^{-10} mol/gm; $^{40}Ar^*/\Sigma^{40}Ar$ = 7%. *Comment:* Dated flow is near the base of the rhyodacite of the Big Lue Mountains, which consists of interlayered lava flows and pyroclastic deposits. Biotite age is believed to be more compatible with the volcanic stratigraphic sequence than the plagioclase age (Ratté, unpubl. mapping 1983).

(biotite) 28.1 ± 1.0 m.y.
(plagioclase) 24.1 ± 1.3 m.y.

212. *USGS(D)—F-3-85* K—Ar
Rhyolite of Bat Cave Wells (33°46'27"N, 108° 12'38"W; sec. 20, T6S, R13W; Bat Cave, Fullerton quad., Catron Co., NM). *Analytical data:* K_20 = 7.00, 6.97%; $^{40}Ar^*$ = 2.773 x $10^{\wedge-10}$ mol/gm; $^{40}Ar^*/\Sigma^{40}Ar$ = 76% . *Comment:* Rhyolite underlies Shelley Peak Tuff at Bat Cave and thus should be older than 28 m.y. Rhyolite of Bat Cave Wells probably correlates with rhyolite of Wye Hill of Bornhorst (1976); see Entries 121 and 122.

(anorthoclase) 27.4 ± 1.0 m.y.

Reference

Aldrich, M. J., Jr., 1974, Structural development of the Hanover-Fierro pluton, southwestern New Mexico: Geological Society of America, Bulletin, v. 85, no. 6, pp. 963-968.

Aldrich, M. J., Jr., 1976, Geology and flow directions of volcanic rocks of the North Star Mesa quadrangle, Grant County, New Mexico; *in* Elston, W. E., and Northrop, S. A. (eds.), Cenozoic volcanism in southwestern New Mexico: New Mexico Geological Society, Special Publication 5, pp. 79-81.

Aldrich, M. J., Jr., and Laughlin, A. W., 1984, A model for the tectonic development of the southeastern Colorado Plateau boundary: Journal of Geophysical Research, v. 89, no. B12, pp. 10,207-10,218.

Bikerman, M., 1972, New K-Ar ages on volcanic rocks from Catron and Grant Counties, New Mexico: Isochron/West, no. 3, pp. 912.

Bikerman, M., 1976, Initial $^{87}Sr/86Sr$ ratios and K-Ar dates of some volcanic rocks from Catron County, New Mexico (abs.): Geological Society of America, Abstracts with Programs, v. 8, no. 5, p. 569.

Bikerman, M., and New, R. A., 1982, A two-biotite dacite—Ar/K dating significance and geochemistry (abs.): Geological Society of America, Abstracts with Programs, v. 14, no. 5, p. 255.

Bornhorst, T. J., 1976, Volcanic geology of the Crosby Mountains and vicinity, Catron County, New Mexico: unpublished M.S. thesis, University of New Mexico, Albuquerque, 113 pp.

Bornhorst, T. J., 1980, Major- and trace-element geochemistry and mineralogy of Eocene to Quaternary volcanic rocks of the Mogollon-Datil volcanic field, southwestern New Mexico: unpublished Ph.D. dissertation, University of New Mexico, Albuquerque, 500 pp.

Bornhorst, T. J., Jones, D. P., Elston, W. E., Damon, P. E., and Shafiqullah, M., 1982, New radiometric ages on volcanic rocks from the Mogollon-Datil volcanic field, southwestern New Mexico: Isochron/West, no. 35, pp. 13-14.

Bromfield, C. S., Eaton, G. P., Peterson, D. L., and Ratté, J. C., 1972, Geological and geophysical investigations of an Apollo 9 photo anomaly near Point of Pines, Arizona: U.S. Geological Survey, Open-file Report 72-51, 19 pp.

Chapin, C. E., and Elston, W. E. (eds.), 1978, Field guide to selected cauldrons and mining districts of the Datil-Mogollon volcanic field, New Mexico: New Mexico Geological Society, Special Publication 7, 149 pp.

Chapin, C. E., and Seager, W. R., 1975, Evolution of the Rio Grande rift in the Socorro and Las Cruces areas: New Mexico Geological Society, Guidebook to 26th Field Conference, pp. 297-322.

Coney, P. J., 1976, Structure, volcanic stratigraphy, and gravity across the Mogollon Plateau, New Mexico; *in* Elston, W. E., and Northrop, S. A. (eds.), Cenozoic volcanism in southwestern New Mexico: New Mexico Geological Society, Special Publication 5, pp. 29-41.

Damon, P. E., and Associates, 1966, Correlation and chronology of ore deposits and volcanic rocks; *in* Annual progress report C00-689-60, Contract AT(11-1)-689, U.S. Atomic Energy Commission: Geochronology Laboratories, University of Arizona, Tucson, 46 pp.

Damon, P. E., and Associates, 1968, Correlation and chronology of ore deposits and volcanic rocks; *in* Annual progress report C00-689-100, Contract AT(11-1)-689, U.S. Atomic Energy Commission: Geochronology Laboratories, University of Arizona, Tucson, p. 65.

Damon, P. E., and Associates, 1969, Correlation and chronology of ore deposits and volcanic rocks; *in* Annual progress report C00-689-120, Contract AT(11-1)-689, U.S. Atomic Energy Commission: Geochronology Laboratories, University of Arizona, Tucson, p. 49.

Damon, P. E., and Associates, 1970, Correlation and chronology of ore deposits and volcanic rocks; *in* Annual progress report C00-689-130, Contract AT(11-1)-689, U.S. Atomic Energy Commission: Geochronology Laboratories, University of Arizona, Tucson, pp. 39-40.

Drewes, H., Houser, B. B., Hedlund, D. C., Richter, D. H., Thorman, C. H., and Finnell, T. L., 1985, Geologic map of the Silver City 1° x 2° quadrangle, New Mexico and Arizona: U.S. Geological Survey, Miscellaneous Investigations Series, Map I-1310-C.

Duffield, W. A., 1986, Preliminary interpretation of field and chemical characteristics of the Taylor Creek Rhyolite, New Mexico (abs.): Geological Society of America, Abstracts with Programs, v. 18, no. 5, pp. 352-353.

Eggleston, T. L., and Norman, D. I., 1986, A summary of the geology, geochemistry, and tin occurrences in the Black Range, New Mexico: New Mexico Geological Society, Guidebook to 37th Field Conference, pp. 173-178.

Elston, W. E., 1968, Terminology and distribution of ash flows of the Mogollon-Silver City-Lordsburg region, New Mexico: Arizona Geological Society, Guidebook to 3rd Field Conference, pp. 231-240.

Elston, W. E., 1976, Glossary of stratigraphic terms of the Mogollon-Datil volcanic province, New Mexico; *in* Elston, W. E., and Northrop, S. A. (eds.), Cenozoic volcanism in southwestern New Mexico: New Mexico Geological Society, Special Publication 5, pp. 131-144.

Elston, W. E., 1984, Mid-Tertiary ash-flow tuff cauldrons, southwestern New Mexico: Journal of Geophysical Research, v. 89, no. B10, pp. 8733-8750.

Elston, W. E., Bikerman, M., and Damon, P. E., 1968, Significance of new K-Ar dates from southwestern New Mexico; *in* Annual progress report C00-689-100, Contract AT(11-1)-689, U.S. Atomic Energy Commission: Geochronology Laboratories, University of Arizona, Tucson, pp. AIV-1-AIV-20.

Elston, W. E., and Damon, P. E., 1970, Significance of 4 new K-Ar dates from the Mogollon Plateau volcanic province, southwestern New Mexico; *in* Annual progress report C00-689-130, Contract AT(11-1)-689, U.S. Atomic Energy Commission: Geochronology Laboratories, University of Arizona, Tucson, pp. AVI-1-AVI-9.

Elston, W. E., Damon, P. E., Coney, P. J., Rhodes, R. C., Smith, E. I, and Bikerman, M., 1973, Tertiary volcanic rocks, Mogollon-Datil province, New Mexico, and surrounding region-K-Ar dates, patterns of eruption, and periods of mineralization: Geological Society of America, Bulletin, v. 84, no. 7, pp. 2259-2274.

Elston, W. E., and Northrop, S. A. (eds.), 1976, Cenozoic volcanism in southwestern New Mexico: New Mexico Geological Society, Special Publication 5, 151 pp.

Elston, W. E., Rhodes, R. C., Coney, P. J., and Deal, E. G., 1976, Progress report on the Mogollon Plateau volcanic field, southwestern New Mexico, no. 3, surface expression of a pluton; *in* Elston, W. E., and Northrop, S. A. (eds.), Cenozoic volcanism in southwestern New Mexico: New Mexico Geological Society, Special Publication 5, pp. 3-28.

Elston, W. E., Rhodes, R. C., and Erb, E. E., Jr., 1976, Control of mineralization by mid-Tertiary volcanic centers, southwestern New Mexico; *in* Elston, W. E., and Northrop, S. A. (eds.), Cenozoic volcanism in southwestern New Mexico: New Mexico Geological Society, Special Publication 5, pp. 125-130.

Farkas, S. E., 1969, Geology of the southern San Mateo Mountains, Socorro and Sierra Counties, New Mexico: unpublished Ph.D. dissertation, University of New Mexico, Albuquerque, 137 pp.

Ferguson, H. G., 1927, Geology and ore deposits of the Mogollon mining district, New Mexico: U.S. Geological Survey, Bulletin 787, 100 pp.

Finnell, T. L., 1976a, Geologic map of the Twin Sisters quadrangle, Grant County, New Mexico: U.S. Geological Survey, Miscellaneous Field Studies Map MF-779.

Finnell, T. L., 1976b, Geologic map of the Reading Mountain quadrangle, Grant County, New Mexico: U.S. Geological Survey, Miscellaneous Field Studies Map MF-800.

Finnell, T. L., Bowles, C. G., and Soule, J. H., 1967, Mineral resources of the Mt. Baldy primitive area, Arizona: U.S. Geological Survey, Bulletin 1230-H, 14 pp.

Fodor, R. V., 1976, Volcanic geology of the northern Black Range, New Mexico; *in* Elston, W. E., and Northrop, S. A. (eds.), Cenozoic volcanism in southwestern New Mexico: New Mexico Geological Society, Special Publication 5, pp. 68-70.

Hedlund, D. C., 1977, Geologic map of the Hillsboro and San Lorenzo quadrangles, Sierra and Grant Counties, New Mexico: U.S. Geological Survey, Miscellaneous Field Studies Map MF-900-A.

Hedlund, D. C., 1978, Geologic map of the C Bar Ranch quadrangle, Grant County, New Mexico: U.S. Geological Survey, Miscellaneous Field Studies Map MF-1039.

Jones, D. P., 1980, Volcanic geology of the Alegros Mountain area, Catron County, New Mexico: unpublished M.S. thesis, University of New Mexico, Albuquerque, 76 pp.

Kedzie, L. L., 1984, High-precision $^{40}Ar/^{39}Ar$ dating of major ash-flow tuff sheets, Socorro, New Mexico: unpublished M. S. thesis, New Mexico Institute of Mining and Technology, Socorro, 197 pp.

Kress, V. C., Laughlin, A. W., and Aldrich, M. J., 1985, K-Ar ages of Cenozoic dikes in Arizona and New Mexico: Isochron/West, no. 43, pp. 3-4.

Lawrence, V. A., 1986, Developments in the Cenozoic volcanic stratigraphy of the Indian Peaks area, northern Black Range, New Mexico: New Mexico Geological Society, Guidebook to 37th Field Conference, pp. 179-182.

Lawrence, V. A., and Richter, D. H., 1986, Geologic map of the Indian Peaks West quadrangle, Catron County, New Mexico: U.S. Geological Survey, Miscellaneous Field Studies Map MF-1849.

Leopoldt, W., and Kortemeier, C. P., 1984, Zircon-fission-track ages of Neogene air-fall ashes from the Gila Group and the Camp Rice Formation, Grant and Dona Ana Counties, New Mexico: Isochron/West, no. 41, pp. 15-18.

Livingston, D. E., Mauger, R. L., and Damon, P. E., 1968, Geochronology of the emplacement, enrichment, and preservation of Arizona porphyry copper deposits: Economic Geology, v. 63, pp. 30-36.

Lopez, D. A., and Bornhorst, T. J., 1979, Geologic map of the Datil area, Catron County, New Mexico: U.S. Geological Survey, Miscellaneous Investigations Series, Map 1-1098.

Marvin, R. F., and Dobson, S. W., 1979, Radiometric ages-compilation B, U.S. Geological Survey: Isochron/West, no. 26, pp. 3-32.

Maxwell, C. H., Foord, E. E., Oakman, M. R., and Harvey, D. B., 1986, Tin deposits in the Black Range tin district: New Mexico Geological Society, Guidebook to 37th Field Conference, pp. 273-282.

McDowell, F. W., 1971, K-Ar ages of igneous rocks from the western United States: Isochron/West, no. 2, pp. 1-16.

McDowell, F. W., 1983, K-Ar dating-incomplete extraction of radiogenic argon from alkali feldspar: Isotope Geoscience, v. 1, pp. 119-126.

McIntosh, W. C., Sutter, J. L., Chapin, C. E., Osburn, G. R., and Ratté, J. C., 1986, A stratigraphic framework for the eastern Mogollon-Datil volcanic field based on paleomagnetism and high precision $^{40}Ar/^{39}Ar$ dating of ignimbrites-a progress report: New Mexico Geological Society, Guidebook to 37th Field Conference, pp. 183-195.

Merrill, R. K., 1974, The late Cenozoic geology of the White Mountains, Apache County, Arizona: unpublished Ph.D. dissertation, Arizona State University, Tempe, 202 pp.

Merrill, R. K., and Péwé, T. L., 1971, The Sheep Crossing Formation-a new late Cenozoic epiclastic formation in east-central Arizona: Journal of Arizona Academy of Science, v. 6, pp. 226-229.

Naeser, C. W., 1976, Fission-track dating: U.S. Geological Survey, Open-file Report 76-190, 68 pp.

Naeser, C. W., 1979, Fission-track dating and geologic annealing of fission tracks; *in* Jager, E., and Hunziker, J. C. (eds.), Lectures in isotope geology: Springer-Verlag, New York, pp. 154-169.

Naeser, C. W., Cunningham, C. G., Marvin, R. F., and Obradovich, J. D., 1980, Pliocene intrusive rocks and mineralization near Rico, Colorado: Economic Geology, v. 75, pp. 122-127.

Osburn, G. R., and Chapin, C. E., 1983, Nomenclature for Cenozoic rocks of northeast Mogollon-Datil volcanic field, New Mexico: New Mexico Bureau of Mines and Mineral Resources, Stratigraphic Chart 1.

Ratté, J. C., 1980, Geologic map of the Saliz Pass quadrangle, Catron County, New Mexico: U.S. Geological Survey, Miscellaneous Field Studies Map MF-1203.

Ratté, J. C., 1981, Geologic map of the Mogollon quadrangle, Catron County, New Mexico: U.S. Geological Survey, Geologic Quadrangle Map GQ-1557.

Ratté, J. C., 1982, Geologic map of the Lower San Francisco Wilderness Study Area and contiguous roadless area, Greenlee County, Arizona, and Catron and Grant Counties, New Mexico: U.S. Geological Survey, Miscellaneous Field Studies Map MF-1463-B.

Ratté, J. C., 1986, Geologic map of the Bull Basin quadrangle, Catron County, New Mexico: U.S. Geological Survey, Open-file Report 86-194.

Ratté, J. C., and Brooks, W. E., 1983, Geologic map of the Mule Creek quadrangle, Grant County, New Mexico: U.S. Geological Survey, Miscellaneous Field Studies Map MF-1666.

Ratté, J. C., and Finnell, T. L., 1978, Road log from Silver City to Reserve via Glenwood and the Mogollon mining district; *in* Chapin, C. E., and Elston, W. E. (eds.), Field guide to selected cauldrons and mining districts of the Datil-Mogollon volcanic field, New Mexico: New Mexico Geological Society, Special Publication 7, pp. 49-63.

Ratté, J. C., and Gaskill, D. L., 1975, Reconnaissance geologic map of the Gila Wilderness Study Area, southwestern New Mexico: U.S. Geological Survey, Miscellaneous Investigations Series, Map 1-886.

Ratté, J. C., Gaskill, D. L., Eaton, G. P., Peterson, D. L., Stotelmeyer, R. B., and Meeves, H. C., 1979, Mineral resources of the Gila Primitive Area and Gila Wilderness, Catron and Grant Counties, New Mexico: U.S. Geological Survey, Bulletin 1451, 225 pp.

Ratté, J. C., and Grotbo, T., 1979, Chemical analyses and norms of 81 volcanic rocks from part of the Mogollon-Datil volcanic field, southwestern New Mexico: U.S. Geological Survey, Open-file Report 79-1435, 33 pp.

Ratté, J. C., and Hedlund, D. C., 1981, Geologic map of the Hells Hole further planning area (RARE II), Greenlee County, Arizona, and Grant County, New Mexico: U.S. Geological Survey, Miscellaneous Field Studies Map MF-1344-A.

Ratté, J. C., Landis, E. R., Gaskill, D. L., Raabe, R. G., and Eaton, G. P., 1969, Mineral resources of the Blue Range Primitive Area, Greenlee County, Arizona, and Catron County, New Mexico: U.S. Geological Survey, Bulletin 1261-E, 91 pp.

Ratté, J. C., Marvin, R. F., Naeser, C. W., and Bikerman, M., 1984, Calderas and ash-flow tuffs of the Mogollon Mountains, southwestern New Mexico: Journal of Geophysical Research, v. 89, no. B10, pp. 8713-8732.

Rhodes, R. C., 1976a, Volcanic geology of the Mogollon Range and adjacent areas, Catron and Grant Counties, New Mexico; *in* Elston, W. E., and Northrop, S. A. (eds.), Cenozoic volcanism in southwestern New Mexico: New Mexico Geological Society, Special Publication 5, pp. 42-50.

Rhodes, R. C., 1976b, Petrologic framework of the Mogollon Plateau volcanic ring complex, New Mexico-surface expression of a major batholith; *in* Elston, W. E., and Northrop, S. A. (eds.), Cenozoic volcanism in southwestern New Mexico: New Mexico Geological Society, Special Publication 5, pp. 103-112.

Rhodes, R. C., and Smith, E. I., 1972, Geology and tectonic setting of the Mule Creek caldera, New Mexico, U.S.A.: Bulletin Volcanologique, v. 36, no. 3, pp. 401-411.

Rhodes, R. C., and Smith, E. I., 1976, Stratigraphy and structure of the northwestern part of the Mogollon Plateau volcanic province, Catron County, New Mexico; *in* Elston, W. E., and Northrop, S. A. (eds.), Cenozoic volcanism in southwestern New Mexico: New Mexico Geological Society, Special Publication 5, pp. 5763.

Richter, D. H., 1978, Geologic map of the Spring Canyon quadrangle, Catron County, New Mexico: U.S. Geological Survey, Miscellaneous Field Studies Map MF-966.

Richter, D. H., Eggleston, T. L., and Duffield, W. A., 1986, Geologic map of the Wall Lake quadrangle, Catron County, New Mexico: U.S. Geological Survey, Miscellaneous Field Studies Map MF1909.

Richter, D. H., Lawrence, V. A., and Duffield, W. A., 1986, Geologic map of the Indian Peaks East quadrangle, Catron County, New Mexico: U.S. Geological Survey, Miscellaneous Field Studies Map MF-1850.

Seamans, S. J., and Elston, W. E., 1987, A third caldera in the Gila Wilderness, SW New Mexico (abs.): Geological Society of America, Abstracts with Programs, v. 19, no. 5, p. 333.

Smith, E. I., 1976, Structure and petrology of the John Kerr Peak dome complex, southwestern New Mexico; *in* Elston, W. E., and Northrop, S. A. (eds.), Cenozoic volcanism in southwestern New Mexico: New Mexico Geological Society, Special Publication 5, pp. 71-78.

Smith, E. I., Aldrich, M. J., Jr., Deal, E. G., and Rhodes, R. C., 1976, Fission-track ages of Tertiary volcanic and plutonic rocks, Mogollon Plateau, southwestern New Mexico; *in* Elston, W. E., and Northrop, S. A. (eds.), Cenozoic volcanism in southwestern New Mexico: New Mexico Geological Society, Special Publication 5, pp. 117-118.

Smith, E. I., and Rhodes, R. C., 1974, Squirrel Springs volcano-tectonic depression-a buried cauldron in southwestern New Mexico: Geological Society of America, Bulletin, v. 85, no. 12, pp. 1865-1868.

Stearns, C. E., 1962, Geology of the north half of the Pelona quadrangle, Catron County, New Mexico: New Mexico Bureau of Mines and Mineral Resources, Bulletin 78, 46 pp.

Steiger, R. H., and Jager, E., 1977, Subcommission on geochronology-convention on the use of decay constants in geo- and cosmochronology: Earth and Planetary Science Letters, v. 36, pp. 359-362.

Stinnett, J. W., Jr., 1980, A geochemical study of calc-alkaline andesites and associated volcanic rocks from the Mogollon-Datil field, southwestern New Mexico: unpublished Ph.D. dissertation, Miami University, Oxford, 271 pp.

Stinnett, J. W., Jr., and Stueber, A. M., 1976, A strontium isotopic and geochemical study of volcanic rocks from the Datil-Mogollon field, southwestern New Mexico (abs.): Geological Society of America, Abstracts with Programs, v. 8, no. 5, pp. 636-637.

Strangway, D. W., Simpson, J., and York, D., 1976, Paleomagnetic studies of volcanic rocks from the Mogollon Plateau area of Arizona and New Mexico; *in* Elston, W. E., and Northrop, S. A. (eds.), Cenozoic volcanism in southwestern New Mexico: New Mexico Geological Society, Special Publication 5, pp. 119-124.

Wahl, D. E., Jr., 1980, Mid-Tertiary volcanic geology in parts of Greenlee County, Arizona, Grant and Hidalgo Counties, New Mexico: unpublished Ph.D. dissertation, Arizona State University, Tempe, 270 pp.

Weber, R. H., 1971, K-Ar ages of Tertiary igneous rocks in central and western New Mexico: Isochron/West, no. 1, pp. 33-45. Weber, R. H., and Bassett, W. A., 1963, K-Ar ages of Tertiary volcanic and intrusive rocks in Socorro, Catron, and Grant Counties, New Mexico: New Mexico Geological Society, Guidebook to 14th Field Conference, pp. 220-223.

Willard, M. E., and Stearns, C. E., 1971, Reconnaissance geologic map of the Pelona thirty-minute quadrangle: New Mexico Bureau of Mines and Mineral Resources, Geologic Map 23.

Selected conversion factors*

TO CONVERT	MULTIPLY BY	TO OBTAIN
Length		
inches, in	2.540	centimeters, cm
feet, ft	3.048×10^{-1}	meters, m
yards, yds	9.144×10^{-1}	m
statute miles, mi	1.609	kilometers, km
fathoms	1.829	m
angstroms, Å	1.0×10^{-8}	cm
Å	1.0×10^{-4}	micrometers, μm
Area		
in^2	6.452	cm^2
ft^2	9.29×10^{-2}	m^2
yds^2	8.361×10^{-1}	m^2
mi^2	2.590	km^2
acres	4.047×10^{3}	m^2
acres	4.047×10^{-1}	hectares, ha
Volume (wet and dry)		
in^3	1.639×10^{1}	cm^3
ft^3	2.832×10^{-2}	m^3
yds^3	7.646×10^{-1}	m^3
fluid ounces	2.957×10^{-2}	liters, l *or* L
quarts	9.463×10^{-1}	l
U.S. gallons, gal	3.785	l
U.S. gal	3.785×10^{-3}	m^3
acre-ft	1.234×10^{3}	m^3
barrels (oil), bbl	1.589×10^{-1}	m^3
Weight, mass		
ounces avoirdupois, avdp	2.8349×10^{1}	grams, gr
troy ounces, oz	3.1103×10^{1}	gr
pounds, lb	4.536×10^{-1}	kilograms, kg
long tons	1.016	metric tons, mt
short tons	9.078×10^{-1}	mt
oz mt^{-1}	3.43×10^{1}	parts per million, ppm
Velocity		
ft sec^{-1} (= ft/sec)	3.048×10^{-1}	m sec^{-1} (= m/sec)
mi hr^{-1}	1.6093	km hr^{-1}
mi hr^{-1}	4.470×10^{-1}	m sec^{-1}

TO CONVERT	MULTIPLY BY	TO OBTAIN
Pressure, stress		
lb in^{-2} (= lb/in^2), psi	7.03×10^{-2}	kg cm^{-2} (= kg/cm^2)
lb in^{-2}	6.804×10^{-2}	atmospheres, atm
lb in^{-2}	6.895×10^{3}	newtons (N)/m^2, N m^{-2}
atm	1.0333	kg cm^{-2}
atm	7.6×10^{2}	mm of Hg (at 0° C)
inches of Hg (at 0° C)	3.453×10^{-2}	kg cm^{-2}
bars, b	1.020	kg cm^{-2}
b	1.0×10^{6}	dynes cm^{-2}
b	9.869×10^{-1}	atm
b	1.0×10^{-1}	megapascals, MPa
Density		
lb in^{-3} (= lb/in^3)	2.768×10^{1}	gr cm^{-3} (= gr/cm^3)
Viscosity		
poises	1.0	gr cm^{-1} sec^{-1} *or* dynes cm^{-2}
Discharge		
U.S. gal min^{-1}, gpm	6.308×10^{-2}	l sec^{-1}
gpm	6.308×10^{-5}	m^3 sec^{-1}
ft^3 sec^{-1}	2.832×10^{-2}	m^3 sec^{-1}
Hydraulic conductivity		
U.S. gal day^{-1} ft^{-2}	4.720×10^{-7}	m sec^{-1}
Permeability		
darcies	9.870×10^{-13}	m^2
Transmissivity		
U.S. gal day^{-1} ft^{-1}	1.438×10^{-7}	m^2 sec^{-1}
U.S. gal min^{-1} ft^{-1}	2.072×10^{-1}	l sec^{-1} m^{-1}
Magnetic field intensity		
gausses	1.0×10^{5}	gammas
Energy, heat		
British thermal units, BTU	2.52×10^{-1}	calories, cal
BTU	1.0758×10^{2}	kilogram-meters, kgm
BTU lb^{-1}	5.56×10^{-1}	cal kg^{-1}
Temperature		
°C + 273	1.0	°K (Kelvin)
°C + 17.78	1.8	°F (Fahrenheit)
°F − 32	5/9	°C (Celsius)

**Divide by* the factor number to reverse conversions.
Exponents: for example 4.047×10^{3} (see acres) = 4,047; 9.29×10^{-2} (see ft^2) = 0.0929.

Editor: Jane Calvert Love
Drafting: U.S. Geological Survey

Typefaces: Text in 10 pt. Palatino, leaded one point
References in 8 pt. Palatino, leaded one point
Display heads in 14 pt. Palatino bold

Presswork: Miehle Single Color Offset
Harris Single Color Offset

Binding: Saddlestiched with softbound cover

Paper: Cover on 17-pt. Kivar
Text on 70-lb white matte

Ink: Cover—PMS 320
Text—Black

Quantity: 900

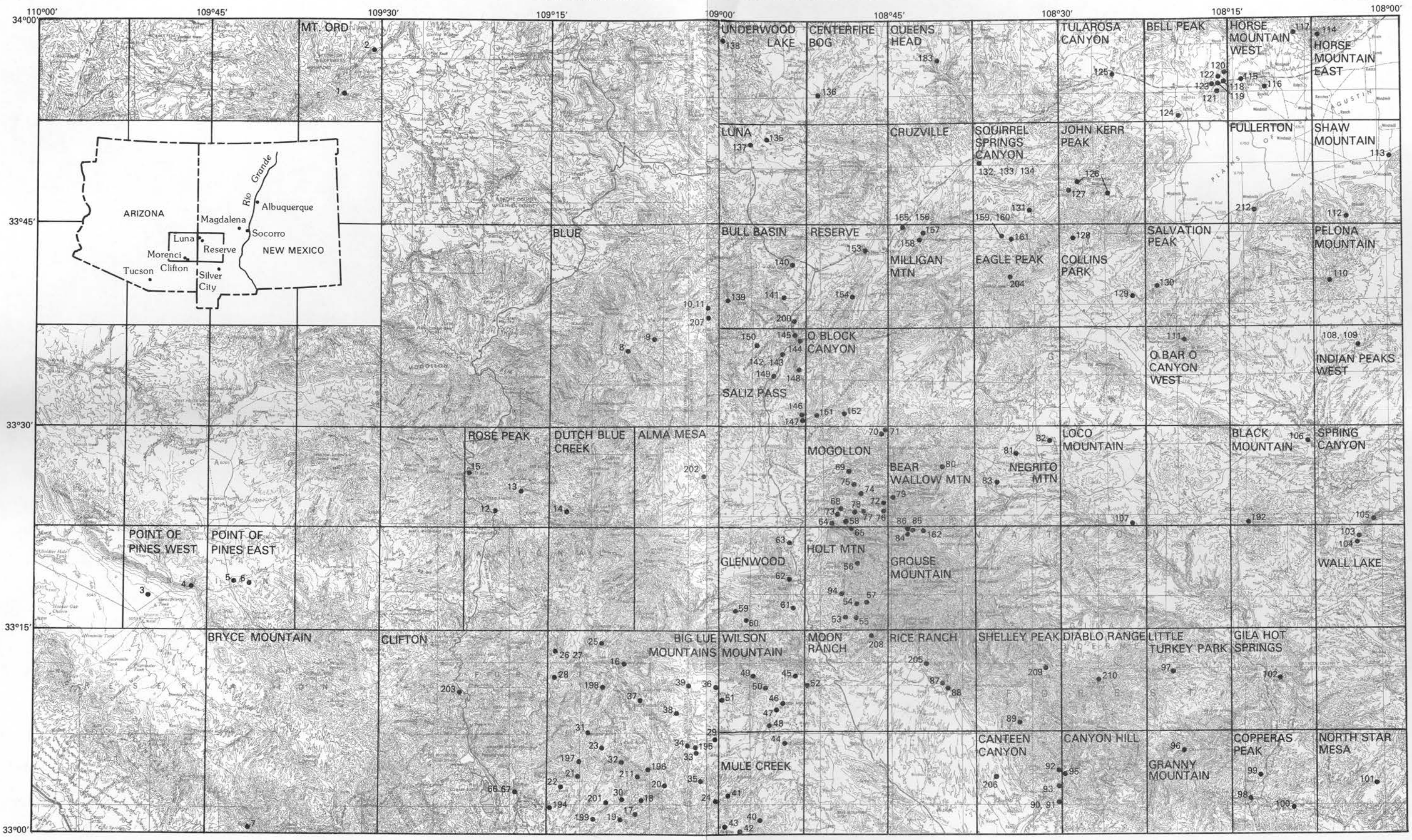
110°00′
109°45′
109°30′
109°15′
109°00′
108°45′
108°30′
108°15′
108°00′
34°00′
33°45′
33°30′
33°15′
33°00′
MT. ORD
UNDERWOOD LAKE
CENTERFIRE BOG
QUEENS HEAD
TULAROSA CANYON
BELL PEAK
HORSE MOUNTAIN WEST
HORSE MOUNTAIN EAST
LUNA
CRUZVILLE
SQUIRREL SPRINGS CANYON
JOHN KERR PEAK
FULLERTON
SHAW MOUNTAIN
BLUE
BULL BASIN
RESERVE
MILLIGAN MTN
EAGLE PEAK
COLLINS PARK
SALVATION PEAK
PELONA MOUNTAIN
O BLOCK CANYON
SALIZ PASS
O BAR O CANYON WEST
INDIAN PEAKS WEST
ROSE PEAK
DUTCH BLUE CREEK
ALMA MESA
MOGOLLON
BEAR WALLOW MTN
NEGRITO MTN
LOCO MOUNTAIN
BLACK MOUNTAIN
SPRING CANYON
POINT OF PINES WEST
POINT OF PINES EAST
GLENWOOD
HOLT MTN
GROUSE MOUNTAIN
WALL LAKE
BRYCE MOUNTAIN
CLIFTON
BIG LUE MOUNTAINS
WILSON MOUNTAIN
MOON RANCH
RICE RANCH
SHELLEY PEAK
DIABLO RANGE
LITTLE TURKEY PARK
GILA HOT SPRINGS
MULE CREEK
CANTEEN CANYON
CANYON HILL
GRANNY MOUNTAIN
COPPERAS PEAK
NORTH STAR MESA
ARIZONA
NEW MEXICO
Rio Grande
Albuquerque
Magdalena
Socorro
Luna
Reserve
Morenci
Clifton
Tucson
Silver City